Lab-on-Chip platforms: label-free detection, separation, patterning and in vitro culture of cells

Tohid Fatanat Didar

Doctor of Philosophy

Department of Biomedical Engineering

McGill University
Montreal, Quebec, Canada
January 2013

A thesis submitted to McGill University in partial fulfillment of the requirements of the degree of Doctor of Philosophy

ABSTRACT

Biomedical devices developed for detection, sorting and *in vitro* culture of cells are important tools in both clinical diagnostics and fundamental research. Recently, with the advances in miniaturization, Lab-on-Chip (LOC) devices have started to play an important role in detection and enrichment of rare cells. Since they do not alter the properties of target cells, label-free methods are a suitable option for cell separation. This dissertation focused on two main label-free approaches, namely adhesion-based and size-based and several novel microchips were introduced for separation of target cells using both size-based and adhesion-based approaches. The first device a multilayered, fully thermoplastic-based microfluidic chip was designed and fabricated for high-throughput size-based separation of micro/nano particles and cells. High-throughput (100 µl/min) separation of micro/nano particles and rare primary cells, with greater than 95% separation efficiency, was successfully demonstrated (Chapters 4 and 5). The second series of microchips were based on adhesion-based separation; multiplex covalently attached microarrays and gradients of biomolecules were produced and embedded inside a single microfluidic chip (chapters 7 and 8). The developed bio-functional interfaces were embedded in a multi-purpose adhesion-based microchip to simultaneously capture, separate, pattern and culture primary and rare cells *in vitro*. Using this chip, oligodendrocyte progenitor cells and cardiomyocytes were successfully separated from rat brain and heart tissues, respectively with greater than 95% separation efficiency in 10min (Chapter 9). Separation of two dissimilar primary cells, in terms of biological properties and initial population, demonstrated the universality of the developed chip towards efficient cell separation. More importantly separated cells can be cultured on the same chip for different subsequent applications such as proliferation for cell therapy or drug testing.

ABRÉGÉ

Les dispositifs biomédicaux développés pour la détection, le triage et la culture cellulaire sont des outils importants en diagnostic clinique et en recherche fondamentale. Récemment, avec les progrès dans le domaine de la miniaturisation et les microfluidiques, les ‘laboratoires-sur-puces’ (LOC) ont commencé à jouer un rôle significatif dans la détection et l'enrichissement des différents types de cellules. Parmi les multitudes LOC développés pour ces applications, ceux n’impliquant pas de marquage représentent une option attrayante, car ils ne modifient pas les propriétés des cellules ciblées par le triage. Séparation à base d'adhérence cellulaire ou en utilisant la différence entre la taille physique des cellules sont les deux approches principales qui ne nécessitent pas de prétraitement des cellules et leur marquage. Dans cette thèse, des micropuces proposées emploient des méthodes sans marquage préalable des cellules ciblées tout en exploitent, soit leurs propriétés d’adhésion et leur affinité pour la biointerface, soit leur différence de taille par rapport la taille des autres cellules dans le mélange initial. En ce qui concerne la première micropuce, nous avons développé un dispositif microfluidique original et multicouche à base de thermoplastique pour la séparation de micro/nanoparticules et de cellules de tailles différentes. Une efficacité de séparation supérieure à 95% a pu être réalisée à haut débit (150 µl/min),

Quant à la séparation basée sur l'adhérence, tout d’abord, nous avons introduit des LOCs pour produire des gradients de concentration de biomolécules dans un seul canal microfluidique. Dans un deuxième temps, ce concept a été utilisé pour fabriquer une puce multifonctionnelle sur laquelle, il était possible de simultanément capturer, séparer des cellules rares de source primaire, paver la surface avec des motifs des cellules et les cultiver sur la même puce. En utilisant cette puce, des cellules progénitrices d'oligodendrocytes (OPC) et des cardiomyocytes provenant respectivement du cerveau et du cœur du rat, ont pu être séparés en 10 min avec une efficacité de séparation supérieure à 95% des autres cellules dans le mélange tissulaire. La séparation de ces deux types de

cellules primaires démontre l’efficacité et l’universalité de cette puce multifonctionnelle pour la séparation d'une gamme de mélanges cellulaires avec différentes concentrations initiales des cellules ciblées par le triage.

ACKNOWLEDGMENTS

I would like to express my gratitude to my supervisor, Professor Maryam Tabrizian, for her insightful guidance and for providing an excellent research environment. Her vision and extraordinary leadership is always inspiring for me. I learnt from her to never give up and always challenge myself for the better. Her enthusiasm and encouragement helped me realize that we can always do better by widening our imagination, goals and efforts to make the impossible, possible. I am also very grateful of her for the opportunities she gave me to participate in various national and international conferences and present the results of my work.

I would like to thank Dr. Teodor Veres for his technical advice, guidance and his help for developing the size-based separation platform at NRC-Canada as well as providing me with the access to the state of the art micro-fabrication facilities at NRC. Also at NRC, I would like to thank Dr. Kebin Li for his help in design, fabrication and test of the size-based separation platform.

I would also like to thank Dr. Guillermina Almazan for her help and advice and providing access to the rat dissection facilities for separation of OPCs and cardiomyocytes. I would like to acknowledge Dr. David Juncker for providing me with the access to his lab and also many valuable scientific discussions.

My special thanks go to all the current and former lab members in Dr. Tabrizian's group, in particular Steve Shapka, Christina Holmes, Samira Taherkhni, Andrew Pearce and Mina Mekhail. I would like to specifically thank Jamal Daoud for his help and advice in most of my experiments, Amir Foudeh for the experiments with contact printing and Kristen Bowey for rat heart isolation experiments.

I would also like to thank Dr. David Juncker's group members specially Sébastien Ricoult, Roozbeh Safavieh and Mohammad Qasaimeh. Special thanks go to Marcio Dipaula for his help regarding rat dissections. I would also like to acknowledge all the administrative support and help from Ms Pina Sorrini and Nancy Abate.

Last but not least, I want to thank my wife, Zeinab for her constant support, patience, understanding and encouragement.

Finally, I would like to acknowledge the funding sources that made this work possible: Natural Sciences and Engineering Research Council of Canada NSERC-CREAT Integrated Sensor Systems (ISS) program, the Fonds Québécois de la Recherche de la Nature et des Technologies (FQRNT), McGill Faculty of Medicine and Biomedical Engineering Department.

CONTRIBUTIONS OF AUTHORS

In accordance with the “Guidelines for Thesis Preparation”, this thesis is presented as a collection of manuscripts written by the candidate with the collaboration of the co-authors. First three chapters include general introduction, objectives and background knowledge. The results section in the form of accepted, submitted or to be submitted manuscripts are included in chapters 4, 5, 6 7 8 and 9. In the final chapters (10 and 11), guidelines for future research are suggested. The manuscripts are based on theoretical, simulation and experimental data generated from experiments designed and executed by the candidate, who was also responsible for data collection and analysis. PhD supervisor appears as co-author on all manuscripts to reflect her supervisory role during the execution of the work and her involvement in the preparation and editing of the manuscripts. On the first and second paper (chapters 4 and 5), Dr. Teodor Veres and Dr. Kebin Li appear as co-authors to acknowledge their contribution in the design and fabrication of the multilayer thermoplastic based microfluidic device as well in the preparation of these manuscripts. Amir Foudeh appears as a co-author in the 4th paper (chapter 7) to acknowledge his help for fabrication and test of the developed microchip. Kristen Bowey appears as a co-author in the 6th paper (chapter 9) to acknowledge her contribution for the experiments in separation of cardiomyocytes from rat heart tissue using the developed microchip in this chapter as well as editing this manuscript.

TABLE OF CONTENTS

LIST OF TABLES

LIST OF FIGURES

Chapter 1: Introduction

1-1 Definition and motivation for cell sorting

In general, any technique that can be used for separation, isolation or enrichment of a specific cell type, is a cell sorting technique (Mattanovich and Borth 2006). Cell sorting techniques employ either physical properties (e.g. density or size), or affinity properties (e.g. electric, magnetic or adhesive specific to each cell type) to sort desired cell types.

The ability to rapidly detect and separate a specific cell type within a complex biological sample is becoming increasingly critical in both basic research and clinical diagnostics and therapeutics. The use of pure cells helps to reduce variations among experiments and thus expedite scientific discovery. Furthermore, cell separation is a basic requirement for cell therapy in the field of regenerative medicine. The fields of biology and biotechnology are the main users of sorting techniques and devices for isolation of rare cell populations. However, the importance of cell sorting is not limited to biology and medicine but also to the fields of molecular genetics, diagnostics and therapeutics where analysis and subsequent cultivation of desired cells from a defined cell population are required.

Despite the progress achieved in isolation of rare cell populations, current devices and methods leave much to be desired. Developing high-throughput and multiplex devices that are portable, label-free, simple and cost effective are the subjects of current research efforts in this field.

1-2 Lab-on-Chip devices for cell sorting

Lab-on-Chip (LOC) devices implement micro/nano fabrication principles to integrate one or several laboratory functions on a small chip. In terms of flow conditions, these devices mostly operate based on the principles of microfluidics. Over the past two decades there have been significant developments in the field of LOC technology where these miniaturized platforms have started to play an increasingly important role in discoveries in cell biology, neurobiology,

pharmacology, and tissue engineering. The major advantages of LOC devices for research and diagnostics include: ability to design cellular microenvironments (Walker, Zeringue et al. 2004), precisely controlled fluid flow rates and velocity fields (Kim, Lee et al. 2008), high surface to volume ratios, portability and reduction of time and cost of cell culture experiments (Walker, Zeringue et al. 2004).

1-3 Label free cell separation

Based on the method used to identify the cells of interest, cell sorting microfluidic devices can be categorized into (i) label-free techniques (e.g. size-based and adhesion-based separation) and (ii) pre-processed techniques (e.g. fluorescence activated cell sorting, FACS (Herzenberg, Sweet et al. 1976, Kruger, Singh et al. 2002, Studer, Jameson et al. 2004, Cho, Chen et al. 2010), and magnetic activated cell sorting, MACS (Miltenyi S, Muller W et al. 1990, Dirican, Ozgun et al. 2008, Marek, Caruso et al. 2008). In the latter, desired cells are tagged with fluorescent dyes (for FACS) or magnetic beads (for MACS) and are exposed to electrical or magnetic fields respectively. These methods can potentially alter the functions of the separated cells due to the presence of attached antibodies (FACS) or magnetic beads (MACS); this is of concern if the isolated cells are designated for specific downstream applications such as tissue regeneration. Conversely, in label-free techniques, there is no need for a pre-processing step and thus the properties of target cells can be maintained.

Size-based filtration and adhesion-based separation are two of the main label-free approaches used in cell sorting. Adhesion-based separation is not dependent on cell size-and targets the affinity of cell membrane to specific adhesion molecules. The significance of adhesion-based separation is not only attributed to its label free nature, but also to its potential for bio-sensing. Such Adhesion-based separation platforms can be further integrated to investigate the target cells after separation, on the same platform, reducing the time, costs and efficiency of subsequent studies.

1-3 Thesis outline

The research described in this dissertation reports the (1) design, (2) microfluidic simulation, (3) microchip fabrication and (4) proof-of-concept demonstration of LOC devices for high-throughput, label-free separation of cells. This document contains 10 chapters; chapter 2 outlines the hypothesis and objectives of the thesis, which is developing enabling LOC technologies for cell sorting. Chapter 3 presents an overview and background knowledge of the field. Chapters 4 to 9 present a collection of published, submitted or “to be submitted” manuscripts where the design, fabrication and function of several LOC devices along with results and discussions have been presented.

During this doctoral work, two label-free approaches based on size or adhesion properties of target cells were implemented in micro-fabricated LOC platforms to detect or separate target cell types. The developed chips have important potential applications not only for detection and separation of cells but also for *in vitro* study of primary and rare cells. The specific contributions of this work are as follows:

1- A novel microfluidic chip for size-based separation of particles and cells was designed and fabricated. This chip not only addresses drawbacks of previously reported devices, but also takes into account commercialization perspectives. Fabrication limitations with Polydimethylsiloxane-based (PDMS-based) devices and also membrane blocking due to laminar flow in microfluidic devices are the main technical drawbacks of the previously reported devices. Low operating flow rate is another issue that limits the use of these devices for practical applications. The developed platform addressed all of the above-mentioned limitations. Generating turbulent flow in a microfluidic channel to avoid membrane blocking at very high flow rates (6000 µl/hr) was the core contribution of this design. This device was fabricated from an integrated thermoplastic elastomer-based (TPE-based) multilayer microfluidic chip with an embedded peristaltic micropump and membrane using hot embossing lithography. High-throughput label-free separation of red blood cells and chosen rare cells (i.e. oligodendrocyte progenitor cells from brain tissue) was successfully demonstrated using this chip.

2- A microfluidic chip with dual simultaneous functionalities was introduced. This novel design provided bio-functional interfaces for applications such as bio-sensing, cell detection, sorting and *in vitro* culture. Following are two original features of this chip:

(a) This chip produces multiplex microarrays of biomarkers in a single microfluidic channel. This was achieved through a combination of micro-contact printing and microfluidic patterning, resulting in shear-resistant, multiplex detection interfaces on a single microfluidic channel.

(b) The developed chip was able to generate concentration gradients of multiple biomolecules, based on hydrodynamic resistances, inside multiple parallel micro-channels. The main advantage of this chip was its ability to perform high-throughput, gradient-dependent experiments in parallel micro-channels with multiplex gradients in each channel. Furthermore, nonlinear polynomial gradients could be produced using this design. Previously reported microfluidic designs were able to generate chemical gradients in only one channel with one gradient profile which limited the application of these devices for high-throughput gradient-dependent experiments. In addition, previous designs resulted in big device footprints—thus minimizing the space available for the actual experiments.

The degree of adhesion of human umbilical vein endothelial cell (HUVEC) to multiplex peptide gradients in parallel channels was successfully demonstrated using this chip. The applicability of this platform could be extended to investigate a variety of biological phenomena such as cancer cells migration, biomarker discovery, cell sorting and stem cell differentiation.

3- A multi-purpose microchip with the ability to simultaneously capture, separate, pattern and culture primary and rare cells *in vitro* was introduced. Using this chip, oligodendrocyte progenitor cells (OPCs) and cardiomyocytes were separated from rat brain and heart tissue, respectively. Results showed over 95% separation efficiency for both cell types in less than 10 min. Separation of two dissimilar primary cells demonstrated the universality of the developed interface

and its functionality towards efficient cell separation from a range of cell mixtures with varying cell concentrations of the target cells in the initial mixture. In addition, attachment of target cells and spreading of each cell was precisely controlled based on the patterns designed on the surface. Viability and differentiation of separated cells *in vitro* was also demonstrated on this platform.

The multi-functionality, versatility, portability and cost effectiveness of this microchip opens a new avenue for separation, patterning, *in vitro* culture and co-culture of rare cells. Furthermore, integration of separation platform with downstream applications (e.g. cell culture) would provide significant advantages, eliminating complex methods such as FACS or MACS and reducing time, cost and manpower.

A list of publications and reports of invention prior to patent application resulted from this project is presented below:

1-4 Articles published or accepted in refereed journals

1- Tohid Fatanat Didar and Maryam Tabrizian, A miniaturized multipurpose platform for rapid, label-free and simultaneous separation, patterning and in vitro culture of primary and rare cells, Advanced H. Materials, Accepted (2013).

2- Tohid Fatanat Didar*, K. Li*, M. Tabrizian and T. Veres, High throughput multilayer microfluidic particle separation platform using embedded thermoplastic-based micro-pumping, Lab on a Chip Accepted, (2013). (*equal contribution).

3- Tohid Fatanat Didar*, K. Li*, M. Tabrizian and T. Veres, Separation of rare oligodendrocyte progenitor cells from brain using a high-throughput multilayer thermoplastic-based microfluidic device, Biomaterials, Accepted. (2013) (*equal contribution).

4- Tohid Fatanat Didar and M. Tabrizian, Generating multiplex gradients of biomolecules for controlling cellular adhesion in parallel microfluidic channels, Lab on a Chip, 12, 4363-4371, (2012).

5- Tohid Fatanat Didar, Amir Foudeh and Maryam Tabrizian, Patterning multiplex protein microarrays in a single microfluidic channel, Analytical Chemistry, 84 (2), 1012-1018, (2012).

6- Tohid Fatanat Didar and Maryam Tabrizian, Adhesion-based detection, sorting and enrichment of cells in microfluidic Lab-on-Chip devices, Lab on a Chip, 10, 3043-3053, (2010).

1-5 Patents

1- T. Fatanat Didar, K. Bowey and M. Tabrizian, Universal microchip for detection separation, isolation and controlled attachment and spreading of rare and primary cells, Provisional patent, (2013).

2- T. Fatanat Didar, Kebin Li, Maryam Tabrizian and Teodor Veres, Integrated multi-level microfluidic system for particles/cells separation and sorting, provisional patent (2013).

References

Cho, S. H., C. H. Chen, F. S. Tsai, J. M. Godin and Y. H. Lo (2010). "**Human mammalian cell sorting using a highly integrated micro-fabricated fluorescence-activated cell sorter (FACS).**" Lab on a Chip - Miniaturisation for Chemistry and Biology **10**(12): 1567-1573.

Dirican, E. K., O. D. Ozgun, S. Akarsu, K. O. Akin, O. Ercan, M. Ugurlu, C. Camsari, O. Kanyilmaz, A. Kaya and A. Unsal (2008). "**Clinical outcome of magnetic activated cell sorting of non-apoptotic spermatozoa before density gradient centrifugation for assisted reproduction**." Journal of Assisted Reproduction and Genetics **25**(8): 375-381.

Herzenberg, L. A., R. G. Sweet and A. Herzenberg (1976). "**Fluorescence-activated cell sorting.**" Scientific American **234**(3): 108-116.

Kim, S. M., S. H. Lee and K. Y. Suh (2008). "**Cell research with physically modified microfluidic channels: A review**." Lab on a Chip - Miniaturisation for Chemistry and Biology **8**(7): 1015-1023.

Kruger, J., K. Singh, A. O'Neill, C. Jackson, A. Morrison and P. O'Brien (2002). "**Development of a microfluidic device for fluorescence activated cell sorting**." Journal of Micromechanics and Microengineering **12**(4): 486-494.

Marek, R., M. Caruso, A. Rostami, J. B. Grinspan and J. D. Sarma (2008). "**Magnetic cell sorting: A fast and effective method of concurrent isolation of high purity viable astrocytes and microglia from neonatal mouse brain tissue.**" Journal of Neuroscience Methods **175**(1): 108-118.

Mattanovich, D. and N. Borth (2006). "A**pplications of cell sorting in biotechnology**." Microbial Cell Factories **5**(1): 12.

Miltenyi S, Muller W, Weichel W and Radbruch A (1990). "**High gradient magnetic cell separation with MACS**." Cytometry **11**: 231-238.

Studer, V., R. Jameson, E. Pellereau, A. Pepin and Y. Chen (2004). **A microfluidic mammalian cell sorter based on fluorescence detection**, Elsevier.

Walker, G. M., H. C. Zeringue and D. J. Beebe (2004). "**Microenvironment design considerations for cellular scale studies**." Lab on a Chip **4**(2): 91-97.

Chapter 2: Hypothesis and Objectives

2-1- Hypothesis

Among different techniques used for cell separation in LOC devices, label-free techniques are of particular interest, because they do not alter the properties of the target cells. This is an important design parameter if the isolated cells are to be used for specific applications such as tissue regeneration or drug screening tests. This led to establish the hypothesis of this thesis as follows: through appropriate LOC design, label-free microchips can be fabricated for separating, patterning and culturing target cells on the same platform. These platforms will allow to sort cells either by difference in their adhesion properties or by difference in their sizes.

2-2 Research objectives

To confirm the aforementioned hypothesis, the main objective of this project was therefore to develop enabling size-based filtration and adhesion-based separation LOC devices for high-throughput label-free detection and sorting of primary and rare cells. Oligodendrocyte progenitor cells (OPCs), with a population of 5-10%, and cardiomyocytes, representing 50-60% in cell mixtures, from brain and heart tissue, respectively, were chosen as the main target cells for separation, due to the large difference in their initial population in their respective cell mixture, in order to assess the dynamic range of developed microfluidic platform. Besides, both cell types have very limited proliferative potential *in vitro* and very often OPCs maturation is limited by inability to obtain pure population. OPCs and cardiomyocytes are frequently used as cell model for *in vitro* and preclinical investigations of various diseases.

The main objective was broken down into two goals as detailed below:

Aim 1: size-based separation- to design and develop a novel multilayered, fully thermoplastic elastomeric-based microfluidic device for high-throughput size-based separation with an embedded commercially available membranes that can

separate target particles/cells while avoiding membrane clogging, which often occur in microfluidic devices operating under laminar flow regime.

Aim 2: Adhesion based separation- to develop LOC devices with embedded bio-functional interfaces for adhesion-based separation through the use of selective biomolecules. This aim encloses three sub-aims:

(a) To pattern surfaces and create regions having various degrees of affinity towards different cell types. Such multiplex shear resistant patterns of several cell-adhesive biomolecules were obtained through covalent binding in a LOC device.

(b) To generate bio-functional interfaces with concentration gradients of different biomolecules in order to discover novel biomarkers as well as investigating the degree of adhesion of target cells to these biomolecules.

(c) To develop a universal chip for separation of primary cell types within a wide range of physical properties and initial populations. In addition to their separation, the goal was to simultaneously pattern and culture target cells on the separation platform to further study separated cells *in vitro*.

Chapter 3: Background knowledge

3-1 Lab-on-Chip devices

A Lab-on-Chip (LOC) is a device fabricated using micro and nano-fabrication techniques that integrates one or several laboratory functions on a single chip of only a few square millimeters in size while consuming small biological sample volumes. They allow studying many analytical processes of biological and chemical samples on a single microchip. Flow conditions in LOC devices follow microfluidic principles. Thus, microfluidics plays an increasingly important role in these devices.

3-2 Principles of microfluidics

Microfluidics refers to the manipulation of liquids at the micrometer scale mainly in micro-fabricated systems with dimensions in the order of hundreds of microns. In fluid mechanics the flow regime is characterized by the Reynolds number (Re). Re number is the ratio of viscous forces to inertial forces and is defined by the following equation:

$$\mathrm{Re} = \frac{\rho \upsilon D_h}{\mu} \quad (3\text{-}1)$$

Where ρ is the fluid density, υ is the velocity of the fluid, μ is the fluid viscosity and D_h is the hydraulic diameter of the channel.

Flow regimes with Re numbers less than 2300 are considered to be laminar. In microfluidic channels the hydraulic diameter is very small resulting in Re numbers less than 2300. Therefore flow regime in microfluidic devices is almost always laminar.

By analogy to electrical resistances in electronics, hydrodynamic resistances are defined for microfluidic channels. The hydrodynamic resistance R_w of a microfluidic channel is defined as:

$$R_w = DP/Q \quad (3\text{-}2)$$

Where *DP* is the applied pressure difference between the two ends of the channel and *Q* is the flow rate. In straight micro-channels, hydrodynamic resistance depends on the channel geometry.

Inherent laminar flow and the ability to control the hydrodynamic resistances of microfluidic channels provide significant advantage for LOC devices over macro scale systems in many applications such as microfluidic patterning (Takayama, Ostuni et al. 2001, Didar, Foudeh et al. 2011), gradient generation (Jeon, Dertinger et al. 2000, Li Jeon, Baskaran et al. 2002, Didar and Tabrizian 2012) and hydrodynamic separation (Huang, Cox et al. 2004, Yamada and Seki 2005).

However, laminar flow can also be problematic; it is hard to implement mixing in a laminar flow regime. Furthermore, when membranes are used for size-based cell separation, laminar flow can result in membrane clogging (Wei, Chueh et al. 2011).

3-3 Surface functionalization and patterning in LOC devices

Optimal surface properties, in terms of topography and roughness, as well as the homogeneous distribution of ligands on the surface, can significantly enhance the efficiency and sensitivity of the device. Consequently, different techniques have been implemented for surface functionalization such as microfluidic patterning and micro-contact printing.

Conventional microfabrication techniques such as photolithography, soft lithography (Whitesides, Ostuni et al. 2001), electrochemical discharge machining (Fatanat Didar, Dolatabadi et al. 2008) and deep reactive ion etching (Lang 1996) are used for patterning micro structures onto surfaces. Several other methods including electron beam lithography (Goto, Tsukahara et al. 2008), electrochemical and chemical etching (Westcott, Lamb et al. 2009), UV-assisted capillary molding (Kwon, Lee et al. 2007), and layer by layer technique (Shaikh-Mohammed, Li et al. 2004) are used for patterning nanostrucutres on microchannel surfaces.

Micro-contact printing (Wilbur, Kumar et al. 1994, Xia and Whitesides 1997) and microfluidic patterning (Schena 1999, Delamarche, Juncker et al. 2005) are two main techniques for immobilization of adhesive ligands onto surfaces of

microchannels (Sin, Murthy et al. 2005, Zhang, Crozatier et al. 2005, Nagrath, Sequist et al. 2007, Plouffe, Njoka et al. 2007, Plouffe, Kniazeva et al. 2009). If covalent ligand attachment to the surface is required silanization (Olbrich, Andersen et al. 1996, Qin, Hou et al. 2007), (Maraldo and Mutharasan 2007), can be implemented to produce strong bunds between the ligand and the surface.

Combination of different methods has also been used to achieve better adhesive properties (Kaji, Hashimoto et al. 2006, Kalinina, Gliemann et al. 2008). Micro/nano structuring of the surface followed by functionalization with the biomolecules of choice (Goto, Tsukahara et al. 2008) or functionalizing micro/nano particles with the adhesive biomolecules (Liu, Guo et al. 2007) were showed to improve adhesive properties.

Table 3-1: LOC devices developed for cell sorting

Sorting Method	Separation property	Limitations	References
FACS*	Fluorescence labeling (Pre-processed)	False detection as separation rate increases, pre-processing is necessary, expensive	(Herzenberg, Sweet et al. 1976, Kruger, Singh et al. 2002, Studer, Jameson et al. 2004, Cho, Chen et al. 2010)
MACS**	Magnetic (Pre-processed)	Needs external magnetic field and pre-processing	(Miltenyi S, Muller W et al. 1990, Dirican, Ozgun et al. 2008, Marek, Caruso et al. 2008)
Physical trapping (Filtering)	Size (Label-free)	Selectivity is only based on the size of the particles, needs complex microfabrication	(Di Carlo, Wu et al. 2006, Di Carlo, Edd et al. 2008, Manbachi, Shrivastava et al. 2008)
Acoustic cell sorting	Optical polarizability (Label-free)	Particle diameter must be less than half of the applied wavelength, requires external field	(Deok-Ho, Haake et al. 2004, Nilsson, Petersson et al. 2004, Adams, Thevoz et al. 2009, Johansson, Nikolajeff et al. 2009)
Optical forces	Optical properties (Label-free)	Based either on size or index of refraction	(Wang, Tu et al. 2005, Jonas and Zemanek 2008)
Hydrodynamic separation	Size (Label-free)	Selectivity is only based on the size of the particles, efficiency is an issue	(Adam and Daniel 2001, Yu-Cheng and Chun-Ping 2002, Takagi, Yamada et al. 2005, Yamada and Seki 2005)

*FACS: Fluorescence activated cell sorting, **MACS: Magnetic activated cell sorting

3-4 Overview of the cell separation techniques in LOC devices

Different techniques have been reported in literature for cell sorting using LOC devices. Table 3-1 describes some of these techniques, categorized based on the implemented cell-specific property for separation. This table summarizes the main focus of research efforts for cell sorting in LOC devices specifying limitations of each method. As mentioned before, these techniques can be categorized into two groups, namely pre-processing and label-free. Following is a brief summary of important techniques used in microfluidics for cell sorting in each of these categories.

3-5 Pre-processed methods

3-5-1 Fluorescence activated cell sorting (FACS)

Fluorescence Activated Cell Sorting (FACS) instruments are based on the principles of flow cytometry and typically use laser-induced fluorescence to count or separate cells stained with fluorescently labeled antibodies (Pappas and Wang 2007). Figure 3-1 shows three main steps for cell sorting using FACS. First, the cells are separated and aligned into a ribbon of cells, a process called cell focusing. In microfluidic systems, this initial step is achieved by generating three parallel laminar streams with a central stream large enough to allow the passage of only one cell at a time (Herzenberg, Sweet et al. 1976, Poletaev, Gnuchev et al. 1987, Kruger, Singh et al. 2002). Next, positive cells, namely the cells that are separated from the other components of the flowing solution, are detected. Several methods for target cells detection have been developed. The large majority of systems however, use fluorescent detection where the cells are either tagged with specific fluorescently labeled antibodies or they express a modified fluorescent protein. The detection event actuates a switch, whose activation directs the positive cells into a separate collection channel. Flow switching can be implemented in several manners such as electromechanical valves, pressure-driven valves, electroosmotic switches or optical valves. In particular, electroosmotic force (EOF) has been frequently employed as it is a robust, rapid and easily miniaturized means of directing flows in microfluidic channels (Fu, Spence et al. 1999).

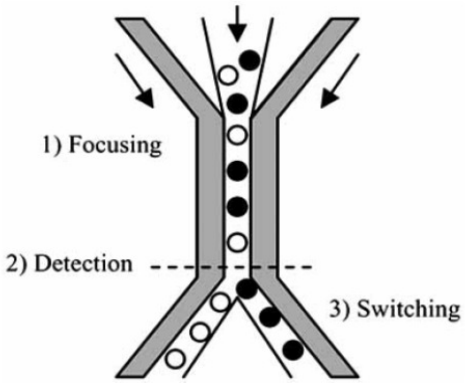

Figure 3-1: Schematic representation of steps for fluorescence activated cell sorting (FACS).

Although FACS is capable of processing 10,000 cells per second, it is a costly procedure which requires large lab space and pre-processing of target cells. In addition FACS is not available in all research centers and requires highly skilled operators.

3-5-2 Magnetic activated cell sorting (MACS)

Magnetic labeling provides a more affordable alternative method for cell separation referred to as MACS. For example, if the desired cells are attached to magnetically labeled antibodies, the positive cells can be attracted into a secondary channel by a magnet positioned on one side of the T-junction. This approach could be described as dynamic, as opposed to a static approach where the target cells are not only re-routed into a secondary channel but are rather magnetically trapped. Magnetic beads with capture moieties can be immobilized inside a micro-channel prior to the injection of the cell containing solution. Such trapping device can consist of external permanent magnets or more conveniently of micro-fabricated electromagnets (Miltenyi S, Muller W et al. 1990, Malic L, Herrmann M et al. 2007, Saliba, Saias et al. 2010, Hoshino, Huang et al. 2011).
Although MACS is a more cost effective technique compared to FACS, it still requires external magnetic fields and also preprocessing of cells which might alter their properties for subsequent applications.

3-6 Label-free cell sorting techniques

Label-free approaches mainly implement inherent properties of the target cells' to separate them from a mixture. These properties include size (Yu-Cheng and Chun-Ping 2002) (Huang, Cox et al. 2004, Takagi, Yamada et al. 2005, Yamada and Seki 2005), acoustic properties (Nilsson, Petersson et al. 2004), optical properties (Wang, Tu et al. 2005, Jonas and Zemanek 2008), and adhesion properties. Among these techniques, size-based and adhesion-based separation have attracted a lot of the interest because they are simple, cost effective and do not expose cells to external optical or acoustic fields. Chapter 6 includes a comprehensive review of adhesion-based separation techniques with a detailed account of prior art and literature survey. In the following paragraphs, a brief survey of the literature on size-based separation is presented.

Size-based particle/cell separation techniques rely purely on microfluidic principles and the interaction of the fluid with the geometries of the microfluidic design. Obstacle induced separation, hydrodynamic filtration (Huang, Cox et al. 2004, Takagi, Yamada et al. 2005), pinched flow fractionation (Bhagat, Hou et al. 2011), inertia and dean flow separation (Kuntaegovvdanahalli, Bhagat et al. 2009, Zhu, Tzeng et al. 2010) are main techniques used for separating cells based on their size difference. Pinches, weirs and posts are common microfluidic obstacle components, which are arranged in microfluidic channels to act as filters, preventing particles from entering certain areas. The above-mentioned techniques require advanced instrumentation to generate precise flow rates and/or complex micro-fabrication.

Among these techniques, embedding thin membranes in microfluidic chips can be a cost effective approach, which in theory can be easily integrated into a miniaturized instrument. However there are major limitations using embedded filters for separation applications. From the fabrication point of view, the main limitation is in non-conformal bonding between the commercially available membranes and microfluidic substrates (e.g. PDMS or glass based devices). Although fabrication and use of PDMS based membranes was recently reported (Luo and Zare 2008), the fabrication steps are complex and also the minimum

pore sizes achieved are around 7 microns. In addition, membrane clogging and low separation flow rates are the main operating drawbacks of previously reported devices (Schirhagl, Fuereder et al. 2011, Wei, Chueh et al. 2011). Size-based cell separation devices, with particular emphasis on implementing membranes and introducing a novel design to address the limitation of previously reported devices, is discussed in chapters 4 and 5.

References

Adam, W. G. and A. H. Daniel (2001). "**Cell separation mediated by differential rolling adhesion.**" Biotechnology and Bioengineering **73**(2): 111-124.

Adams, J. D., P. Thevoz, H. Bruus and H. T. Soh (2009). "**Integrated acoustic and magnetic separation in microfluidic channels.**" Applied Physics Letters **95**(25): 254103 (254103 pp.).

Bhagat, A. A. S., H. W. Hou, L. D. Li, C. T. Lim and J. Han (2011). "**Pinched flow coupled shear-modulated inertial microfluidics for high-throughput rare blood cell separation.**" Lab on a Chip **11**(11): 1870-1878.

Cho, S. H., C. H. Chen, F. S. Tsai, J. M. Godin and Y. H. Lo (2010). "**Human mammalian cell sorting using a highly integrated micro-fabricated fluorescence-activated cell sorter (μFACS)**." Lab on a Chip - Miniaturisation for Chemistry and Biology **10**(12): 1567-1573.

Delamarche, E., D. Juncker and H. Schmid (2005). "**Microfluidics for processing surfaces and miniaturizing biological assays.**" Advanced Materials **17**(24): 2911-2933.

Deok-Ho, K., A. Haake, S. Yu, A. P. Neild, J. E. Ihm, J. Dual, J. A. Hubbell, J. Byeong-Kwon and B. J. Nelson (2004). **High-throughput cell manipulation using ultrasound fields**, Piscataway, NJ, USA, IEEE.

Di Carlo, D., J. F. Edd, D. Irimia, R. G. Tompkins and M. Toner (2008). "**Equilibrium Separation and Filtration of Particles Using Differential Inertial Focusing.**" Analytical Chemistry **80**(6): 2204-2211.

Di Carlo, D., L. Y. Wu and L. P. Lee (2006). "**Dynamic single cell culture array.**" Lab on a Chip **6**(11): 1445-1449.

Didar, T. F., A. M. Foudeh and M. Tabrizian (2011). "**Patterning Multiplex Protein Microarrays in a Single Microfluidic Channel.**" Analytical Chemistry.

Didar, T. F. and M. Tabrizian (2012). "**Generating multiplex gradients of biomolecules for controlling cellular adhesion in parallel microfluidic channels.**" Lab Chip **12**(21): 4363-4371.

Dirican, E. K., O. D. Ozgun, S. Akarsu, K. O. Akin, O. Ercan, M. Ugurlu, C. Camsari, O. Kanyilmaz, A. Kaya and A. Unsal (2008). "**Clinical outcome of magnetic activated cell sorting of non-apoptotic spermatozoa before density gradient centrifugation for assisted reproduction.**" Journal of Assisted Reproduction and Genetics **25**(8): 375-381.

Fatanat Didar, T., A. Dolatabadi and R. Wüthrich (2008). "**Characterization and modeling of 2D-glass micro-machining by spark-assisted chemical engraving (SACE) with constant velocity.**" Journal of Micromechanics and Microengineering **18**(6): 5016.

Fu, A. Y., C. Spence, A. Scherer, F. H. Arnold and S. R. Quake (1999). "**A microfabricated fluorescence-activated cell sorter.**" Nat Biotechnol **17**(11): 1109-1111.

Goto, M., T. Tsukahara, K. Sato and T. Kitamori (2008). "**Micro- and nanometer-scale patterned surface in a microchannel for cell culture in microfluidic devices.**" Analytical and Bioanalytical Chemistry **390**(3): 817-823.

Herzenberg, L. A., R. G. Sweet and A. Herzenberg (1976). "**Fluorescence-activated cell sorting.**" Scientific American **234**(3): 108-116.

Hoshino, K., Y.-Y. Huang, N. Lane, M. Huebschman, J. W. Uhr, E. P. Frenkel and X. Zhang (2011). "**Microchip-based immunomagnetic detection of circulating tumor cells.**" Lab on a Chip.

Huang, L. R., E. C. Cox, R. H. Austin and J. C. Sturm (2004). "**Continuous Particle Separation Through Deterministic Lateral Displacement.**" Science **304**(5673): 987-990.

Jeon, N. L., S. K. W. Dertinger, D. T. Chiu, I. S. Choi, A. D. Stroock and G. M. Whitesides (2000). "**Generation of Solution and Surface Gradients Using Microfluidic Systems.**" Langmuir **16**(22): 8311-8316.

Johansson, L., F. Nikolajeff, S. Johansson and S. Thorslund (2009). **"On-chip fluorescence-activated cell sorting by an integrated miniaturized ultrasonic transducer.**" Analytical Chemistry **81**(13): 5188-5196.

Jonas, A. and P. Zemanek (2008). "**Light at work: The use of optical forces for particle manipulation, sorting, and analysis**." Electrophoresis **29**(24): 4813-4851.

Kaji, H., M. Hashimoto and M. Nishizawa (2006). "**On-Demand Patterning of Protein Matrixes Inside a Microfluidic Device.**" Analytical Chemistry **78**(15): 5469-5473.

Kalinina, S., H. Gliemann, M. Lopez-Garcia, A. Petershans, J. Auernheimer, T. Schimmel, M. Bruns, A. Schambony, H. Kessler and D. Wedlich (2008). "**Isothiocyanate-functionalized RGD peptides for tailoring cell-adhesive surface patterns**." Biomaterials **29**(20): 3004-3013.

Kruger, J., K. Singh, A. O'Neill, C. Jackson, A. Morrison and P. O'Brien (2002). "**Development of a microfluidic device for fluorescence activated cell sorting**." Journal of Micromechanics and Microengineering **12**(4): 486-494.

Kuntaegovvdanahalli, S. S., A. A. S. Bhagat, G. Kumar and I. Papautsky (2009). "Inertial microfluidics for continuous particle separation in spiral microchannels." Lab on a Chip **9**(Copyright 2010, The Institution of Engineering and Technology): 2973-2980.

Kwon, K. W., S. H. Lee, B. Kim, M. C. Park, P. Kim and K. Y. Suh (2007). **Label-free, microfluidic separation of human breast carcinoma and epithelial cells by adhesion difference**, Lyon, France, Inst. of Elec. and Elec. Eng. Computer Society.

Lang, W. (1996). "**Silicon microstructuring technology.**" Materials Science and Engineering R: Reports **17**(1): 1-55.

Li Jeon, N., H. Baskaran, S. K. W. Dertinger, G. M. Whitesides, L. Van De Water and M. Toner (2002). "**Neutrophil chemotaxis in linear and complex gradients of interleukin-8 formed in a microfabricated device.**" Nat Biotech **20**(8): 826-830.

Liu, Y.-J., S.-S. Guo, Z.-L. Zhang, W.-H. Huang, D. Baigl, M. Xie, Y. Chen and D.-W. Pang (2007). "**A micropillar-integrated smart microfluidic device for specific capture and sorting of cells.**" ELECTROPHORESIS **28**(24): 4713-4722.

Luo, Y. and R. N. Zare (2008). "**Perforated membrane method for fabricating three-dimensional polydimethylsiloxane microfluidic devices.**" Lab on a Chip **8**(10): 1688-1694.

Malic L, Herrmann M, Hoa X and T. M. (2007). "**Current State of Intellectual Property in Microfluidic Nucleic Acid Analysis**." Recent Patents on Engineering **1**.

Manbachi, A., S. Shrivastava, M. Cioffi, C. Bong Geun, M. Moretti, U. Demirci, M. Yliperttula and A. Khademhosseini (2008). "**Microcirculation within grooved substrates regulates cell positioning and cell docking inside microfluidic channels.**" Lab on a Chip **8**(5): 747-754.

Maraldo, D. and R. Mutharasan (2007). "**Optimization of antibody immobilization for sensing using piezoelectrically excited-millimeter-sized cantilever (PEMC) sensors**." Sensors and Actuators B: Chemical **123**(1): 474-479.

Marek, R., M. Caruso, A. Rostami, J. B. Grinspan and J. D. Sarma (2008). "**Magnetic cell sorting: A fast and effective method of concurrent isolation of high purity viable astrocytes and microglia from neonatal mouse brain tissue**." Journal of Neuroscience Methods **175**(1): 108-118.

Miltenyi S, Muller W, Weichel W and Radbruch A (1990). "**High gradient magnetic cell separation with MACS**." Cytometry **11**: 231-238.

Nagrath, S., L. V. Sequist, S. Maheswaran, D. W. Bell, D. Irimia, L. Ulkus, M. R. Smith, E. L. Kwak, S. Digumarthy, A. Muzikansky, P. Ryan, U. J. Balis, R. G. Tompkins, D. A. Haber and M. Toner (2007). "**Isolation of rare circulating tumour cells in cancer patients by microchip technology**." Nature **450**(7173): 1235-U1210.

Nilsson, A., F. Petersson, H. Jonsson and T. Laurell (2004). "**Acoustic control of suspended particles in micro fluidic chips**." Lab on a Chip **4**(2): 131-135.

Olbrich, K. C., T. T. Andersen, F. A. Blumenstock and R. Bizios (1996). "**Surfaces modified with covalently-immobilized adhesive peptides affect fibroblast population motility**." Biomaterials **17**(8): 759-764.

Pappas, D. and K. Wang (2007). "**Cellular separations: A review of new challenges in analytical chemistry**." Analytica Chimica Acta **601**(1): 26-35.

Plouffe, B. D., T. Kniazeva, J. E. Mayer, Jr., S. K. Murthy and V. L. Sales (2009). "**Development of microfluidics as endothelial progenitor cell capture technology for cardiovascular tissue engineering and diagnostic medicine."** FASEB J. **23**(10): 3309-3314.

Plouffe, B. D., D. N. Njoka, J. Harris, J. Liao, N. K. Horick, M. Radisic and S. K. Murthy (2007). "**Peptide-mediated selective adhesion of smooth muscle and endothelial cells in microfluidic shear flow.**" Langmuir **23**(9): 5050-5055.

Poletaev, A. I., N. V. Gnuchev and A. V. Zelenin (1987). **"Flow-Cytometry and cell sorting - current status and prospect for application in molecular biology (brief review)**." Molecular Biology **21**(1): 17-20.

Qin, M., S. Hou, L. Wang, X. Feng, R. Wang, Y. Yang, C. Wang, L. Yu, B. Shao and M. Qiao (2007). "**Two methods for glass surface modification and their application in protein immobilization**." Colloids and Surfaces B: Biointerfaces **60**(2): 243-249.

Saliba, A.-E., L. Saias, E. Psychari, N. Minc, D. Simon, F.-C. Bidard, C. Mathiot, J.-Y. Pierga, V. Fraisier, J. Salamero, V. Saada, F. Farace, P. Vielh, L. Malaquin and J.-L. Viovy (2010). "**Microfluidic sorting and multimodal typing of cancer cells in self-assembled magnetic arrays.**" Proceedings of the National Academy of Sciences **107**(33): 14524-14529.

Schena, E. M. (1999). **DNA Microarrays: A Practical Approach.** Oxford, UK, Oxford University Press.

Schirhagl, R., I. Fuereder, E. W. Hall, B. C. Medeiros and R. N. Zare (2011). "**Microfluidic purification and analysis of hematopoietic stem cells from bone marrow.**" Lab on a Chip.

Shaikh-Mohammed, J., M. Li, D. Terala and M. J. McShane (2004). **Integrated Micro/Nano-Fabrication of Cell Culture Scaffolds with Selective Cell Adhesion and Fluorescent Indicators**, San Jose, CA., United states, SPIE.

Sin, A., S. K. Murthy, A. Revzin, R. G. Tompkins and M. Toner (2005). "**Enrichment using antibody-coated microfluidic chambers in shear flow: Model mixtures of human lymphocytes.**" Biotechnology and Bioengineering **91**(7): 816-826.

Studer, V., R. Jameson, E. Pellereau, A. Pepin and Y. Chen (2004). **A microfluidic mammalian cell sorter based on fluorescence detection,** Elsevier.

Takagi, J., M. Yamada, M. Yasuda and M. Seki (2005). "**Continuous particle separation in a microchannel having asymmetrically arranged multiple branches.**" Lab on a Chip **5**(7): 778-784.

Takayama, S., E. Ostuni, P. LeDuc, K. Naruse, D. E. Ingber and G. M. Whitesides (2001). "**Laminar flows: Subcellular positioning of small molecules**." Nature **411**(6841): 1016-1016.

Wang, M. M., E. Tu, D. E. Raymond, J. M. Yang, H. Zhang, N. Hagen, B. Dees, E. M. Mercer, A. H. Forster, I. Kariv, P. J. Marchand and W. F. Butler (2005). "**Microfluidic sorting of mammalian cells by optical force switching.**" Nature Biotechnology **23**(1): 83-87.

Wei, H., B.-h. Chueh, H. Wu, E. W. Hall, C.-w. Li, R. Schirhagl, J.-M. Lin and R. N. Zare (2011). **"Particle sorting using a porous membrane in a microfluidic device.**" Lab on a Chip **11**(2): 238-245.

Westcott, N. P., B. M. Lamb and M. N. Yousaf (2009). "**Electrochemical and chemical microfluidic gold etching to generate patterned and gradient substrates for cell adhesion and cell migration.**" Analytical Chemistry **81**(9): 3297-3303.

Whitesides, G. M., E. Ostuni, S. Takayama, X. Jiang and D. E. Ingber (2001). "**Soft lithography in biology and biochemistry**." Annual Review of Biomedical Engineering **3**(1): 335-373.

Wilbur, J. L., A. Kumar, E. Kim and G. M. Whitesides (1994). **"Microfabrication by microcontact printing of self-assembled monolayers**." Advanced Materials **6**(7-8): 600-604.

Xia, Y. and G. M. Whitesides (1997). "**Extending Microcontact Printing as a Microlithographic Technique**." Langmuir **13**(7): 2059-2067.

Yamada, M. and M. Seki (2005). "**Hydrodynamic filtration for on-chip particle concentration and classification utilizing microfluidics.**" Lab on a Chip **15**: 1233-1239.

Yu-Cheng, L. and J. Chun-Ping (2002). "**Mechanism of hydrodynamic separation of biological objects in microchannel devices.**" Lab on a Chip **2**(3): 164-169.

Zhang, Z. L., C. Crozatier, M. Le Berre and Y. Chen (2005). "**In situ bio-functionalization and cell adhesion in microfluidic devices."** Microelectronic Engineering **78-79**: 556-562.

Zhu, J., T. R. J. Tzeng and X. Xuan (2010). **"Continuous dielectrophoretic separation of particles in a spiral microchannel."** Electrophoresis **31**(8): 1382-1388.

Chapter 4. High throughput multilayer microfluidic particle separation platform using embedded thermoplastic-based micro-pumping

4-1 Connecting text

This chapter reports on the development of the microfluidic chip for size-based separation of particles/cells as the first main goal of this thesis. The design, fabrication details and application of the chip for particle separation have been demonstrated in this chapter.

This research resulted in the following contributions:

Patent: Tohid Fatanat Didar, K. Li, M. Tabrizian and T. Veres, (2013), Integrated microfluidic system for size based particles/cells separation.

Journal paper: Tohid Fatanat Didar*, K. Li*, M. Tabrizian and T. Veres, (2012), High throughput multilayer microfluidic particle separation platform using embedded thermoplastic-based micro-pumping, Lab on Chip, Accepted (*equal contribution).

4-2 Abstract

We present an integrated thermoplastic elastomer (TPE) based multilayer microfluidic device with embedded peristaltic micropump and through-holes membrane for high throughput particle sorting and separation. Fluidic and pneumatic layers of the device were fabricated using hot-embossing lithography and commercially available polycarbonate membranes were successfully sandwiched between two thermoplastic elastomer fluidic layers integrated to a peristaltic micropumping layer. The integrated peristaltic micropump induces turbulence at the top-microfluidic layer ring, which successfully avoids particles aggregation and membrane blocking, even at nano-range size. We present herein the general design of the device structure and pumping characteristics for three devices with membrane pore sizes of 10 μm, 5 μm and 800 nm. By using this design we have successfully demonstrated separation efficiency as high as 99% of the polystyrene microbeads with different sizes and most importantly the separation of 390 nm particles from 2 μm beads was achieved. Using this device, we were also able to separate red blood cells with size of about 6–8 μm from osteoblasts typically larger than 10 μm to demonstrate the potential applicability of this platform for biological samples. The produced microfluidic chip operating at flow rates up to 100 μl/min allows us to achieve efficient high-throughput sorting and separation of target particles/cells.

4-3 Introduction

Particle sorting involves excluding desired particles from a suspension based on their properties. Many techniques have been developed for particle sorting which can be categorized into active and passive approaches (Sun Min, Sung Hoon et al. 2008, Didar and Tabrizian 2010, Lenshof and Laurell 2010). Active separation employs physical forces from external sources such as dielectrophoretic (Barbulovic-Nad, Xuan et al. 2006), optical (Wang, Tu et al. 2005, Jonas and Zemanek 2008, Lin, Chen et al. 2008), magnetic (Dirican, Ozgun et al. 2008, Zhou, Wang et al. 2010, Hoshino, Huang et al. 2011, Issadore, Shao et al. 2011), or acoustic forces (Nilsson, Petersson et al. 2004). However, most of them are complicated and expensive due to the need for external fields, and often additional steps which make the device fabrication complex and difficult to integrate with conventional Lab-on-Chip (LOC) components. On the other hand, passive separation approaches do not utilize external forces but rely on microfluidic behavior and the interaction of the fluid with the geometries of the microfluidic chip. Passive methods include obstacle induced separation, hydrodynamic filtration (Huang, Cox et al. 2004, Takagi, Yamada et al. 2005), pinched flow fractionation (Bhagat, Hou et al. 2011), inertia and dean flow separation (Kuntaegovvdanahalli, Bhagat et al. 2009, Zhu, Tzeng et al. 2010). Pinches, weirs and posts are common microfluidic obstacle components which are introduced in microfluidic channels to act as filters, preventing particles from entering certain areas. Physical filtering is among the few separation techniques that do not require pre-processing steps or external actuation.

For size-based separation, commercially available membranes can be embedded in microfluidic chips. As such in addition to being cost effective, they could easily be integrated into a miniaturized instrument. However there are major limitations using embedded filters for separation applications in microfluidic devices. These limitations can be divided into fabrication issues and operational drawbacks.

From the fabrication point of view, the main limitation is in non-conformal bonding between the commercially available membranes and microfluidic layers (e.g. PDMS or glass based devices). In 2008, Luo *et al.* (Luo and Zare 2008) reported

fabrication of PDMS based membranes that were easily sandwiched between PDMS substrates, although it required complicated fabrication steps and the minimum pore sizes achieved were around 7 microns. Later, the same group produced smaller pore size membranes, around 3 microns, by aligning two or three membrane layers with a small gap on top of each other (Wei, Chueh et al. 2011). This requires precise control during the aligning step and a small misalignment would significantly change the pore size. Conversely, the multiple membrane approach increases the overall depth of the filtering layer, which could cause membrane occlusion during the operation.

For the operation of the device, membrane blocking and low separation flow rates are the main concerns. Laminar flow in microfluidic channels cause particle clogging and membrane blocking. Increasing the shear force of the flow, and/or the pressure difference across the membrane could be implemented to delay the clogging effect or to drive the flow components through the partially clogged perforation. Wei *et al*. (Wei, Chueh et al. 2011) proposed the use of a PDMS membrane with pores in defined areas where the membrane acts simultaneously as both a filter and a valve. The dual function of the membrane allows the chip's user to stop irreversible clogging by sequential flushing and filtering. By using this technique, devices with 10 μm pore size membranes were reported for particle/cell separation at flow rates of around 3 μl/min. Obviously, the operating flow rate is quiet low which limits the developed devices application for high throughput particles/cells sorting.

Micropumps and microvalves are two important components of microfluidic devices and their integration has been actively pursued over the past few years to entail diverse functionality. Various actuation mechanisms such as piezoelectric, thermo-pneumatic, pneumatic, and electromagnetic has been explored (Zhang, Xing et al.). Among them, peristaltic micropumps driven by injecting compressed air (pressure mode) or vacuum (vacuum mode) have attracted considerable interest. Most of the pneumatic, membrane-based microvalves and micropumps reported to date are made of PDMS substrates. However, the large scale use of LOC systems requires fabrication technologies

and materials amenable for rapid and low-cost fabrication, simple procedures for bonding as well as stable surface treatments for bio-molecule capture and immobilization. Hence, it is desirable to develop new technologies for rapid fabrication of microfluidic devices at low cost, based on thermoplastic elastomers (TPEs) and thermoforming processes namely hot embossing and injection moulding. TPEs have been recently used as biocompatible substrates for cellular adhesion and guidance, prototyping of miniaturized microfluidic systems for patterning of DNA arrays as well as complex microfluidic devices. This was achieved due to TPE's remarkable properties such as soft fabrication, raw material cost and speed of processing which are comparable or superior to PDMS in many aspects. TPE can form water-tight bonding on the thermal plastic substrates similar to polymethylmethacrylate (PMMA) and cyclo-olefin polymers (COP). Therefore, in contrast to PDMS substrates requiring oxygen plasma treatment for binding, TPE can be easily bonded with thermoplastic materials to form fully thermoplastic-based microfluidic devices.

Herein, we report on fabrication of a fully thermoplastic-based multilayer microfluidic device integrating a pneumatic peristaltic micropump and microvalves with embedded commercially available polycarbonate (PC) membrane filters. Pumping characteristics and different pumping modes of the peristaltic micropump are introduced and their separation efficiency is discussed. Separation of micro beads using 10 μm membrane pore size applying two different pumping modes is demonstrated and each mode's separation efficiency is discussed. Separation of 390 nm particles from 2 μm beads with a separation efficiency of 99% is also presented. To demonstrate the applicability of the device to separate cells of different sizes, separation of red blood cells of 6 to 8 microns from osteoblasts (larger than 10 microns) is also demonstrated.

4-4 Materials and methods

4-4-1 Materials

TPE sheets with initial thickness of 300 μm and 1 mm were extruded at a temperature of 165^{o}C from the as-received pellets of Mediprene of 400M (GLS Corp., McHenry, IL, USA). SU8 photoresist (GM1070 or GM1075) was

purchased from Gersteltec, Pully, Switzerland. Photo-plotted transparent films printed at a resolution of 36000 dpi from NP, Montreal, Canada were used as photo-masks in the fabrication of molds by using standard photo-lithography process. The molds used in hot-embossing were treated by vapour phase deposition of trichloro (1H, 1H, 2H, and 2H-) perfluoro-octyl)silane (97%, Sigma-Aldrich Co., St. Louis, MO, USA). The hot-embossing process described later on was performed with an EVG520 system (EV Group, Schärding, Austria). Isopore polycarbonate (PC) with pore size of 10um, 5um, and 800 nm were purchased from Millipore (Whitby, ON, Canada). Fluorescence micro/nano beads were purchased from Thermo-Scientific (Fremont, CA, USA).

4-4-2 Integrated multilayer microfluidic design

Figure 4-1 shows a schematic of the microfluidic design. Figure 4-1a is a 3D representation of the design and figure 4-1b depicts a cross section of the device in the circular channel area. Different layers of the device have also been shown in figure 4-1c. The design consists of four layers, i.e., the bottom microfluidic channel layer (BFL), a PC porous membrane layer (ML), the top microfluidic layer (TFL) and a pneumatic air control layer (PL). Bottom fluidic layer (shown in yellow) represents the bottom microfluidic channel with 1 mm width and 100 μm depth. BFL consists of a circular channel, a straight channel and an outlet. Supporting posts (200 μm in diameter and 100 μm in height with 1 mm spacing) were fabricated in the middle of the bottom fluidic channel to avoid collapse of the membrane layer on the bottom channel. The TFL, colored by blue, consists of a straight channel for in taking source fluid and outgoing retentive and a circular channel for filtration that is aligned with its corresponding circular ring on the BFL. TFL has three access holes that can be used as inlets or outlets; depending on the peristaltic micro-pumping configuration. The PC porous membrane is sandwiched between the bottom and top microfluidic layers. The liquid exchange between the top and bottom microfluidic channels can only occur in the circular channel area. The pneumatic air control layer is aligned with the top microfluidic layer. The air chamber of the pneumatic air control layer is designed in a fanlike sector which is wider than the channel width of the top microfluidic channel. The

top and bottom microfluidic layers, as well as the air control layers, are replicated from Si wafer patterned with SU8 resist (SU8 molds) by using the hot-embossing technique.

In the introduced design, the peristaltic micropump is operated by the activation of four membranes disposed in a circular fashion. Pumping rate can be increased by increasing the total length of the activation membrane (an increment of the displacement of a single stroke volume) within a relative compact area. This also allows operation of the micropump at high flow rates with higher dynamic back pressure mode, which is very useful in applications requiring higher maximum backpressure.

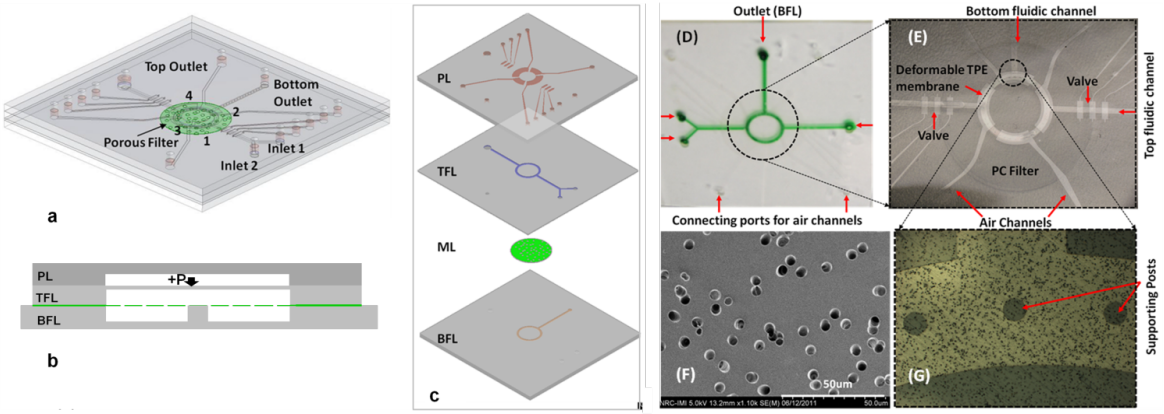

Figure 4-1: Multilayer TPE microfluidic design and fabrication. a) 3D representation of the device, b) cross section of the device in the circular channel area, c) different layers of the microfluidic chip, starting from the bottom: bottom fluidic layer (BFL), membrane layer (ML), top fluidic layer (TFL) and pneumatic air layer or pumping layer (PL), d) a picture of the microlfuidic device showing different access holes, both the top and bottom fluidic channels were filled with green colored ink, (e) magnified image of the circular channel area, f) scanning electron microscope (SEM) image of an embedded polycarbonate membrane with 5 µm pore sizes, g) optical microscope image of the membrane layer placed on the bottom fluidic layer at the circular channel area intersection with the bottom fluidic channel.

4-4-3 Fabrication of the microfluidic device

All of the microfluidic layers (TFL, BFL and PL) were fabricated on TPE by hot-embossing process on an EVG520 system (St. Florian am Inn, Austria) using SU8 molds. The SU8 molds were produced using standard photolithography techniques. The patterns for the device were printed on transparent films at a resolution of 36000 dpi which were used as photo masks. A layer of SU-8 (GM1070 or GM1075) photoresist with a thickness of 100 µm was spin-coated

onto a 4 inch silicon wafer, followed by pre-bake at 40 ^{o}C for 30 min and at 120 ^{o}C for 30 min. It was then exposed to UV light using an EVG 6200 mask aligner through a transparent mask, followed by a post bake at 95 ^{o}C for 1 hour. The photoresist development was then performed in propylene glycol monomethyl ether acetate and the wafer was rinsed with isopropanol and dried with a stream of nitrogen gas. It was then hard-baked at 160 °C for 2 hours. The SU-8 molds were finally treated with trichloro (1H, 1H, 2H, and 2H-perfluorooctyl) silane using vapor phase deposition to obtain an anti-adhesive layer and to facilitate the release of thermoformed TPE from the mold after hot embossing.

The maximum operating temperature and embossing force of the EVG520 was 200 ^{o}C, and 40 KN, respectively. Heating and cooling modules were active on both upper and lower plates at a rate of 20 and 10 ^{o}C/min, respectively. The base pressure inside the chamber was about 0.1 mbar. Typical embossing conditions were: 5 min at 150 ^{o}C with 10 KN applied force for the bottom microfluidic and pneumatic control layers with a starting thickness of 1 mm. For fabrication of the top microfluidic channel, the starting thickness of TPE sheets was 0.3 mm. By adjusting the hot-embossing condition as well as the starting thickness of the TPE sheets, the residue TPE thickness of the top microfluidic channel was controlled around 100 μm in order to avoid collapse of the top microfluidic channel during the operation of the peristaltic micropump and microvalves (up to 15 psi).

Figure 4-1D shows a picture of the fabricated microfluidic device. Strong irreversible bonding between the porous filter and TPE layers was achieved and no leakage was observed during the flow testing. Figure 4-1F shows a scanning electron microscope (SEM) image of a polycarbonate membrane with 5 μm diameter pore sizes. Figure 4-1G depicts an optical microscope image of the bottom microfluidic channel with supporting pillars after placing the PC porous membrane on top of the channel.

Since all the necessary layers were fabricated on TPE, watertight bonding among the TPE layers could easily be formed at room temperature without any additional plasma or thermal treatment. The assembling process of the multilevel

microfluidic device was straightforward. Once the BFL was fabricated, the PC porous membrane was placed on top of the TPE layer to cover the circular channel area. Then the TFL, facing down, is aligned on top of the BFL layer under an optical microscope to ensure that the circular channel on top layer is well aligned with its counterpart on the bottom layer. This is followed by alignment of the PL on top of the TFL using an optical microscope to ensure the air chambers are well aligned with the circular channel of the top microfluidic layer. Finally a hard thermoplastic cover (Zeonor 1060R) with connecting ports is bonded on top of the assembled device.

4-4-4 Operation of the embedded peristaltic micropump

Operation of the integrated peristaltic micropump was carried out on a homemade 12-channel pneumatic control manifold. It consisted of 24 electromagnetic valves (EMV) controlled by Lab View Software. The maximum output pressure of the manifold was 30 psi. When the air chamber in the pneumatic control layer is injected with compressed air of a few psi, the residue layer of the TPE is deformed, pushing the liquid underneath forward and backward. A net flow can be generated when more than three membranes are operated in a sequential way and the flow direction is dependent on the membranes activation sequence. That's the typical working principle of a peristaltic micropumps based on three microvalves' configuration. As shown in Figures 4-2 a and b, a typical peristaltic micropump cycle consists of following different steps: 1) all four chambers are pressurized, therefore all four TPE membranes are deformed; 2) pressure is released from chamber 1 which is closer to the desired inlet access hole and membrane 1 relaxes back to its initial state aspirating the liquid from the inlet towards the direction of the membrane 1; 3) chamber 1 is kept in the vent state, and the pressure inside chambers 2 and 3 are simultaneously released, the deformed TPE membranes 2 and 3 relax back to their initial state, resulting in further liquid aspiration from the inlet towards the direction of membrane 1 and then to membranes 2 and 3; 4) chambers 1, 2 and 3 are kept in the vent state and pressure inside chamber 4 is released, the liquid is therefore aspirated further towards membrane 4; 5) chambers 2, 3, and 4 are

in vent state and chamber 1 is pressurized pushing half of the stroke volume of the liquid back to the inlet direction and the other half towards the outlet direction; 6) chamber 1 is kept in pressurized state, chambers 2 and 3 are simultaneously pressurized, pushing the liquid towards the membrane 4 and then towards the outlet direction; 7) chambers 1, 2 and 3 are kept in the pressure state and chamber 4 is pressurized, pushing the liquid towards the outlet; 8) releasing pressure in chamber 1, restarts to aspirate the liquid from the inlet. Repeating the operation cycle shown in Fig. 4-2b allows for continuously pump the liquid from the inlet to the outlet. For the case of the microfluidic design presented herein, the microvalves operated by pneumatic air pressure were integrated on top of the microfluidic channel. Once the sample containing the particles that need to be size separated is introduced on the top circular channel, and the access valve is closed, the sample is then pumped from the inlet to the direction of the circular channel and then pass through the porous filter and eventually the smaller particles are pushed to the bottom outlet. Because of the turbulent agitation of the peristaltic operation mentioned above, the smaller microbeads can efficiently pass through the porous filter to the bottom microfluidic channel and to the bottom outlet. The bigger microbeads remain on top of the filter. To avoid clogging and ensure an efficient filtering, after a certain time of circulation on the top circular channel, the liquid containing the microbeads larger than the membrane pore size are washed away. The washing liquid that is introduced from inlet 2 is pumped into the circular channel area, and passed through the porous PC filter and then to the bottom outlet to make sure that all the small particles have been pumped to the bottom outlet. Then the valve between the circular channel and the top outlet is opened and therefore the bigger particles are removed from the surface of the PC filter and pumped out from the top outlet. By repeating these two procedures, we can continue the separation of smaller particles without clogging the porous PC filter.

4-4-5 Sample preparation and analysis

15 μm green and 2 μm blue fluorescence microbeads suspension was prepared in deionized water with a concentration of 5×10^4 p/ml each. Mixed suspensions

were then prepared with equal volumes of each suspension and used in the experiments. For nano-particles' separation red fluorescence 390 nm particles were prepared at a concentration of 4.5×10^5 p/ml and mixed with the 2μm blue fluorescence bead suspension at a concentration of 1.5×10^4 p/ml.

Initial and collected samples at each outlet were analyzed with an inverted fluorescence microscope (Nikon TE 2000-E). Collected microbeads were further analysed using a Fluorescence Activated Cell Sorting (FACS) system. Separated nano size particles were also assessed using a Multi Angle Particle Sizer (Brookhaven Instruments Corporation).

Osteoblasts were cultured in *Dulbecco modified eagle medium* (DMEM) 10% fetal bovine serum (FBS), 1% penicillin streptomycin (PS) in cell culture incubator (at 37 °C, 5% CO2) and trypsinized prior to all experiments.

4-5 Results and discussion

4-5-1 Pumping characteristics of the device

Device operation and flow rates for three different devices using 10 μm, 5 μm and 800 nm membrane pore sizes were investigated. 9 psi pressure with a pumping frequency of 3Hz was applied and flow rates at the top and bottom outlets were measured simultaneously (Figure 4-2c). The overall flow rate at the inlet channel in all three devices was about 100 μl/min. This flow rate is much higher compared to previously reported microfluidic devices for primary cells purification (3 μl/min using a 10μm pore size membrane). As depicted in figure 4-2c, the top outlet has a higher flow rate which is expected due to the higher hydrodynamic resistance of the membrane layer. We did not observe significant variation in the top and bottom outlets flow rates using different membrane pore sizes. The slight changes observed (+/- 3 μl/min) in the flow rate can be explained by the very small differences in the top and bottom channel width in the circular area due to alignment differences and also because of small changes in the membranes porosity.

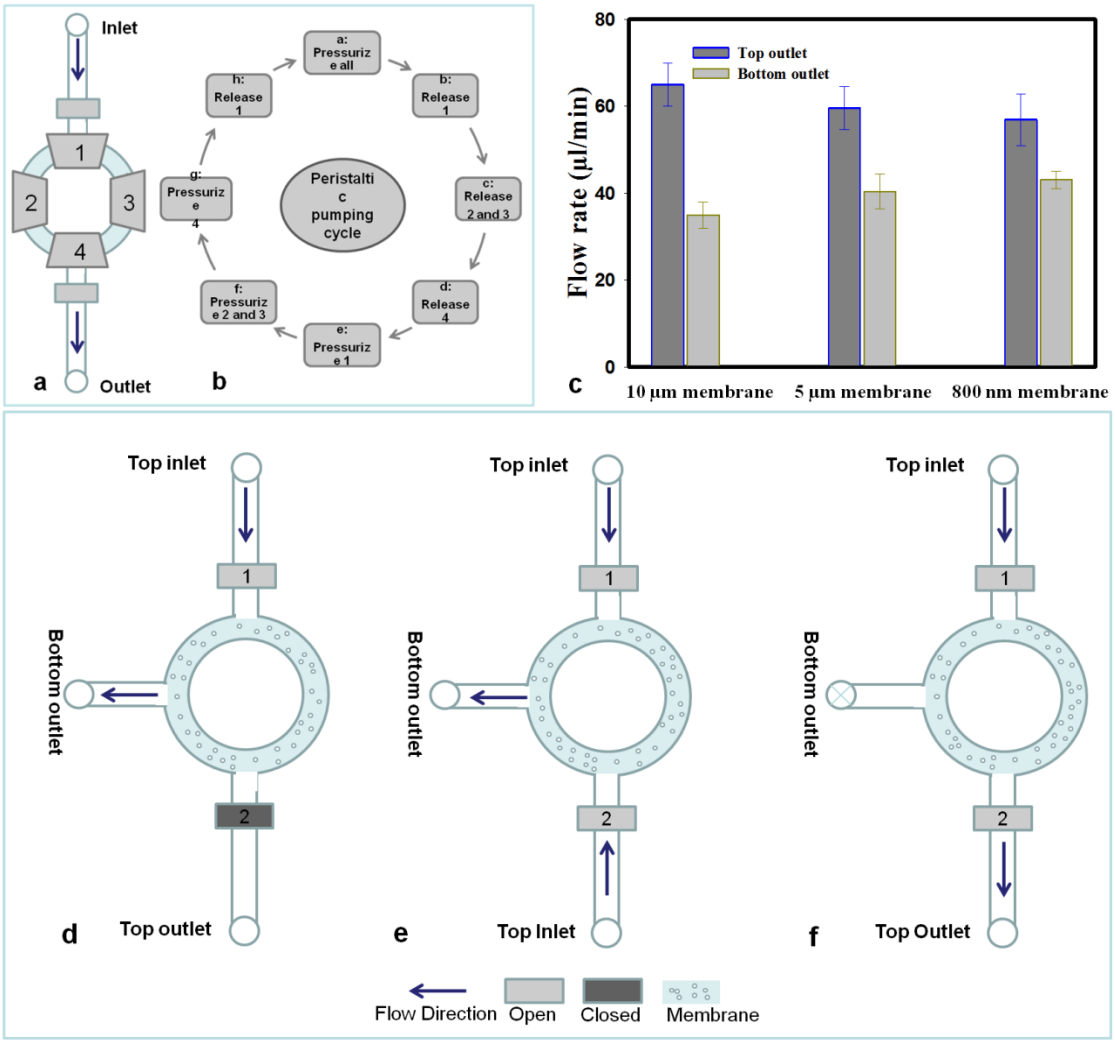

Figure 4-2: a and b) depict a schematic presentation of the circular channel with 4 pneumatic layers for peristaltic micropumping with eight different steps of the peristaltic pumping cycle, c) measured flow rates for three different chips with 10 µm, 5 µm and 800 nm pore size at the top and bottom outlets applying a pressure of 9psi with a pumping frequency of 3Hz, d-f) three different pumping configurations: top inlet and bottom outlet are used while top outlet is closed (d), both top access holes are used as inlets and bottom access hole as outlet (e) and bottom outlet is closed and there is flow only at the top microfluidic layer (f).

4-5-2 Application for microbeads separation

Separation of 2 µm and 15 µm polystyrene micro-beads populations was performed using the 10 µm pore size membrane by applying two different pumping modes. The separation efficiency, defined as the ratio of the number of target particles to the total number of particles collected at each outlet, was then investigated for both conditions (Wei, Chueh et al. 2011).

In the first configuration, the top outlet valve was closed and bead mixture entered from the top inlets and passes through the membrane to the bottom outlet (Figure 4-2d). This was followed by washing of the membrane using the same pumping configuration to remove any remaining small beads. At the end, the top outlet valve was opened and the 15 μm beads exit from the top outlet (figure 4-2f). 9 psi of compressed air pressure with a pumping frequency of 3Hz was applied in the pumping layer resulting in an overall applied flow rate of 100 μl/min. Figure 4-3l shows collected beads concentration at each outlet using the aforementioned pumping configuration. Figures 4-3a-c show selected images of the initial mixture and collected beads at each outlet channel for the first pumping mode.

For the second pumping configuration, both top fluidic layer's access holes were used as inlets (Figure 4-2e). The beads mixture entered from the initial inlet and pure solution containing no beads was introduced from the other top access hole. 9psi of air pressure with a 3 Hz pumping frequency was used for this purpose and 2 μm beads were collected at the bottom outlet (Movie S4-1). After pumping the mixture, a washing step was performed using the same pumping configuration to remove any remaining small beads. Finally, by changing the pumping mode, flow was directed towards the top outlet (Figure 4-2f) and 15 μm beads were collected at this outlet. Figure 4-3m depicts the collected beads concentration using this pumping mode. Selected corresponding fluorescence images are also shown in figures 4-3d and 3e. Collected samples analysis using FACS machine for the second pumping mode has been shown in figures 4-3f-g. These results depict successful separation of beads and confirm the fluorescence microscopy results.

In both pumping modes no 15 μm beads were collected from the bottom outlet. Using the first pumping mode small beads got trapped at the entrance of top outlet channel. Therefore about 15% of the collected sample at the top outlet contained 2 μm beads. This drawback was addressed by changing the pumping mode to the second mode in which the incoming flow from the top outlet channel stopped smaller beads from entering into the top outlet channel. Using the

second pumping mode, greater than 99% separation efficiency was achieved for the separation of 2 μm beads from 15 μm beads.

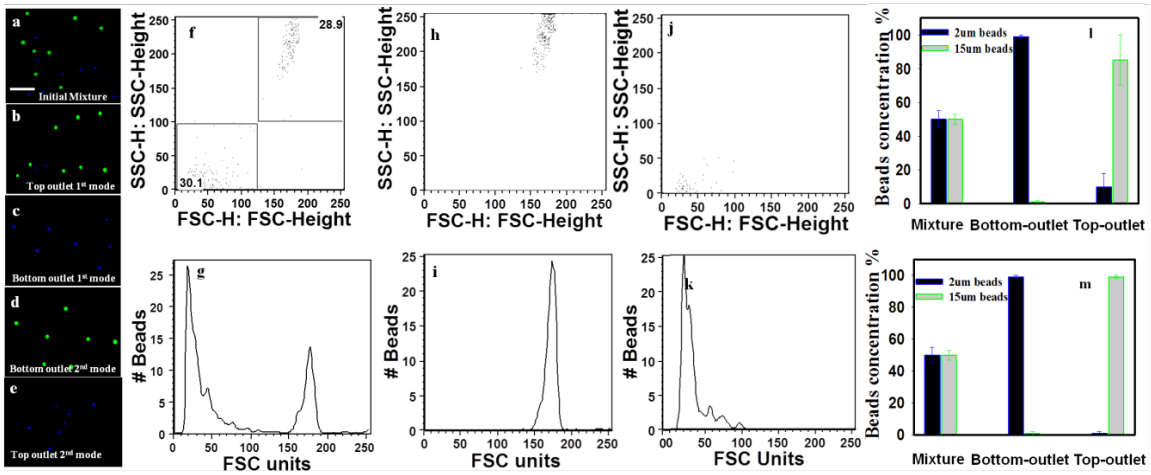

Figure 4-3: Microbeads separation results. a-e) selective fluorescence microscopy images of the initial mixture and collected samples at the top and bottom outlet applying two different pumping modes, f and g) FACS results for size distribution of the initial mixture, h and i) FACS results for size distribution of collected sample at the top outlet applying the second pumping mode, j and k) FACS results for size distribution of collected sample at the bottom outlet applying the second pumping mode, l and m) show mixed beads initial concentration and collected beads concentration at the top and bottom outlet channels applying the first (l) and second (m) pumping modes respectively. Error bars represent standard deviation for the concentration analysis using 10 different fluorescence microscopy images.

4-5-3 Application for separation of sub-micron size particles

The original design of the device allowed for the separation of 390 nm from 2 μm beads using 800 nm membrane pore size and the second pumping strategy (Figure 4-2e). After washing the membrane to remove any remaining nano particles, 2 μm beads were collected at the top outlet applying the pumping mode shown in figure 4-2f. The selective fluorescence microscopy images of initial mixture, bottom outlet and top outlet are shown in figures 4a, 4b and 4c respectively. Collected samples from the bottom outlet were analyzed using a particle sizer and the results showed a size distribution of 392 nm with a standard deviation of 5 nm. These results indicated an efficiency of higher than 99% for the separation of 390 nm particles from 2 μm beads (Figure 4-4d).

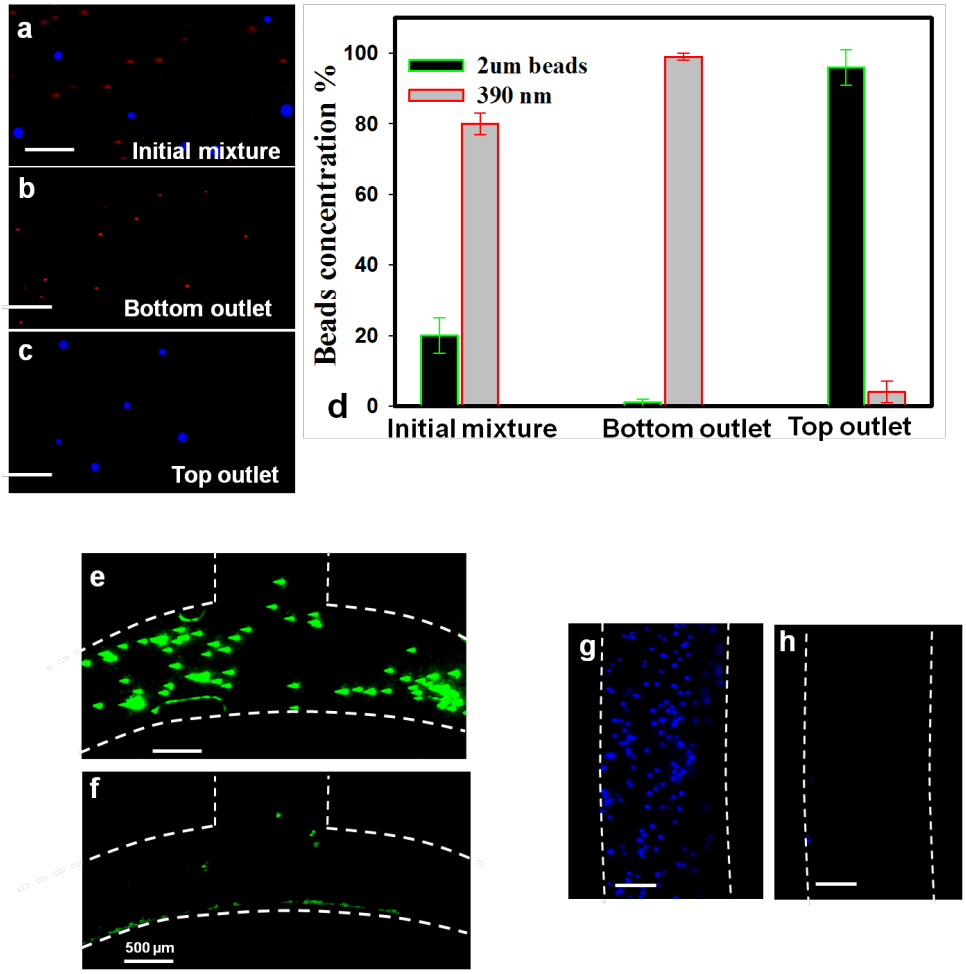

Figure 4-4: Results for separation of 390 nm particles and 2 µm beads. a, b and c) are selected fluorescence microscopy images of initial mixture and collected samples at each outlet. d) depicts concentration of each particle in the initial mixture and the collected samples from bottom and top outlets. Error bars represent standard deviation for the concentration analysis using 10 different fluorescence microscopy images. e and f) represent the 10 µm pore size membrane surface after pumping and washing steps, respectively (used for separation of 2 µm beads from 15 µm beads). Both images show the same area of the circular channel. g and h) show the 800 nm pore size membrane surface after the pumping and washing steps, respectively (used for separation of 390 nm beads from 2 µm beads). Both images show the same area of the circular channel. As shown in these images bigger particles can be successfully removed and collected from the membrane surface without any aggregation or blocking.

4-5-4 Turbulent washing efficiency and membrane clogging

As mentioned, particle aggregation and membrane clogging is the main operational limitation for membrane based microfluidic separation devices as a result of laminar flow in microfluidic chips. To overcome this limitation, a peristaltic micropump was embedded inside the chip to create necessary turbulence to avoid blocking of the membrane, but also provide the ability to

rapidly change the flow direction for optimum separation. Fluorescence images in figure 4-4e-h show the membrane surface area in the circular channel at different steps of the separation process for the separation of 2 µm-15 µm and 2 µm-390 nm particles. Figure 4-4e depicts the presence of 15 µm beads on membrane surface after the pumping step using the 10 µm pore size chip. The same surface is shown in figure 4-4f after the washing step where only a few beads could be found on the membrane surface. Figures 4-4g and 4-4h are fluorescence images of the 800 nm membrane surfaces in the circular channel after collecting 390 nm particles and washing step, respectively. Almost all of the 2 µm beads attached to the membrane surface at this area could be detached and collected. These results indicate that the induced turbulence enabled removing undesirable particles from the surface allowing for the repetitive use of the chip without further cleaning of the membrane area.

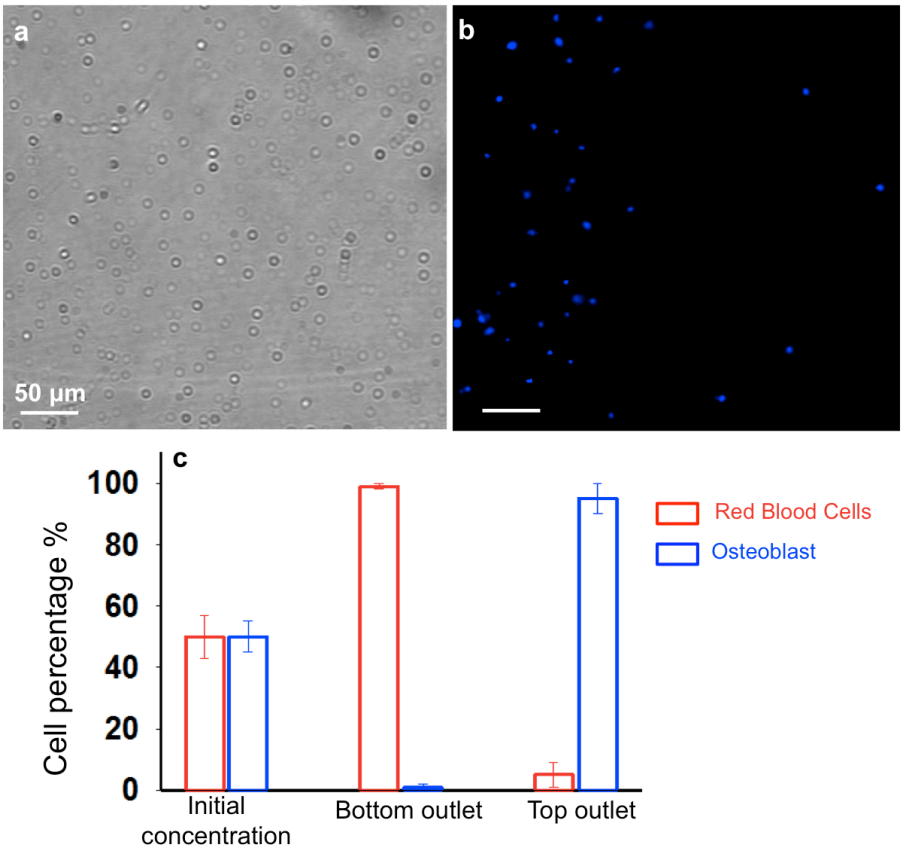

Figure 4-5: a) Optical microscope image of collected red blood cells from the bottom outlet. b) collected osteoblasts from the top outlet live stained with Cy5 conjugated dye. No osteoblast cells were collected at the bottom outlet.

4-5-5 Application for cell separation

To demonstrate that the device can potentially be used for the separation of biological micoparticles such as cells, red blood cells (6 to 8 microns) and osteoblasts (larger than 10 microns) were mixed at a concentration of 10^5 cells/ml each. Osteoblasts were live stained with a fluorescence dye prior to mixing. Second pumping mode (figure 4-2e) with 10 μm pore size membrane was implemented to separate and collect red blood cells from the bottom and osteoblasts from top outlets (Movie S4-2). Analysis of collected samples showed that more then 99% of the cells collected at the buttom outlet were red blood cells and the top outlet contained greater than 95% osteoblast cell types (Figure 4-5).

4-6 Conclusions

A microfluidic microparticle separation platform with an embedded peristaltic micro-pumping system and commercially available membranes was presented for particles/cells separation. The introduced multilayer microfluidic platform was fabricated using hot-embossing lithography on thermoplastic elastomeric substrates providing high-throughput fabrication and lower cost compared to PDMS based devices. Because of the intrinsic mechanism of the peristaltic micropump, the generated turbulent recirculation of particle above the membrane resulted in high separation efficiency without membrane clogging. More than 99% separation efficiency was achieved for both micro and nano size particles separation using different membrane pore sizes. As a proof of concept for biological applications, separation of red blood cells from osteoblasts was demonstrated. The operating flow rate of up to 100 μl/min provides high throughput sorting and separation of particles which is a significant advantage compared to previously reported microchips. We showed that the developed platform could be used to integrate commercially available membranes with desired pore sizes to separate a wide range of particle sizes eliminating the limitations of PDMS membranes to achieve smaller pore sizes. Combined with the desired characteristics of the TPE materials and the multilayer structure of the device, the introduced platform can be easily modified for multi level particle/cell separation with different size ranges.

4-7 Acknowledgments

The authors would like to acknowledge National Research Council of Canada, National Science and Engineering Research, Council of Canada-Collaborative Research program and Discovery program, Genome Canada/ Génome Québec, for their financial support for the development of microfluidic platforms and diagnostic tools. T.F.D. would like to thank the Faculty of medicine at McGill and Fonds de Recherche du Quebec - Nature et Technologies (FQRNT) for financial support.

References

Barbulovic-Nad, I., X. Xuan, J. S. H. Lee and D. Li (2006). "**DC-dielectrophoretic separation of microparticles using an oil droplet obstacle**." Lab on a Chip **6**(2): 274-279.

Bhagat, A. A. S., H. W. Hou, L. D. Li, C. T. Lim and J. Han (2011). "**Pinched flow coupled shear-modulated inertial microfluidics for high-throughput rare blood cell separation.**" Lab on a Chip **11**(11): 1870-1878.

Didar, T. F. and M. Tabrizian (2010). "**Adhesion based detection, sorting and enrichment of cells in microfluidic Lab-on-Chip devices**." Lab on a Chip **10**(22): 3043-3053.

Dirican, E. K., O. D. Ozgun, S. Akarsu, K. O. Akin, O. Ercan, M. Ugurlu, C. Camsari, O. Kanyilmaz, A. Kaya and A. Unsal (2008). "**Clinical outcome of magnetic activated cell sorting of non-apoptotic spermatozoa before density gradient centrifugation for assisted reproduction**." Journal of Assisted Reproduction and Genetics **25**(8): 375-381.

Hoshino, K., Y.-Y. Huang, N. Lane, M. Huebschman, J. W. Uhr, E. P. Frenkel and X. Zhang (2011). "**Microchip-based immunomagnetic detection of circulating tumor cells.**" Lab on a Chip.

Huang, L. R., E. C. Cox, R. H. Austin and J. C. Sturm (2004). "**Continuous Particle Separation Through Deterministic Lateral Displacement**." Science **304**(5673): 987-990.

Issadore, D., H. Shao, J. Chung, A. Newton, M. Pittet, R. Weissleder and H. Lee (2011). "**Self-assembled magnetic filter for highly efficient immunomagnetic separation**." Lab on a Chip - Miniaturisation for Chemistry and Biology **11**(1): 147-151.

Jonas, A. and P. Zemanek (2008). **"Light at work: The use of optical forces for particle manipulation, sorting, and analysis**." Electrophoresis **29**(24): 4813-4851.

Kuntaegovvdanahalli, S. S., A. A. S. Bhagat, G. Kumar and I. Papautsky (2009). **"Inertial microfluidics for continuous particle separation in spiral microchannels.**" Lab on a Chip **9**(Copyright 2010, The Institution of Engineering and Technology): 2973-2980.

Lenshof, A. and T. Laurell (2010). **"Continuous separation of cells and particles in microfluidic systems.**" Chemical Society Reviews **39**(3): 1203-1217.

Lin, C.-C., A. Chen and C.-H. Lin (2008). **"Microfluidic cell counter/sorter utilizing multiple particle tracing technique and optically switching approach."** Biomedical Microdevices **10**(1): 55-63.

Luo, Y. and R. N. Zare (2008). **"Perforated membrane method for fabricating three-dimensional polydimethylsiloxane microfluidic devices.**" Lab on a Chip **8**(10): 1688-1694.

Nilsson, A., F. Petersson, H. Jonsson and T. Laurell (2004). **"Acoustic control of suspended particles in micro fluidic chips.**" Lab on a Chip **4**(2): 131-135.

Sun Min, K., L. Sung Hoon and S. Kahp Yang (2008). "**Cell research with physically modified microfluidic channels: a review.**" Lab on a Chip **8**(Copyright 2009, The Institution of Engineering and Technology): 1015-1023.

Takagi, J., M. Yamada, M. Yasuda and M. Seki (2005). "**Continuous particle separation in a microchannel having asymmetrically arranged multiple branches.**" Lab on a Chip **5**(7): 778-784.

Wang, M. M., E. Tu, D. E. Raymond, J. M. Yang, H. Zhang, N. Hagen, B. Dees, E. M. Mercer, A. H. Forster, I. Kariv, P. J. Marchand and W. F. Butler (2005). "**Microfluidic sorting of mammalian cells by optical force switching.**" Nature Biotechnology **23**(1): 83-87.

Wei, H., B.-h. Chueh, H. Wu, E. W. Hall, C.-w. Li, R. Schirhagl, J.-M. Lin and R. N. Zare (2011). "**Particle sorting using a porous membrane in a microfluidic device.**" Lab on a Chip **11**(2): 238-245.

Zhang, C., D. Xing and Y. Li "Micropumps, microvalves, and micromixers within PCR microfluidic chips: Advances and trends." Biotechnology Advances **25**(5): 483-514.

Zhou, Y., Y. Wang and Q. Lin (2010). "**A microfluidic device for continuous-flow magnetically controlled capture and isolation of microparticles.**" Journal of Microelectromechanical Systems **19**(4): 743-751.

Zhu, J., T. R. J. Tzeng and X. Xuan (2010). "**Continuous dielectrophoretic separation of particles in a spiral microchannel.**" Electrophoresis **31**(8): 1382-1388.

Chapter 5. Separation of rare oligodendrocyte progenitor cells from brain using a high-throughput multilayer microfluidic device

5-1 Connecting text

In chapter 4, a microfluidic chip was introduced for size-based separation of particles and cells, which included design and fabrication details and device characterization. In this chapter the application of this chip for separation of oligodendrocyte progenitor cells from rat brain tissue has been demonstrated. This chapter addresses the first major goal of the project for size-based separation of rare primary cells.

This research resulted in the following contributions:

Patent: Tohid Fatanat Didar, K. Li, M. Tabrizian and T. Veres, (2013), Integrated microfluidic system for size based particles/cells separation.

Journal paper: Tohid Fatanat Didar*, K. Li*, M. Tabrizian and T. Veres, (2013), Separation of rare oligodendrocyte progenitor cells from brain using a high-throughput multilayer microfluidic device, Biomaterials, Accepted, (*equal contribution).

5-2 Abstract

Despite the advances made in the field of regenerative medicine, the progress in cutting-edge technologies for separating target therapeutic cells are still at early stage of development. These cells are often rare cells, such as stem cells or progenitor cells that their overall properties should be maintained during the separation process for their subsequent application in regenerative medicine. This work, presents a case report where we have undertaken the separation of oligodendrocyte progenitor cells (OPCs) from rat brain primary cultures using an integrated thermoplastic elastomeric (TPE) based multilayer microfluidic device fabricated using hot-embossing technology. OPCs are frequently used in recovery, repair and regeneration of central nervous system after injuries. Indeed, their ability to differentiate *in vitro* into mylinating oligodendrocytes, are extremely important for myelin repair. OPCs form 5-10% of the glial cells population. The traditional macro scale techniques for OPCs separation require pre-processing of cells and/or multiple time consuming steps with low efficiency leading very often to alteration of their properties. The proposed methodology implies to separate OPCs based on their smaller size compared to other cells from the brain tissue mixture. Using aforementioned microfluidic chip embedded with a 5 μm membrane pore size and micropumping system, a separation efficiency more than 99% was achieved. This microchip was able to operate at flow rates up to 100 μl/min, capable of separating OPCs from a confluent 75 cm2 cell culture flask in less than 10 min, which provides us with a high-throughput and highly efficient separation, while preventing membrane clogging due to turbulent flow generated during separation process.

5-3 Introduction

Using stem/progenitor cells is now a well-established approach in regenerative and reconstructive medicine. As our understanding about the development of cell functions and their role in regeneration of tissue and organs becomes more sophisticated, it is increasingly important to isolate various cell types and more importantly pluripotent cells from non-pluripotent cells. Despite the advances made in the field of regenerative medicine over the past several years, the technology for separating target therapeutic cells hasn't changed much. As the promise of regenerative medicine is gradually realized, cell separation technologies are also required to arrive at label-free separation with higher processing speed. Therefore, separating pure population of rare cells, such as stem cells or progenitor cells, without altering their properties is a critical step for cell therapy.

Based on the applied method, cell sorting techniques can be divided into label-free and pre-processed techniques (Didar and Tabrizian 2010). Fluorescence activated cell sorting (FACS)(Bonner WA, Hulett HR et al. 1972), and magnetic activated cell sorting (MACS)(Stefan, Werner et al. 1990) are two commercialized examples of pre-processed techniques. In contrast to label-free methods, pre-processed techniques often alter the separated cells' functions. This is a great concern when the isolated cells are destined for specific applications such as tissue regeneration. In terms of separation principle, differences in target cells physical properties (e.g. density or size) or affinity (e.g. electric, magnetic or adhesive properties specific to each cell type) is employed to separate target cells from a mixture derived from primary tissues. Among these techniques, size based separation is a label-free, cost effective, simple and rapid approach which can also be implemented in microfluidic devices, making it a suitable choice for cell separation (Huang, Cox et al. 2004, Di Carlo, Irimia et al. 2007, Wei, Chueh et al. 2011). Indeed, with the advances in miniaturization, microfluidics have opened new avenues for the development of LOC devices for the analytical investigation of biological and chemical samples. The cell sorting field has also benefited from the major advantages of microfluidic devices, namely the precise

flow control (Sun Min, Sung Hoon et al. 2008), and reduction in time and cost of cell separation (Walker, Zeringue et al. 2004).

Among different size-based cell separation techniques, implementing thin membrane layers, embedded in microfluidic chips, is a straightforward and cost effective approach that, in theory, can be easily integrated into a miniaturized instrument. However there are major fabrication and operational limitations using embedded filters for separation applications. Non-conformal bonding between the commercially available membranes and polydimethylsiloxane (PDMS) based microfluidic layers and achieving desired membrane pore sizes are two main fabrication limitations in PDMS based microfluidic devices. Conversely, membrane blocking and low separation flow rates are usually the main operating drawbacks in the membrane embedded microfluidic chips (Luo and Zare 2008, Schirhagl, Fuereder et al. 2011, Wei, Chueh et al. 2011).

Recently we introduced a multilayer thermoplastic-based microfluidic platform for size-based separation of particles (Fatanat Didar, Li et al. 2013). This design distinguishes itself from previously developed membrane based cell sorting chips by four main features: 1) The chip possesses an embedded pneumatic peristaltic micro-pump (Zhang, Xing et al. , Unger, Chou et al. 2000, Roy, Geissler et al. 2011) 2) uses commercially available polycarbonate (PC) membrane filters 3) it is fabricated using thermoplastic elastomeric-based (TPE) material by hot embossing lithography and 4) operates at flow rates higher than 100 µl/min. As such, the design could generate turbulent flow in the porous membrane area by a peristaltic micropump layer allowing for high-throughput size-based separation of particles and particle-like structures such as cells while avoiding membrane clogging.

The work presented in this paper is a case study where this chip has been used to separate rare oligodendrocyte progenitor cells (OPCs) from rat brain tissue. Currently, the limited regenerative potential of the adult stem cells in the central nervous system has directed the preclinical trauma research on reducing secondary degeneration and promoting regeneration through implementing OPCs. Oligodendrocytes are the myelinating glial cells in the central nervous

system (which are critical in facilitating the rapid conduction of neuronal action potentials and supporting axonal survival (Baumann and Pham-Dinh 2001, Chen, Balasubramaniyan et al. 2007). Oligodendrocytes are generated from OPCs. There are several stages for oligodendrocytes maturation (Zhang 2001). OPCs proliferate and migrate throughout the central nervous system during late embryonic development, and later differentiate into mature myelinating oligodendrocytes (Zhang 2001).

A primary rich natural sources of OPCs, namely glial cells from central nervous system, contain mostly neurons, microglia and astrocytes and less than 10% of OPCs. So far, FACS (Sim, McClain et al. 2011), MACS (Cizkova, Cizek et al. 2009), differential gradient centrifugation or shaking methods based on differential adherent properties of glial cells (Scolding, Rayner et al. 1999) have been attempted to separate OPCs from astrocyte and microglia cells in the mixed glial culture extracted from central nervous system. As previously mentioned, these methods require pre-processing of cells and/or involve multiple time consuming steps to separate OPCs.

So far, none of these methods exploited the difference in OPCs size compared to other cells in the cell mixture. Indeed, among glial cells, OPCs are smaller in size (< 7 microns) compared to microglia (> 10 microns) and astrocytes (> 12 microns). This provided us with a great opportunity to use the developed chip for label-free and straightforward size-based sorting of OPCs from the glial cell mixture without altering their properties. For this purpose, the multilayer microfluidic devise with 10 μm and 5 μm membrane pore sizes was used in two sets of experiments. Applying optimum experimental conditions and 5 μm membrane pore size, we could achieve 99% pure OPC populations. To ensure the OPCs maintained their viability and phenotypes, separated cells were cultured *in vitro* for up to 10 days. Cultured OPCs could differentiate to mature oligodendrocytes after 7 days in culture. The results were validated by immunostaining using A2B5 antibodies, a primary cell surface marker used to identify OPCs (Sim, McClain et al. 2011) along with staining against GalC (galactocerebrosidase gene) for the identification of mature oligodendrocytes as

an indication of separated OPCs differentiation *in vitro*. Changes in cell morphology from bipolar or tripolar structure to extensions during OPCs maturation was also followed with fluorescence microscopy.

5-4 Materials and methods

5-4-1 Materials

Pellets of Mediprene of 400M were purchased from GLS corp., McHenry, IL, USA and were extruded at a temperature of 165°C to form films and/or sheets of several meters long with thicknesses of either ~200 µm or 1000 µm. SU8 photoresist was purchased from GM1075; Gersteltec, Pully, Switzerland. Photo-plotted films printed at a resolution of 36000 dpi (NP, Montreal, Canada) were used as the photolithography masks. Anti-adhesive layer (1H, 1H, 2H, 2H-perfluoro-octyltrichlorosilane) was purchased from Sigma-Aldrich, St. Louis, MO, USA. The hot-embossing process was performed with an EVG520 system (EV Group, Schärding, Austria). Isopore polycarbonate (PC) membranes with pore sizes of 10 µm and 5 µm were purchased from Millipore (whitby, ON, Canada).
A2B5 mouse and GalC rat primary antibodies, FITC conjugated IgG mouse, Cy3 conjugated IgG1 secondary antibodies and DAPI (4',6-Diamidino-2-Phenylindole, Dihydrochloride) were purchased from Invitrogen.

5-4-2 Design and fabrication of the microfluidic chip

A schematic representation of the microfluidic design has been shown in figure 5-1. This figure depicts a 3D representation of the design (Figure 5-1a) and a cross section of the device in the circular channel area (figure 5-1b). The microfluidic device was composed of four different layers: a bottom microfluidic channel layer (BFL), PC porous membrane layer (ML), top microfluidic layer (TFL) and a pneumatic air control layer (PL). Yellow dashed lines represent the bottom fluidic layer (1 mm width and 100 µm depth). This layer consists of a circular channel, a straight channel and an outlet. Blue lines, represent the top fluidic layer (TFL) which consists of a straight channel and a circular channel aligned with its counterpart on the BFL underneath of the ML. TFL has three access holes which can be used as inlets or outlets depending on the peristaltic micro-pumping

configuration. The PC porous membrane (20 mm in diameter) was embedded between the bottom and top microfluidic layers. Bottom and top fluidic layers are connected through the membrane only in the circular channel area where liquid exchange occurs. Finally, the pneumatic air control layer is aligned with the top microfluidic layer. The top and bottom microfluidic layers as well as the air control layer were fabricated on TPE substrates by hot embossing. SU8 patterned silicon wafers were micro-fabricated using standard photolithography techniques and were later on used as molds in hot embossing lithography to fabricate different TPE layers.

Four thin membranes of the pneumatic layer, arranged in a circular fashion, were actuated by pressurized air to operate the peristaltic micro-pumping system. Pumping rate can be increased by increasing the total length of the activation membrane, an increment of the displacement of a single stroke volume, within a relative compact area. For instance, this offers the possibility of modulating the air pressure in the device to achieve desired flow rates required for cell sorting.

Since all of the necessary layers were fabricated on TPE, watertight bonding among the TPE layers could be easily formed at room temperature without any additional plasma or thermal treatment.

Figures 5-1d and 1e are pictures of the assembled device illustrating different parts of the chip in detail. Figure 5-1f shows an optical microscopic image of a PC membrane with 10 μm pore size and Figure 5-1g is an optical microscope image of the bottom fluidic channel and PC membrane constructed with pillars to support the membrane between the TFL and BFL. Figure 5-1 h shows a picture of the chip after final assembly and tubing. More detailed information regarding the design and device fabrication as well as peristaltic pumping characteristics of the device can be found in the (Fatanat Didar, Li et al. 2013).

The microfluidic device was then connected to a homemade 12-channels pneumatic control manifold using silastic laboratory tubing with inner diameter (ID) of 640 μm and outer diameter (OD) of 1.19 mm (from Dow Corning Corporation) through the PTFE tubes, which were connected to the air ports of the device.

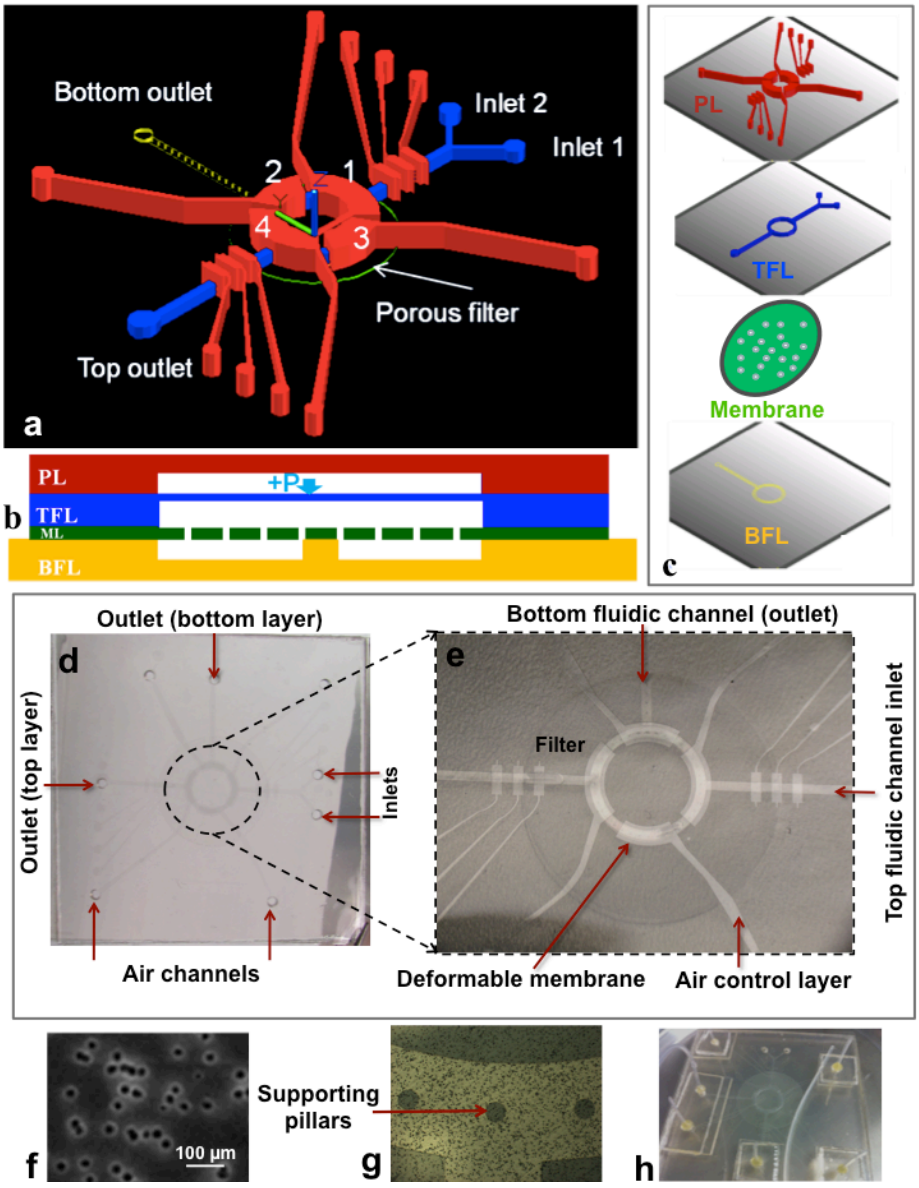

Figure 5-1: Multilayer microfluidic design used for OPCs separation. (a) 3D representation of the device, (b) shows a schematic representation of a cross section of the device in the circular channel area and (c) represents different layers of the microfluidic chip, starting from the bottom: bottom fluidic layer (BFL), membrane layer (ML), top fluidic layer (TFL) and pneumatic air layer or pumping layer (PL). (d-e) Images of the TPE based device indicating different access holes, (f) Optical microscope image of a 10 um pore size membrane, (g) supporting pillars embedded in the BML to support the membrane, (h) An image of the microfluidic device.

5-4-3 Peristaltic micro-pumping strategy for OPCs separation

In our previous report, we demonstrated different pumping configurations of the chip and showed that the second pumping mode (Figure S5-5) provides higher separation efficiency (Fatanat Didar, Li et al. 2013).

Therefore this pumping mode was applied for OPCs separation. Briefly, both top fluidic layers' access holes were used as inlets (Figure S5-5b). Cell mixture entered from the initial inlet and pure cell media containing no beads was introduced from the other top access hole. 9psi of air pressure with a 3 Hz pumping frequency was used and OPCs were collected at the bottom outlet. After pumping the cell mixture, a washing step was performed using the same pumping configuration to remove any remaining OPCs. Because of the turbulence generated by the peristaltic pumping, smaller cells efficiently passed through the porous filter to the bottom microfluidic channel and to the bottom outlet while avoiding membrane clogging by larger cells. Finally, by changing the pumping mode, flow was directed towards the top outlet (Figure S5-5c) and the remaining larger cells were flushed out of the device.

5-4-4 Brian tissue extraction and culture

Using a protocol approved by McGill University Animal Care Ethic Committee, OPC mixed primary cultures were prepared from brains of newborn Sprague-Dawley rats. The meninges and blood vessels were removed from the cerebral hemispheres in Ham's F-12 medium. The tissues were gently forced through a 230-μm nylon mesh. Dissociated cells were then gravity-filtered through a 100-μm nylon mesh. This second filtrate was centrifuged for 7 min at 1000 rpm, and the pellet was re-suspended in DMEM supplemented with 12.5% fetal calf serum, 50 units/ml penicillin, and 50 μg/ml streptomycin. Cells were plated on poly-L-ornithine coated 75-cm^2 flasks and incubated at 37 °C with 5% CO_2. The mixed cell flasks were then used for subsequent separation experiments.

5-4-5 Evaluation of OPCs initial concentration

Primary mixed cell flasks include OPCs, astrocytes and microglia cells. The cell mixture was trypsinized (0.25% trypsin for 10 min), diluted to a concentration of 4×10^4 cells/ml and were cultured on tissue culture treated petri dishes and kept in an incubator under 5% CO_2 for 24 hrs. Immunocytochemsitry was then performed to determine the initial percentage of OPCs in this mixture as described in the next section.

5-4-6 Immunocytochemistry

Different immunocytochemistry steps were performed to identify OPCs and their differentiation into mature oligodendrocytes before and after separation. To determine the initial OPCs concentration, cells were live-stained in pre-warmed media with A2B5 antibody (50 µg/ml) for 30 min at 37ºC. For OPCs differentiation, in addition to previous step, GalC marker at a concentration of 50 µg/ml was added to the cell media to discriminate differentiated OPCs from undifferentiated ones. The cells were then washed with pre-warmed media and were fixed using 4% paraformaldehyde in PBS for 30 min at room temperature. Secondary antibodies (anti-mouse FITC-IgG1 and anti-rabbit Cy3-IgG3) at a concentration of 100 µg/ml were mixed and incubated with the fixed cells for 1hr. Cells were then rinsed twice with PBS. Nucleus staining dye (DAPI 1:1000) in PBS was applied for 15 minutes, rinsed three times with sterile PBS and then cells were observed by fluorescence microscopy. Separated cells were incubated with the secondary antibody only as a control. A negative control was also performed by similarly staining NIH 3T3 fibroblasts.

5-4-7 Fluorescence microscopy

An inverted fluorescence microscope (Nikon TE 2000-E) was used to monitor separated OPCs staining at different stages of in vitro culture. Secondary antibodies conjugated with three different fluorescent dyes (Cy3, DAPI and FITC) were used in cell staining and results were observed through appropriate filters. All images were captured using a CCD camera (Photometrics CoolSNAP HQ2) and analyzed by MBF_ImageJ (MacBiophotonics, McMaster University).

5-5 Results and discussion

5-5-1 Assessment of OPCs initial population and size

Figure 5-2 reports on the initial concentration of OPCs as determined by immunocytochemistry. The results showed that OPCs form 7±1% of the initial primary cell cultures' concentration. This is in very good agreement with previously reported OPC population (5-10%) (Cizkova, Cizek et al. 2009, Sim, McClain et al. 2011). An optical microscope image of pure populations of each

cell type in the mixture confirmed that OPCs are smaller in size compared to astrocytes and microglia cells. At the initial stage of growth, floating OPCs are about 5 ± 2 microns in diameter while microglia cells are in average larger than 10 µm and astrocytes larger than 12 µm in diameter. This size difference was the basis of our strategy to use high-throughput multilayered microfluidic device for separation of OPCs using either membrane with 5 µm or 10 µm pore sizes.

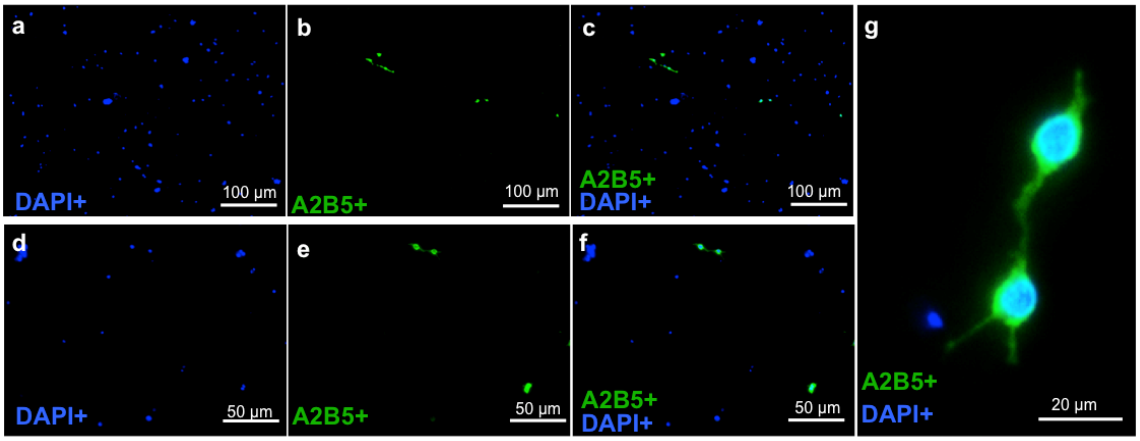

Figure 5-2: Representative fluorescence microscopy image of stained initial cell mixture. A2B5 staining was performed to identify OPCs (green) (b, e) and DAPI nucleus stain (a, d) was used to visualize all types in the mixture for overall counting. (c, d) are the superimposed fluorescence images showing both A2B5 and DAPI, (g) represents a magnified image of the identified OPCs in the primary cell mixture. Analysing more than 4 brain primary mixture cultures showed 7% OPCs initial populations in average.

5-5-2 Separation efficiency using devices with different membrane pore sizes

Figure 5-3a shows optical microscope image of cell mixture before separation. Cells mixture at a concentration of 5.5×10^7 cells/ml was prepared and introduced into the microfluidic device using either a 10 µm or a 5 µm pore size membrane. Figures 5-3b and 5-3c show optical microscope images of the cells just after they were collected from bottom outlets of the chips with 10 µm and 5 µm membrane pore sizes respectively.

Isolated OPCs remained viable and their well-known bipolar morphology (Sim, McClain et al. 2011) was preserved after 2 days culture as shown in optical microscope image of cells separated with 5 µm membrane pore size (figure 5-3d).

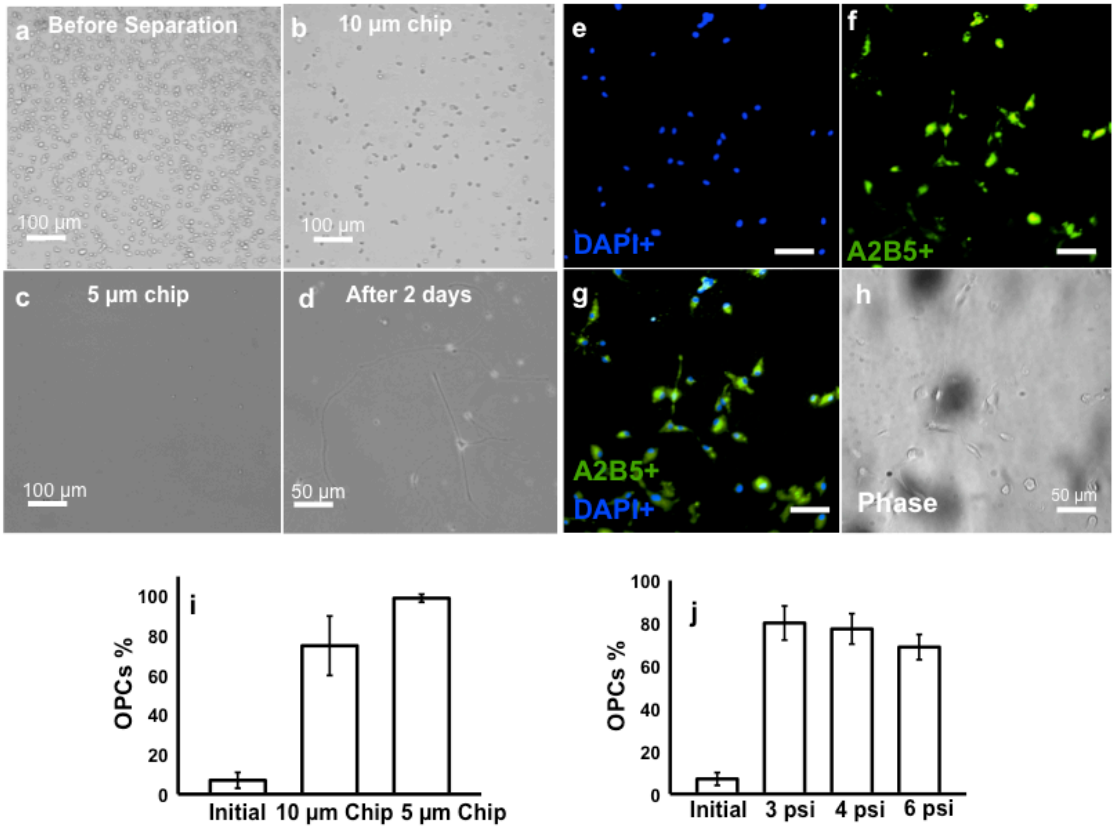

Figure 5-3: (a) optical microscope images of initial cell mixture before separation, (b) and (c) cells collected from the bottom outlet of the chips with 10 µm and 5 µm membrane pore sizes respectively, (d) cultured cells separated using the chip with 5 µm membrane pore size after 2 days in vitro culture, (e), (f) and (g) Immunocytochemistry results and evaluation of OPCs population after separation showing representative fluorescence microscope images of collected cells at the bottom outlet of the chip with 5 µm membrane pore size. OPCs were stained with specific marker (A2B5) shown in green and also nucleus stain DAPI to represent the overall cell population, (h) shows the representative phase image, (i) depicts purity of OPCs in the initial cell mixture and after separation using chips with 10 µm and 5 µm membrane pore sizes, (j) the effect of applied air pressure on the separation efficiency of OPCs using the chip with 10 µm membrane pore size. Error bars represent standard deviation of analyzing 30 fluorescence microscope images obtained from three different experiments.

The immunocytochemistry results presented in Figure 5-3j confirmed the purity of OPCs after separation by either membrane. Representative fluorescence microscope images of separated OPCs stained with A2B5 specific marker indicated 80% and 99% OPC population with 10 µm and 5 µm membrane pore sizes, respectively (Figures 5-3e-i). Therefore, with an initial cell mixture concentration of 5.5×10^7 cells/ml introduced into the device, it was possible to separate OPCs from a fully confluent mixture detached from a 75 cm^2 cell flask in less than 10 min.

5-5-3 The effect of applied pumping air pressure on cell separation

Operation of the developed microfluidic platform, using embedded peristaltic micro-pump, provides several advantages as well as differences compared to conventional external pumping systems for cell sorting. For instance, applying lower air pressure results in a lower flow rate, which can affect the separation time for high-throughput separation. In attempt to increase the separation efficiency of OPCs with 10 μm membrane pore size to the level of 5 μm membrane pore size (80% versus 99%), the capabilities of the device in working under various compressed air pressures were explored. Three different operating conditions were applied by varying the air pressure to investigate the purity of obtained OPCs from the bottom outlet using a 10 μm membrane pore size. As shown in Figure 5-3j, lower applied pressures tend to result in higher separation efficiency. Although this difference does not seem to be significant, it indicates that during the peristaltic micropumping operation, applied air pressure plays an important role in determining the flow rate and separation efficiency of cells.

5-5-4 Viability and differentiation of separated OPCs

To examine the differentiating ability of separated OPCs after passing through the microfluidic device under applied pressure, separated cells were cultured on petri dishes treated with poly-L-ornithine and their differentiation into mature oligodendrocytes was investigated. Cultured OPCs were stained with OPC and mature oligodendrocyte markers at days 7 and 10 after separation. Separated OPCs remained viable during *in vitro* culture and differentiated into mature oligodendrocytes. Figure 5-4 (a-b) represents optical microscope images of separated OPCs after day 3 and 7 *in vitro* culture, respectively. As shown, in figure 5-4, OPCs display bipolar morphology after 1 day, tripolar morphology with some extensions after 3 days and at day 7, they grow extensions as an indication of differentiation into mature oligodendrocytes (Sim, McClain et al. 2011, Mekhail, Almazan et al. 2012). Figure 5-4 (d-h) also shows representative fluorescence microscope images of stained OPCs after 7 and 10 days in which cells where both A2B5-positive (OPCs) and GalC-positive (mature oligodendrocyte) at day 7 and only GalC-positive at day 10.

These results showed that not only OPCs can be isolated to greater than 99% pure OPC populations, but also their differentiation capabilities into mature oligodendrocytes is not affected by the separation process. In addition to achieving viable pure OPC populations, the high-throughput operation (100 µl/min) of the device allows for time efficient separation. Similar devices have reported separation of hematopoietic stem cells with flow rates not higher than 17.2 µl/min (Schirhagl, Fuereder et al. 2011).

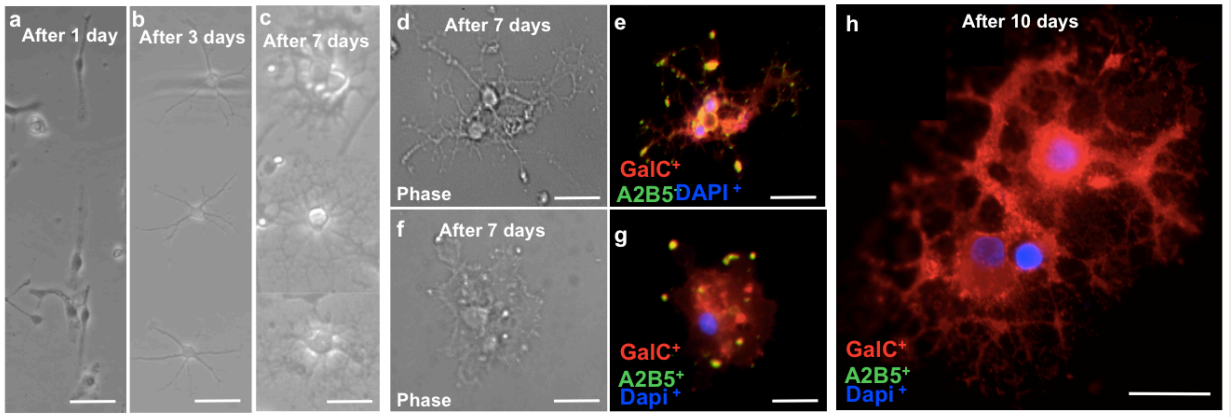

Figure 5-4: a), (b) and (c) representative optical microscope images of separated OPCs after 1, 3 and 7 days in vitro culture respectively. (d-e) and (f-g), phase image and fluorescence microscope images of separated OPCs cultured in vitro and stained with A2B5 (green) and GalC (red) markers after 7 days. After 7 days cells express both OPC and mature oligodendrocyte markers. (h) Flourescence microscope image of OPCs after 10 days in culture where cells express only mature oligodendrocyte marker, GalC, (red). Scale bars represent 50µm.

5-6 Conclusion

In this study, we extended the application of a multilayer thermoplastic-based microfluidic device with embedded peristaltic micro-pump and commercially available polycarbonate membrane to separate oligodendrocyte progenitor cells from rat brain tissue. This method is revealed to be rapid, straightforward and cost effective for isolation and purification of OPCs. Using the chip with 5 µm membrane pore size, separation efficiency of greater than 99% was achieved. The device was also capable of operating at flow rates up to 100 µl/min allowing effective OPCs separation from a mixture of 75 cm^2 culture flasks in less than 10 minutes. We showed that isolated OPCs can be cultured when further studies of these cells are required, for instance in investigating the fundamental of OPCs and their involvement in myelination/remyelination of central nervous system

related injuries. The application of the developed device can further be extended to high-throughput size based separation of other biological targets, such as circulating tumor cells or pathogens in various mixtures and fluids including blood.

5-7 Supporting Information

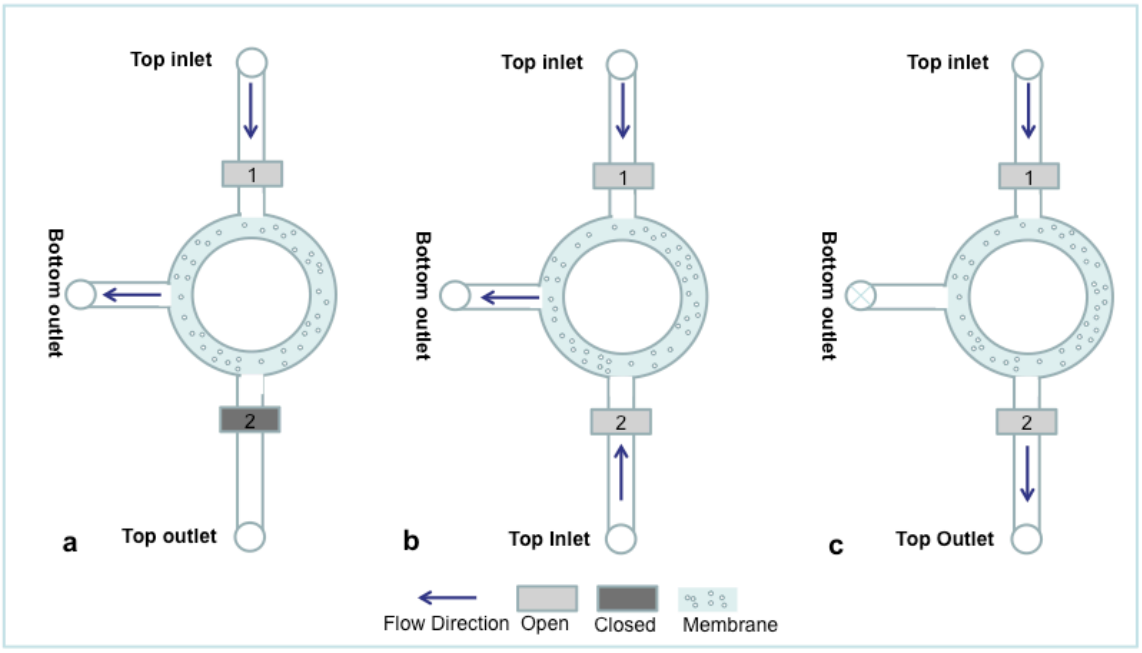

Figure S5-5: Schematic representation of different pumping strategies: (a) top fluidic layer includes one inlet and one outlet, (b) both outlets at the top fluidic layer are used as inlets which results in higher separation efficiency for the smaller cells (OPCs), (c) the bottom outlet is closed and remaining larger cells are flushed through the top outlet.

5-8 Acknowledgment

The authors would like to acknowledge National Science and Engineering Research Council of Canada-Collaborative Research program and Discovery program, Genome Canada/ Génome Québec, for their financial support for the development of microfluidic platforms and diagnostic tools. The authors would also like to thankd Dr. Guillermina Almazan for valuable comments, discussions and help about. Mr Mina Mekhail for useful discussions as well as Marcio Dipaula for his assistance with the cell isolation experiments. T.F. Didar would like to thank the Faculty of Medicine and Department of Biomedical Engineering at

McGill, the Fonds de recherche du Quebec - Nature et technologies (FQRNT) and NSERC-CREATE “Integrated Sensor Systems” for their financial support.

References

Baumann, N. and D. Pham-Dinh (2001). "**Biology of Oligodendrocyte and Myelin in the Mammalian Central Nervous System.**" Physiological Reviews **81**(2): 871-927.

Bonner WA, Hulett HR, Sweet RG and H. LA: (1972). "**Fluorescence activated cell sorting.**" Rev Sci Instrum **43**: 404-409.

Chen, Y., V. Balasubramaniyan, J. Peng, E. C. Hurlock, M. Tallquist, J. Li and Q. R. Lu (2007). "**Isolation and culture of rat and mouse oligodendrocyte precursor cells.**" Nat. Protocols **2**(5): 1044-1051.

Cizkova, D., M. Cizek, M. Nagyova, L. Slovinska, I. Novotna, S. Jergova, J. Radonak, J. Hlucilova and I. Vanicky (2009). "**Enrichment of rat oligodendrocyte progenitor cells by magnetic cell sorting.**" Journal of Neuroscience Methods **184**(1): 88-94.

Di Carlo, D., D. Irimia, R. G. Tompkins and M. Toner (2007). "**Continuous inertial focusing, ordering, and separation of particles in microchannels.**" Proceedings of the National Academy of Sciences **104**(48): 18892-18897.

Didar, T. F. and M. Tabrizian (2010). "**Adhesion based detection, sorting and enrichment of cells in microfluidic Lab-on-Chip devices.**" Lab on a Chip **10**(22): 3043-3053.

Fatanat Didar, T., K. Li, T. Veres and M. Tabrizian (2013). "**Multilayer thermoplastic based microfluidic chip for high-throughput particle/cell separation.**"Biomaterials, In press.

Huang, L. R., E. C. Cox, R. H. Austin and J. C. Sturm (2004). "**Continuous Particle Separation Through Deterministic Lateral Displacement.**" Science **304**(5673): 987-990.

Luo, Y. and R. N. Zare (2008). "**Perforated membrane method for fabricating three-dimensional polydimethylsiloxane microfluidic devices.**" Lab on a Chip **8**(10): 1688-1694.

Mekhail, M., G. Almazan and M. Tabrizian (2012). "**Oligodendrocyte-protection and remyelination post-spinal cord injuries: a review.**" Prog Neurobiol **96**(3): 322-339.

Roy, E., M. Geissler, J.-C. Galas and T. Veres (2011). "**Prototyping of microfluidic systems using a commercial thermoplastic elastomer.**" Microfluidics and Nanofluidics **11**(3): 235-244.

Schirhagl, R., I. Fuereder, E. W. Hall, B. C. Medeiros and R. N. Zare (2011). "**Microfluidic purification and analysis of hematopoietic stem cells from bone marrow**." Lab on a Chip.

Scolding, N. J., P. J. Rayner and D. A. S. Compston (1999). "**Identification of A2B5-positive putative oligodendrocyte progenitor cells and A2B5-positive astrocytes in adult human white matter.**" Neuroscience **89**(1): 1-4.

Sim, F. J., C. R. McClain, S. J. Schanz, T. L. Protack, M. S. Windrem and S. A. Goldman (2011). "**CD140a identifies a population of highly myelinogenic, migration-competent and efficiently engrafting human oligodendrocyte progenitor cells.**" Nat Biotech **29**(10): 934-941.

Stefan, M., M. Werner, W. Walter and R. Andreas (1990). "**High gradient magnetic cell separation with MACS.**" Cytometry **11**(2): 231-238.

Sun Min, K., L. Sung Hoon and S. Kahp Yang (2008). "**Cell research with physically modified microfluidic channels: a review.**" Lab on a Chip **8**(Copyright 2009, The Institution of Engineering and Technology): 1015-1023.

Unger, M. A., H. P. Chou, T. Thorsen, A. Scherer and S. R. Quake (2000). "**Monolithic microfabricated valves and pumps by multilayer soft lithography.**" Science **288**(5463): 113-116.

Walker, G. M., H. C. Zeringue and D. J. Beebe (2004). "**Microenvironment design considerations for cellular scale studies.**" Lab on a Chip **4**(2): 91-97.

Wei, H., B.-h. Chueh, H. Wu, E. W. Hall, C.-w. Li, R. Schirhagl, J.-M. Lin and R. N. Zare (2011). "**Particle sorting using a porous membrane in a microfluidic device.**" Lab on a Chip **11**(2): 238-245.

Zhang, C., D. Xing and Y. Li "**Micropumps, microvalves, and micromixers within PCR microfluidic chips: Advances and trends.**" Biotechnology Advances **25**(5): 483-514.

Zhang, S. C. (2001). "**Defining glial cells during CNS development.**" Nat Rev Neurosci **2**(11): 840-843.

Chapter 6. Adhesion based detection, sorting and enrichment of cells in microfluidic lab-on-chip devices

6-1 Connecting text

In chapters 4 and 5 the first label free approach, size-based separation, was demonstrated. In chapters 6, 7, 8 and 9 the second label free approach, adhesion-based separation, will be discussed. In this chapter a comprehensive review of the microfluidic devices for adhesion based separation is presented. In addition to previously reported approaches future trends and technologies in the filed has also been discussed.

The literature review resulted in the following critical review paper:

- Tohid Fatanat Didar and M. Tabrizian, (2010), Adhesion-based detection, sorting and enrichment of cells in microfluidic Lab-on-Chip devices, Lab on a Chip, 10, 3043-3053.

6-2 Abstract

The detection, isolation and sorting of cells are important tools in both clinical diagnostics and fundamental research. Advances in microfluidic cell sorting devices have enabled scientists to attain improved separation with comparative ease and considerable time savings. Despite the great potential of Lab-on-Chip cell sorting devices for targeting cells with desired specificity and selectivity, this field of research remains unexploited. The challenge resides in the detection techniques, which has to be specific, fast, cost-effective, and implementable within the fabrication limitations of microchips. Adhesion-based microfluidic devices seem to be a reliable solution compared to the sophisticated detection techinques used in other microfluidic cell sorting systems. It provides the specificity in detection, label-free separation without requirement for a preprocessing step, and the possibility of targeting rare cell types. This review elaborates on recent advances in adhesion-based microfluidic devices for sorting, detection and enrichment of different cell lines, with a particular focus on selective adhesion of desired cells on surfaces modified with ligands specific to target cells. The effect of shear stress on cell adhesion in flow conditions is also discussed. Recently published applications of specific adhesive ligands and surface functionalization methods have been presented to further elucidate the advances in cell adhesive microfluidic devices.

6-3 Introduction

The isolation and sorting of cells is frequently used in laboratories for clinical diagnostics or basic research. Separation of human lymphocytes from blood for HIV diagnosis tests (Wysocki LJ and VL 1978, Murthy, Sin et al. 2004, Sin, Murthy et al. 2005), enrichment of stem cells (M., R. et al. 2006), and cytosensors for detection of different diseases (Nagrath, Sequist et al. 2007, Xu, Phillips et al. 2009) are some examples of the need for cell sorting. The fields of biology and biotechnology are the main users of sorting techniques and devices for isolation of rare cell populations. The importance of cell sorting has not been solely limited to biology and medicine but also analysis and subsequent cultivation of desired cells from a defined cell population in the fields of molecular genetics, diagnostics and therapeutics. On the other hand, use of pure cells help reduce variations among experiments and thus expedite scientific discovery.

Cell sorting technique is defined as any procedure which can be used for separation, isolation or enrichment of a specific cell type (Mattanovich and Borth 2006). In this technique, either physical properties, such as density or size, or affinity such as electric, magnetic or adhesive properties specific to each cell type is used to sort cells. Conventional techniques for the separation of cells include filtration, centrifugation and sedimentation, which are carried out either in a batch or continuous manner and can be easily implemented in large-scale operation. However, where cell size differences are not significant, effective separation is impeded. This issue becomes more significant when small sample volumes are employed. The other conventional techniques for cell sorting are: panning (Wysocki LJ and VL 1978), fluorescence activated cell sorting (FACS) (Bonner WA, Hulett HR et al. 1972), and magnetic activated cell sorting (MACS) (Stefan, Werner et al. 1990).

Recent developments in lab-on-a-chip devices have opened new avenues for the analytical study of biological and chemical samples in a single microfluidic device, and have begun to play an increasingly important role in cell biology, neurobiology, pharmacology, and tissue engineering. The cell sorting technology has also started to benefit from the major advantages of microfluidic devices,

namely the ability to design cellular microenvironments (Walker, Zeringue et al. 2004), precise control of fluid flow (Sun Min, Sung Hoon et al. 2008), and reduction of time and cost of cell culture assays (Walker, Zeringue et al. 2004). Many microfluidic devices with different flow channel designs have been introduced as cell sorting devices based on the physical properties. Physical-based cell sorting methods such as filtration (Di Carlo, Wu et al. 2006, Manbachi, Shrivastava et al. 2008), sedimentation and hydrodynamic force (Yu-Cheng and Chun-Ping 2002, Takagi, Yamada et al. 2005, Yamada and Seki 2005) are mainly limited to the differences in size or density of the target cell(s) and other cell types within a mixture. A comprehensive review of these devices has been published by Kim et al. (Sun Min, Sung Hoon et al. 2008) Compared to physical-based sorting methods, affinity-based techniques include a wide array of approaches, taking advantage of electric, magnetic, optical and adhesive properties of cells.

Table 6-1: Microfluidic devices developed for cell sorting

Sorting Method	Separation property	Limitations	References
FACS*	Fluorescence	False detection as separation rate increases, pre-processing is necessary, expensive	(Herzenberg, Sweet et al. 1976, Kruger, Singh et al. 2002, Studer, Jameson et al. 2004, Cho, Chen et al. 2010)
Hydrodynamic separation	Size	Selectivity is only based on the size of the particles, efficiency is an issue	(Adam and Daniel 2001, Yu-Cheng and Chun-Ping 2002, Takagi, Yamada et al. 2005, Yamada and Seki 2005)
Physical trapping (Filtering)	Size	Selectivity is only based on the size of the particles, needs complex microfabrication	(Di Carlo, Wu et al. 2006, Di Carlo, Edd et al. 2008, Manbachi, Shrivastava et al. 2008)
DEP**	Dielectric particles	Requires external electric field	(Kang and Li 2009, Nilsson, Evander et al. 2009)
Acoustic cell sorting	Size	Particle diameter must be less than half of the applied wavelength, requires external field	(Deok-Ho, Haake et al. 2004, Nilsson, Petersson et al. 2004, Adams, Thevoz et al. 2009, Johansson, Nikolajeff et al. 2009)
Optical forces	Optical polarizability	Based either on size or index of refraction	(Wang, Tu et al. 2005, Jonas and Zemanek 2008)
MACS***	Magnetic properties	Needs external magnetic field and pre-processing	(Miltenyi S, Muller W et al. 1990, Dirican, Ozgun et al. 2008, Marek, Caruso et al. 2008)

*FACS: Fluorescence activated cell sorting, **Dielectrophoresis, ***MACS: Magnetic activated cell sorting

FACS, MACS, (Miltenyi S, Muller W et al. 1990, Dirican, Ozgun et al. 2008, Marek, Caruso et al. 2008), acoustic cell sorting (Deok-Ho, Haake et al. 2004, Nilsson, Petersson et al. 2004, Adams, Thevoz et al. 2009, Johansson, Nikolajeff et al. 2009), optical cell sorting (Wang, Tu et al. 2005, Jonas and Zemanek 2008), dielectrophoresis (DEP) (Kang and Li 2009, Nilsson, Evander et al. 2009) and adhesion-based sorting are among those devices which provide more flexibility and precision in targeting and separating desired cell types. Table 6-1 depicts cell sorting techniques implemented in microfluidic chips.

Based on the detection method used, cell sorting microfluidic devices can be divided into label-free and pre-processed techniques. In latter techniques which include FACS and MACS, desired cells are tagged with fluorescent dyes or magnetic beads respectively and are exposed to electrical or magnetic fields. Although in label-free techniques, such as filtration and hydrodynamic separation, there is no need for a pre-processing step, the sorting options are limited to physical properties or external forces, such as acoustic or optical fields. In contrast to label free methods, pre-processed techniques might alter the separated cells' functions due to the presence of attached magnetic beads (MACS) or antibodies (FACS). This might be a great concern if the isolated cells are designated to specific applications such as tissue regeneration. Adhesive-based sorting devices are among the few label-free sorting techniques which are not dependent on the size of the particles, making them a suitable option for cell sorting. The significance of adhesive based separation is not only attributed to its label free nature, but also to its ability to achieve specific adhesion of target cell types on the surface of microchannels. This paper reports on adhesion based microfluidic devices for sorting different cell types, enrichment of rare cells and the detection and diagnostics of diseased cells. Despite the availability of several review papers dedicated to cell sorting principles (Pappas and Wang 2007, Chen, Feng et al. 2008, Kumar and Bhardwaj 2008, Sun Min, Sung Hoon et al. 2008, Nilsson, Evander et al. 2009, Tsutsui and Ho 2009) there is so far no review with a primary focus on adhesion-based cell sorting microchips. Herein, surface patterning and modification techniques for microfluidic devices as well as

the effect of shear stress on cell adhesion are discussed. Particular emphasis is on the new trends for separation or detection of desired cell types using cell-specific adhesion molecules including proteins, peptides and aptamers.

6-4 Factors affecting cell adhesion in microfluidic devices

Cell adhesiveness is cell type dependent. This feature has been used to develop multiple techniques and devices to study the adhesion properties of different cell types (Chang, Lee et al. 2005, Nalayanda, Kalukanimuttam et al. 2007, Stroumpoulis, Haining et al. 2007, Xunli, Jones et al. 2008, Min-Hsien 2009). With the recent progress in the development of microfluidic devices, their use is frequently investigated for the separation of various cell types in one device using parallel channels modified with different molecules. This reduces tremendously the assay time due to higher surface contact between target cells and modified surfaces.

Shear stress and flow rate, surface topography, concentration and specificity of cell adhesive molecules, are main factors affecting cell adhesion in microfluidic devices. However, the surface properties represent the main driving force that influences the composition and orientation of adsorbed proteins and subsequent cellular events, such as adhesion, proliferation, and differentiation (Gristina, D'Aloia et al. 2009). Common surface modification approaches consist of micro/nano structuring of the surface and/or functionalization with specific ligands. These ligands referred to as cell adhesion molecules are involved in cell-cell and cell-surface interactions and are commonly used in the design of sorting, sensing and diagnostic devices to target desired cell types. Not all cell adhesion molecules have the same strength of binding, some are strong and some are weak and dynamic (Buckley, Rainger et al. 1998). Nevertheless, there are many unknowns about cell adhesive molecules, particularly about the role of mechanical and chemical signals generated by them to facilitate the crosstalk between cell and extracellular environment.

6-5 Preparation of cell-adhesive surfaces

Optimal surface properties, in terms of topography and roughness, as well as the homogeneous distribution of ligands on the surface, can significantly enhance the

efficiency and sensitivity of the device. Consequently, different techniques have been implemented for surface modification including micro/nano patterning and adhesive ligand coating.

Conventional microfabrication techniques such as photolithography, soft lithography (Whitesides, Ostuni et al. 2001), electrochemical discharge machining (Fatanat Didar, Dolatabadi et al. 2008) and deep reactive ion etching (Lang 1996) are used for patterning micro structures onto surfaces. Several other methods including electron beam lithography (Goto, Tsukahara et al. 2008), electrochemical and chemical etching (Westcott, Lamb et al. 2009), UV-assisted capillary molding (Kwon, Lee et al. 2007), and layer by layer technique (Shaikh-Mohammed, Li et al. 2004) are used for patterning nanostrucutres on microchannel surfaces. Silanization (Olbrich, Andersen et al. 1996, Qin, Hou et al. 2007), (Maraldo and Mutharasan 2007), microcontact printing (Wilbur, Kumar et al. 1994, Xia and Whitesides 1997) and microfluidic printing (Schena 1999, Delamarche, Juncker et al. 2005) are three main techniques for immobilization of adhesive ligands onto surfaces of microchannels (Sin, Murthy et al. 2005, Zhang, Crozatier et al. 2005, Nagrath, Sequist et al. 2007, Plouffe, Njoka et al. 2007, Plouffe, Kniazeva et al. 2009). Table 6-2 compares the advantages over the disadvantages of these three methods for protein/peptide/aptamer modification on microchannel surfaces. Combination of different methods has also been used to achieve better adhesive properties (Kaji, Hashimoto et al. 2006, Kalinina, Gliemann et al. 2008). Micro/nano structuring of the surface followed by functionalization with the biomolecules of choice (Goto, Tsukahara et al. 2008) or functionalizing micro/nano particles with the adhesive biomolecules (Liu, Guo et al. 2007) were showed to improve adhesive properties.

6-6 The effect of flow and shear stress on cell adhesion

The main difference of cell adhesion in microfluidic devices compared to conventional cell adhesion flasks is the flow characteristics and the resulted shear stress exerted on the suspended cells. Different groups have reported adhesion and detachment of different cell types under varying shear stresses (Jian, Usami et al. 1997, Lu, Koo et al. 2004, Zhang, Jones et al. 2007, Gutierrez,

Petrich et al. 2008, Cheung, Zheng et al. 2009, Joong Yull, Sung Ju et al. 2009, Lovchik, Bianco et al. 2009, Murthy, Taslim et al. 2009). The first device for systematically investigating the effect of shear stress on cell adhesion was introduced by Shunichi et al. (Shunichi, Hsuan-Hsu et al. 1993) Based on the Hele-Shaw flow theory between parallel plates, the authors fabricated a nozzle shaped microfluidic channel in which shear stress decreased linearly along the channel length (Fig. 6-1).

According to eqn (6-1), shear stress exerted on the suspended particles depends on the geometry of the channel (w: inlet width, L: length and h: depth), volumetric flow rate (Q) and viscosity of suspension (μ):

$$\tau_{\omega} = \frac{6\mu Q}{wh^2} \qquad (6\text{-}1)$$

Using this design, the group showed that the adhesion of platelets on fibrinogen coated glass surfaces was shear dependant (Shunichi, Hsuan-Hsu et al. 1993). This design has been used by other groups (Murthy, Sin et al. 2004, Plouffe, Njoka et al. 2007, Green and K. 2009) to study cell adhesion under different shear stresses to obtain optimum adhesion conditions.

In general, increasing the shear stress decreases the adhesion rate. This is an important consideration in designing a microchannel for separating different cell types at different local points of a microchannel. The results for adhesion of smooth muscle cells and endothelial cells on specific peptides indicate that the number of cells adhering on the surface strongly depends on shear stress (Plouffe, Njoka et al. 2007). For instance, in a suspension of mixed endothelial cells (ECs) and smooth muscle cells (SMCs), 83% of the SMCs adhered onto the surface coated with their specific peptide (VAPG) at a shear stress of 2.9 dyn/cm2 while the highest adhesion rate (86%) for ECs was achieved at a shear stress of 1.9 dyn/cm2 (Plouffe, Njoka et al. 2007). For endothelial progenitor cells (EPCs) the optimum shear stress was reported to be 1.47 dyn/cm2 (Plouffe, Kniazeva et al. 2009).

Microchannel geometry also plays an important role in cell adhesion and should be taken into consideration, particularly for subsequent modification of the device to introduce adhesive regions on the channels surface. Eqn (4-1) depicts the shear stress along the axis passing through the center of the microchannel (Fig. 6-1). Shear stress also varies along the microchannel's width especially when turns are included in the design. In general, channels with sharp turns are not optimal for cell adhesion. When turns are needed in the design, they should be curved to obtain uniform velocity. For straight microchannels, cell adhesion is independent of the length of the microchannel up to 100 mm. For capturing rare cell types where a small adhesion surface is needed, straight microchannels are better options. When a large amount of cells and a large surface area is required for adhesion, spiral shape microchannels are alternative choices as the shear stress remains almost constant in the entire width (Murthy, Taslim et al. 2009).

Table 6-2: Comparison of surface modification techniques for peptide/protein/aptamer immobilization

Surface Modification Technique	Advantages	Disadvantages
Silanization	Reliable, Easy procedure,	Long process, Needs an oxygen free atmosphere, Needs subsequent assembly for use in microfluidics, Not selective,
Micro-contact Printing	Fast, Applicable to a variety of patterns, Repeatable, Selective,	Needs more precision, Needs to be assembled later for use in microfluidic, Difficult to control ligand concentration
Microfluidics	Is performed on the final microfluidic device, Fast, No sterilization needed, Selective, Controllable ligand density	Needs oxygen free atmosphere, Patterned geometries are limited to open network structures

As of yet, there remains a need for a comprehensive report on the detachment of adhered cells by shear stress and flow rate. Zhang et al. (Xunli, Jones et al. 2008) have investigated Chinese hamster ovary (CHO) cell detachment from surfaces modified with collagen, silane and glutaraldehyde under different shear stresses. Cells, adhered on non-treated glass surface, detached easily from the surface, while collagen coated surface had the highest adhesion force. The authors have also shown the effect of shear stress on the detachment of Chinese hamster ovary (CHO), T47D, NCTC 2544, CaC02 and U937 cell lines from silane coated glass surface. CHO cell line needed the lowest shear stress for

detachment whereas U937 cell line required the highest detachment shear stress.

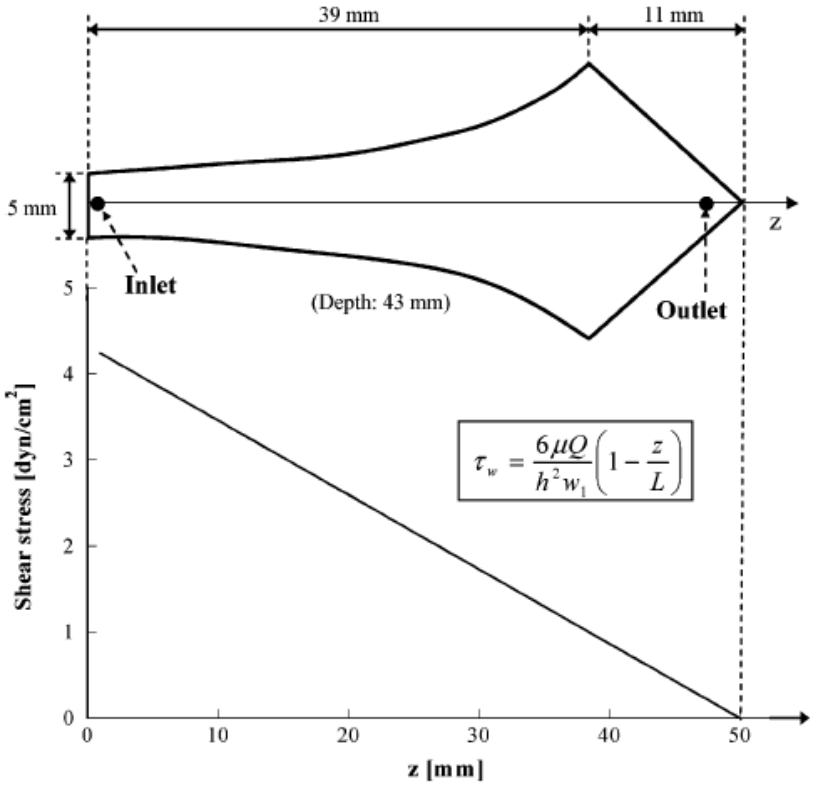

Figure 6-1: Flow chamber geometry and shear stress profile(Murthy, Sin et al. 2004). The relationship between shear stress (τw) and axial position (z) is given by the equation derived by Shunichi et al. (Shunichi, Hsuan-Hsu et al. 1993) (Reproduced from reference (Murthy, Sin et al. 2004) with permission from American Chemical Society).

Interestingly, all cell lines and surfaces had almost the same detachment percentage when the shear stress increased to more than 100 dyn/cm2.

Lu et al. (Lu, Koo et al. 2004) also investigated fibroblast adhesion onto surfaces coated with different concentrations of fibronectin under different shear stresses using microfluidic platforms and showed that detachment rate decreases by increasing the concentration of cell adhesive ligand on the surface. Fibroblast detachment was about 10% at high concentrations of adhesive ligand (10 µg/ml) while almost all of the adhered cells were detached at lower ligand concentration (0.1 µg/ml) under a relatively low shear stress.

In a flow acceleration assay, low flow acceleration (0.032 ml/min^2) induced the deformation of prostate cancer cells attached on a protein-modified surface, while

at higher flow acceleration rate (0.32 ml/min^2) the deformation was negligible and the detachment was significant (Cheung, Zheng et al. 2009).

6-7 Adhesion based Microfluidic cell sorting devices

6-7-1 Cell adhesion on micro/nano structured surfaces

Cell adhesion, separation and proliferation can significantly increase by changing the surface topography (Shaikh-Mohammed, Li et al. 2004, Keon Woo, Sung Sik et al. 2007, Goto, Tsukahara et al. 2008, Hengyu, Jeong-Hwan et al. 2008).

Adhesion of COS-7 fibroblasts on PDMS surfaces modified by Al microstructures (Patrito, McCague et al. 2007) and mouse fibroblast NIH/3T3 cells on 300 nm wide and 150 nm high gold features (Young, Wheeler et al. 2007) are examples of cell adhesion in micro/nano patterned microfluidic devices. Hengyu et al. (Hengyu, Jeong-Hwan et al. 2008) reported that the adhesion of Escherichia coli on micro/nano-textures patterned on glass surface is twice as high as on a smooth surface.

Separation of human breast cancer cells from epithelial cells in a microfluidic device with patterned microchannels was achieved by Kown et al. (Keon Woo, Sung Sik et al. 2007) Various nanostructures (pillar, perpendicular and parallel lines) of 400 nm were fabricated on PDMS surfaces using UV-assisted capillary moulding (Fig 6-2). The adhesion strength of MCF10A cells was found to be higher than that of MCF7 cells regardless of pre-culture time and surface nanotopography at all flow rates. For the separation of cancer cells, the optimum conditions were achieved by a 2-hour pre-culture on perpendicular line patterns (Fig. 6-2e) followed by flow-induced detachment at 200 µl/min. Applying these conditions, the fraction of MCF7 cancer cells in the effluent increased from 0.36 to 0.83. Although this device can enhance the enrichment of MCF7 cells from MCF10A cells, the long pre-incubation time (2 hrs), difficulty in controlling the experimental parameters to reach the optimum conditions, and low specificity of the device are the major limitations for its practical applications.

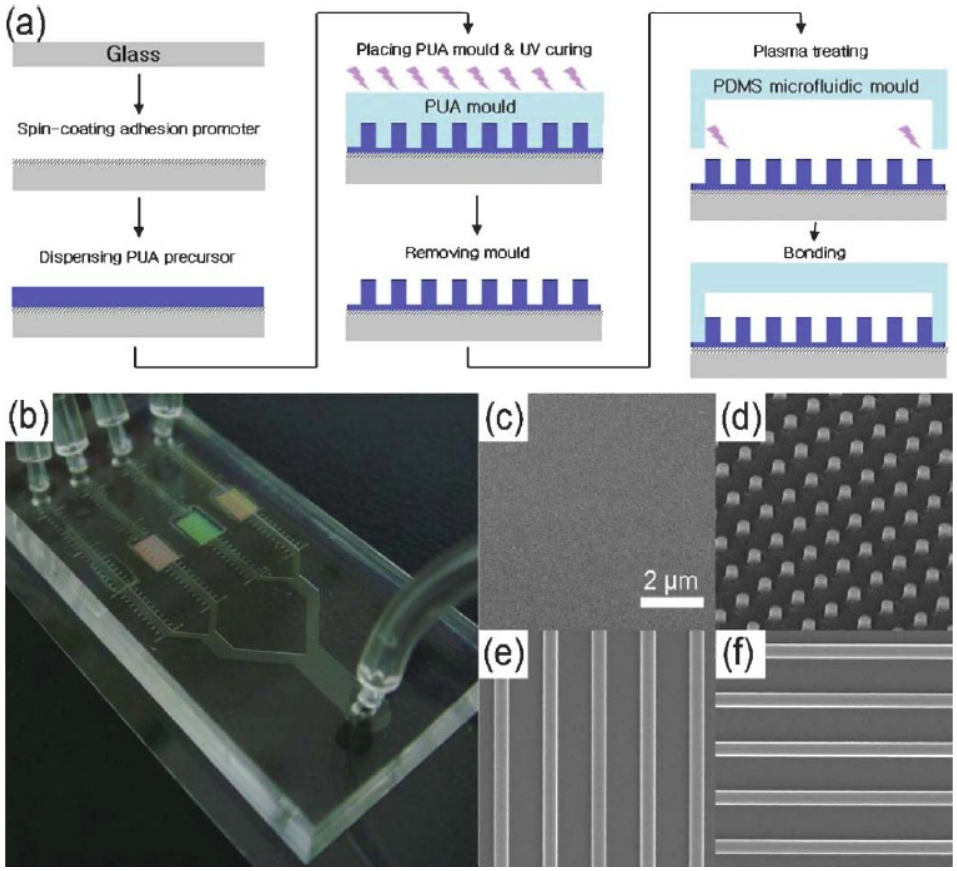

Figure 6-2: (a) A scheme of fabrication of microfluidic channels integrated with a nanopatterned substrate. PUA nanostructures were fabricated using UV-assisted capillary moulding onto glass substrate. (b) Fabricated microfluidic channel. (c–f) SEM images of flat or three PUA nanostructures fabricated inside a microfluidic channel: (c) PUA flat surface, (d) 400 nm pillars (e) 400 nm perpendicular lines, and (f) 400 nm parallel lines. (Reproduced from reference (Keon Woo, Sung Sik et al. 2007) with permission from Royal Society of Chemistry).

A new approach in adhesion based microfluidic devices which uses hybrid glass/gold micro/nanostructures was reported by Westcot et al. (Westcott, Lamb et al. 2009) Different patterns were tested for cell adhesion on this hybrid substrate (Fig. 6-3). Fibroblasts did not adhere to these surfaces with an EG4C11SH (tetra(ethylene glycol) undecane thiol) monolayer on the surface, and interestingly, did not bind to the gold gradient region until HDT (hexadecanethiol) was added to the gold in the microchannel (Westcott, Lamb et al. 2009).

6-7-2 Ligand-specific cell adhesion

Specific adhesion of cells on modified surfaces is a reliable and highly sensitive approach which has recently gained growing attention for separation of different cell lines. Specificity of cell adhesion in microfluidic devices can be achieved

using proteins, peptides and aptamers to capture desired cell types. The key point, however, remains in finding of the biomolecule which is specific to the targeted cell membrane.

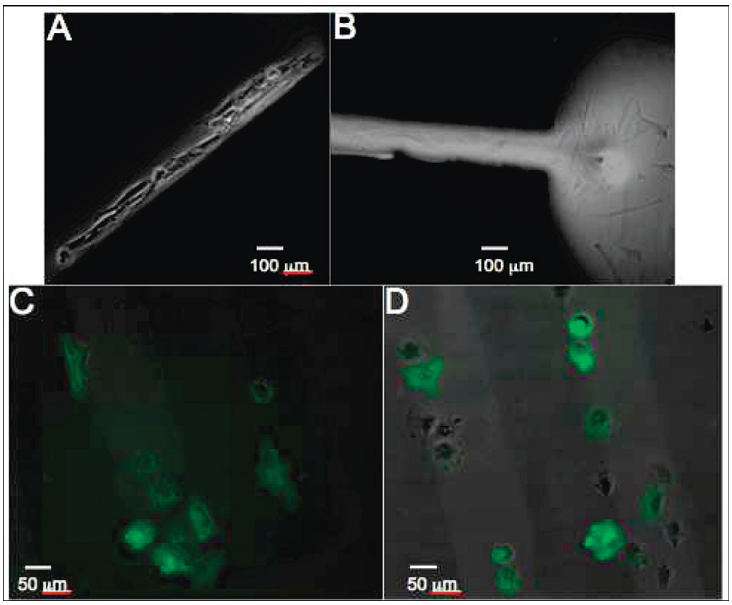

Figure 6-3: Cell attachment to microfluidic generated partially etched and functionalized gold substrates. (A) Cells adhered specifically to the etched line pattern presenting HDT. (B) Cells adhered to a circular pattern. (C) Stably transfected Rat2 fibroblasts expressing GFPcoronin attached to the partially etched pattern. (D) The same fluorescent cells bound to a line pattern. The cells only adhere to partially etched regions of the gold allowing for live-cell visualization of cells on patterned surfaces. (Reproduced from reference (Westcott, Lamb et al. 2009) with permission from American Chemical Society).

6-7-2-1 Protein-specific cell adhesion

One of the pioneering works pertaining to the capture and detection of circulating tumour cells (CTC) in a microfluidic device was reported by Nagrath et al. (Nagrath, Sequist et al. 2007). Specific adhesive antibodies namely EpCAM and TACSTD1 which are both anti-epithelial cell-adhesion-molecules, were used to capture the CTCs (Fig. 6-4).

In two separate studies, Epithelial Membrane Antigen (EMA) and Epithelial Growth Factor Receptor (EGFR) were reported as potential capture antigens for breast cancer cells (Evron, Dooley et al. 2001), (Fuqua, Wiltschke et al. 2000). The specificity of EMA was between 60% to 78% (Fuqua, Wiltschke et al. 2000) and EGFR was over expressed in 45% of breast cancer cells (Evron, Dooley et al. 2001). Du et al. (Du, Cheng et al. 2007) used this concept to fabricate a

simple microfluidic device coated with EMA and EGFR to specifically capture breast cancer cells in a mixture with normal cells. The capture rate for breast cancer cells in the proposed microchip was more than 30% while less than 5% of the normal cells adhered to the surface after three minutes at a flow rate of 15 µl/min.

Separation of Endothelial progenitor cells (EPCs) and vascular endothelial cells (VECs) were also reported through the use of antibody modified surfaces. EPCs showed more tendencies to adhere to anti-CD34 modified surface and VECs adhered mainly to surfaces modified by anti-CD31 (Plouffe, Kniazeva et al. 2009). Some non-specific adhesion was also reported in this work.

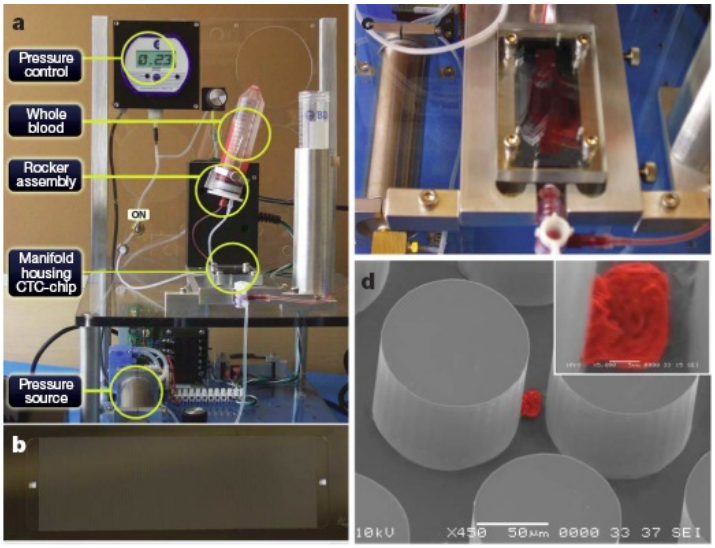

Figure 6-4: Isolation of CTCs from whole blood using a microfluidic device. a) The workstation setup for CTC separation. The sample is continually mixed on a rocker, and pumped through the chip using a pneumatic pressure-regulated pump. b) The CTC-chip with microposts etched in silicon. c) Whole blood flowing through the microfluidic device. d) Scanning electron microscope image of a captured NCI-H1650 lung cancer cell spiked into blood (pseudo coloured red). The inset shows a high magnification view of the cell. (Reproduced from reference (Nagrath, Sequist et al. 2007) with permission from Nature publishing group).

Combinations of different cell separation techniques can help increase the efficiency and specificity of separation. As an example, Hashimoto et al. (Hashimoto, Kaji et al. 2009) combined the principle of DEP with adhesion-based separation in a microfluidic chip to increase the reliability and specificity of the separation. The device was functionalized with anti-CD16b to selectively separate neutrophils from a suspension of mixed leukocytes (Fig. 6-5). After antibody immobilization, an AC voltage was applied to the microelectrode array

to concentrate the neutrophils from the flowing suspension and subsequently capture the desired cell type by its specific antibody on the surface. This approach was also effective for capturing Eosinophil cells once anti-eosinophil was immobilized on the surface

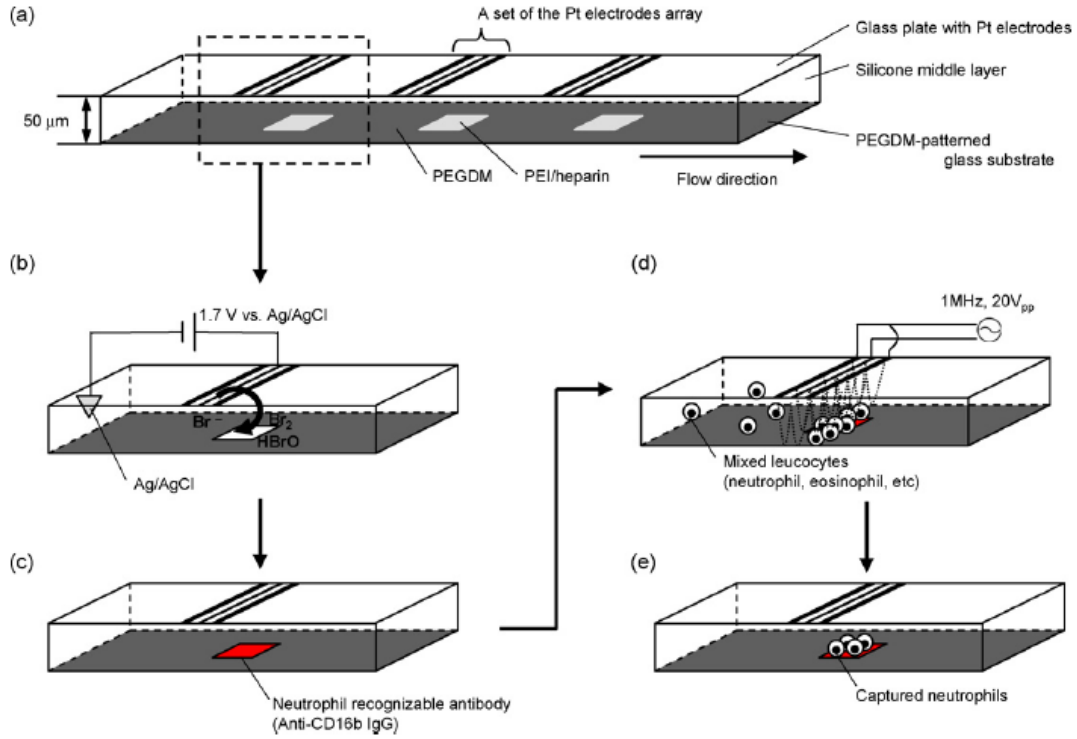

Figure 6-5: Schematic representations of selective capture of neutrophils from mixed leukocytes within a microchannel. (a) Construction of the microfluidic device. A PEGDM-free region covered with PEI/heparin layer is positioned under a set of the Pt electrodes array. (b) The PEI/heparin layer is removed by HBrO generated at the central electrode to allow protein adsorption. (c) Neutrophil-specific antibody is immobilized on the protein-adsorptive region. (d) Leukocytes are concentrated at the antibody-immobilized region by negative DEP force. (e) Neutrophils are biochemically captured by the antibody and unbound cells are washed away. (Reproduced from reference (Hashimoto, Kaji et al. 2009) with permission from ELSEVIER).

Another approach to the adhesion-based cell separation could be achieved by modifying micro and nano particles with the specific protein to trap the cells inside the flow. An interesting design for separation of A549 cancer cells, using a combination of modified magnetic nanoparticles and magnetic micropillars was reported by Liu et al. (Liu, Guo et al. 2007). The authors used photolithography to integrate Nickel micropillars on the microchannels surfaces. A549 cancer cells attached to the supermagnetic beads, functionalized with WGA (Fig. 6-6) were

trapped using a magnetic field created by the micropillars. A capture efficiency of 62% to 74% was achieved.

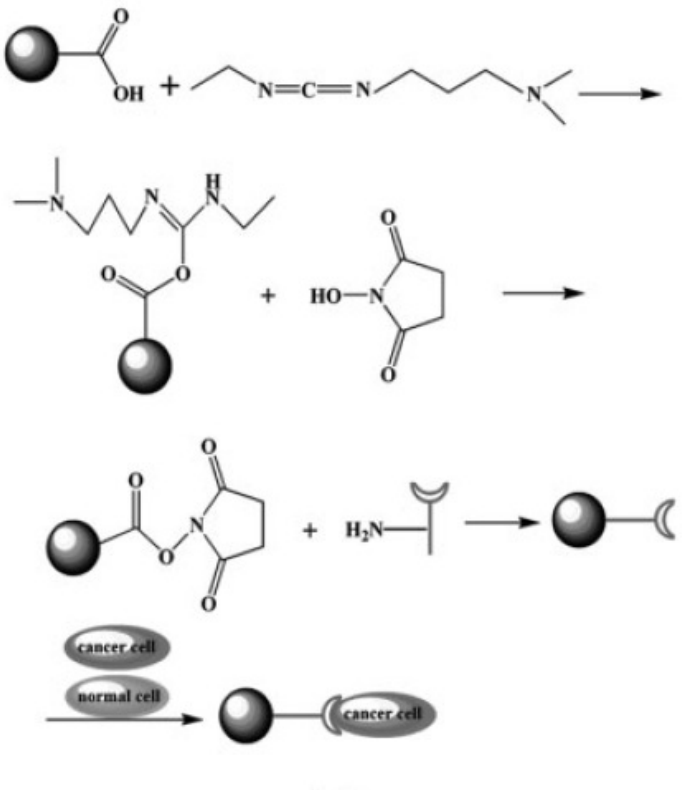

Figure 6-6: Covalent binding of the specific protein to the magnetic beads and subsequent adhesion of the cancer cell. (Reproduced from reference (Liu, Guo et al. 2007) with permission from Wiley InterScience).

6-7-2-2 Peptide-specific cell adhesion

Patterning selected peptides can direct adhesion of specific cell lines exclusively to predetermined regions on microchannel surfaces. Recently Hasenbein et al. (Hasenbein, Andersen et al. 2002) used microcontact printing to pattern a surface with Arginine–Glycine–Aspartic Acid–Serine (RGDS), Lysine–Arginine–Serine–Arginine (KRSR), Arginine-Aspartic Acid-Glycine-Serine (RDGS) and Lysine-Serine-Serine-Arginine (KSSR) peptides. Following four hours incubation, adhesion of either osteoblasts or fibroblasts on surfaces patterned with the RDGS and KSSR was not significant but both osteoblasts and fibroblasts adhered and formed clusters onto areas modified with the adhesive RGDS,

whereas only osteoblasts adhered and formed clusters onto the areas modified with KRSR.

Plouffe et al. (Plouffe, Njoka et al. 2007) used Arg-Glu-Asp-Val (REDV) and Val-Ala-Pro-Gly (VAPG) peptide sequences to separate smooth muscle and endothelial cells respectively in a microfluidic device. By controlling the shear stress and flow conditions a separation purity of 82% was obtained. KYSFNYDGSE peptide, a sequence of 10 amino acids, has also been reported as the cell adhesive biomolecule for the adhesion of neural retina cells (Rao, Wu et al. 1992).

Negative enrichment of target cells is also an attractive option for separation and enrichment of rare cell types. In this technique the surface of the microchannel is coated with the ligands specific to the non-target cell types in the suspension resulting in adhesion of all cell types except target cells. This method has the advantage of eliminating the difficulty in detaching target cell types from surface after separation. Implementing this technique, adipose-derived stem cells (ADSCs) could be isolated from a suspension of endothelial cells (ECs), smooth muscle cells (SMCs) and fibroblasts (FBs) in a three-stage spiral shape microfluidic platform coated with peptides specific to ECs, SMCs and FBs adhesion (Fig 6-7) (Green and K. 2009).

Using peptides for specific targeting of cells has not been limited to surfaces. Recently, peptide functionalized hydrogel, namely alginic acid, was used to capture fibroblasts in a microfluidic device (Plouffe, Brown et al. 2009). First the alginate was absorbed on the glass surface and then by using Ca2+ ionic solution, it was converted to hydrogels. After capturing the target cells by hydrogel, ethylene diamine tetraacetic acid (EDTA) was used to dissolve the alginate and release the cells. It should be noticed that specific cell capture using gels is a different approach compared to the use of shear stress for cell detachment, in which the cells are released after the gel dissolution. The use of gel for cell entrapment and release might provide an advantage over other cell separation techniques, since it maintains cell integrity

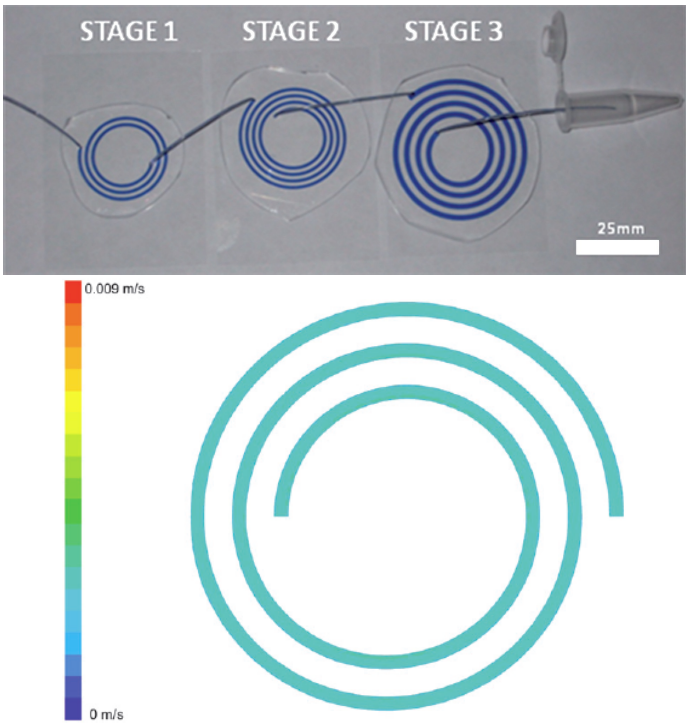

Figure 6-7: a) Experimental set up of the ADSC recovery experiments. From left to right; REDV stage (266 mm2), VAPG stage (491 mm2), and the RGDS stage (793 mm2). (Reproduced from reference(Green and K. 2009) with permission from Royal Society of Chemistry). b) Velocity profile for a microchannel with spiral geometry obtained by CFD modeling. The inner radius of the spiral is 1.9 mm and the profile shown is uniform throughout the length and cross-section of the channel at all locations. (Reproduced from reference (Murthy, Taslim et al. 2009) with permission from Royal Society of Chemistry).

6-7-2-3 Aptamer-specific cell adhesion

A recent technique, referred to as Systematic Evolution of Ligands by Exponential Enrichment (SELEX), utilizes RNA, ssDNA or modified nucleic acids as aptamers to selectively target organic molecules, proteins (Csordas, Gerdon et al. 2010), antibodies (Xu and Ellington 1996) or desired cell types (Ulrich, Ippolito et al. 1998, Ulrich, Magdesian et al. 2002, Daniels, Chen et al. 2003, Shangguan, Li et al. 2006, Wu, Sefah et al. 2010, Zhang, Jia et al. 2010). SELEX, introduced first by Gold et al. (Tuerk C 1990) and Szostak et al. (Ellington and Szostak 1990), is an important tool in the diagnosis of diseases as well as in research and therapeutics. Cell SELEX, as an extended development of the SELEX technique, recognizes differences in surface molecule expression between any two types of cells. This technique relies on obtaining a specific

probe for a cell type without having any knowledge of molecular differences between cell types (Nery, Wrenger et al. 2009). Cell SELEX technique has been used to specifically target human red blood cells (Morris, Jensen et al. 1998), cancer cells (Daniels, Chen et al. 2003, Herr, Smith et al. 2006, Chen, Medley et al. 2008, Shangguan, Meng et al. 2008) and to separate stem cells (Guo, SchÄfer et al. 2006). The cell SELEX procedure includes incubation of the combinatorial RNA or ssDNA library with target cells and the subsequent removal of unbound oligonucleotides (Fig. 6-8).

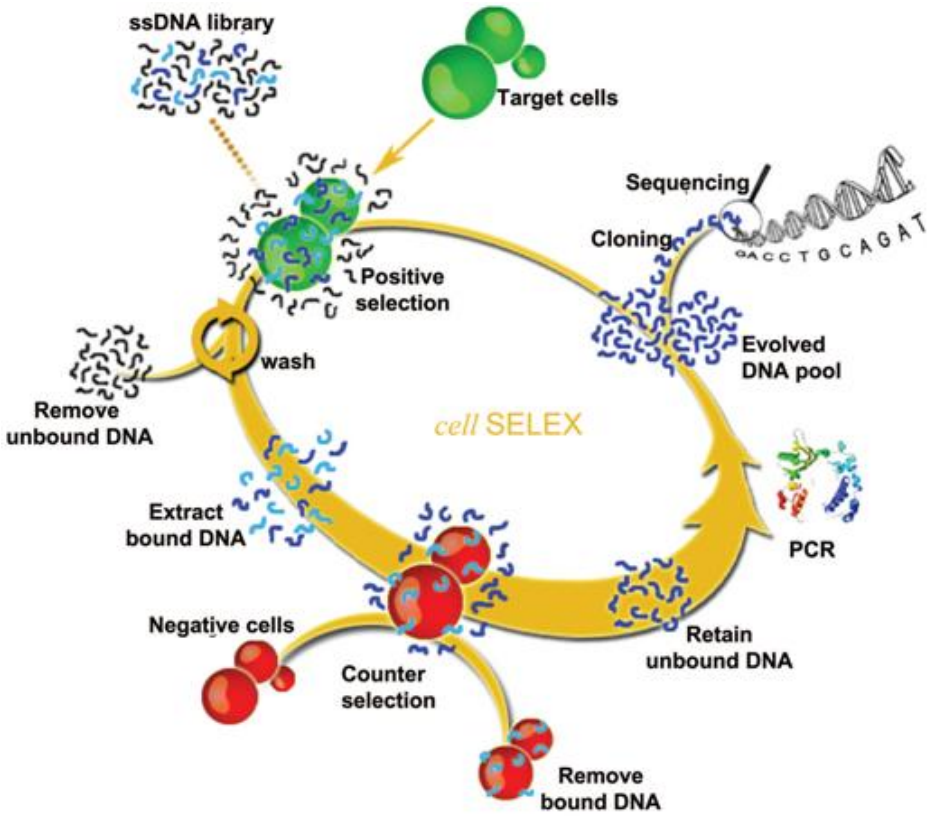

Figure 6-8: Schematic representation of the cell-based aptamer selection. The ssDNA pool was incubated with target cells (CCRF-CEM cells in this study). After washing, the bound DNAs were eluted by heating to 95°C. The eluted DNAs were then incubated with negative cells (Ramos cells in this study) for counter selection. After centrifugation, the supernatant was collected and the selected DNA was amplified by PCR. The PCR products were separated into ssDNA for next-round selection or cloned and sequenced for aptamer identification in the last-round selection. (Reproduced from reference (Shangguan, Li et al. 2006) with permission from Proceedings of the National Academy of Sciences).

The bound sequences are then eluted from the cell surfaces and amplified by RT-PCR or PCR for the next SELEX cycles. To overcome unspecific binding of RNA or DNA pools to other sites on cell surfaces other than the desired target site, the pre-selected RNA or DNA pool is exposed to control cells and only the unbound RNA/DNA fractions are used for the next SELEX cycle. After cycles of target selection and subtraction rounds, a homogenous population of aptamers are found to specifically bind to the target cell (Nery, Wrenger et al. 2009).

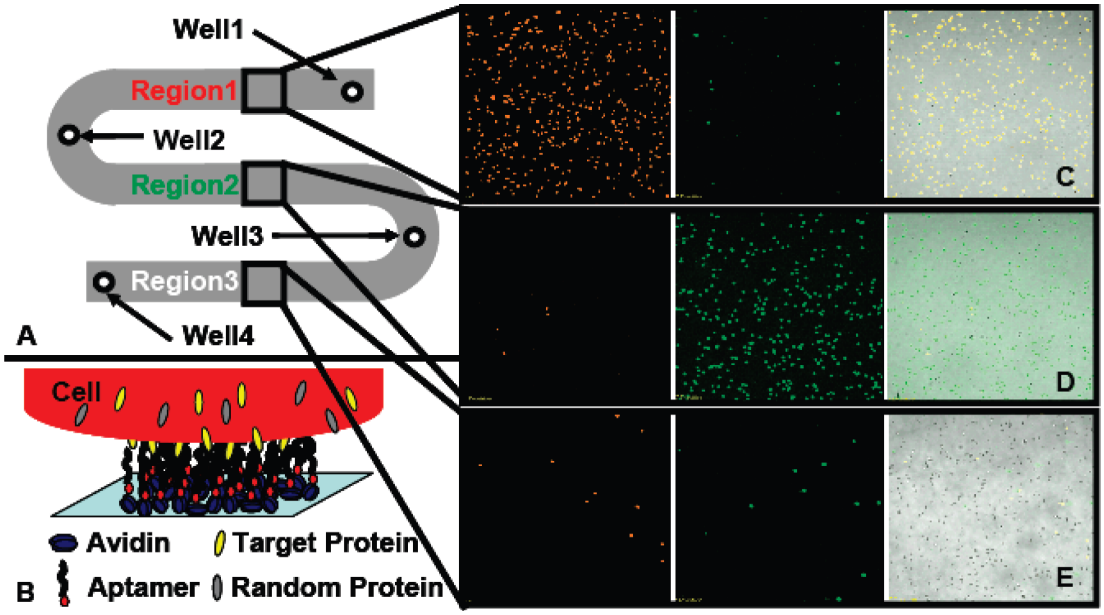

Figure 6-9: Microfluidic device and multiplexed detection of 3 different cancer cell lines. (A) Schematic of microfluidic device, showing three regions used for aptamer immobilization and four wells used for channel preparation and cell sample injection. (B) Aptamer immobilization scheme, showing avidin adsorbed to the glass surface and biotinylated aptamers capturing a cell through specific molecular interactions. (C) The Sgc8 aptamer enriches the red-stained CEM cells. (D) The TD05 aptamer enriches the green-stained Ramos cells. (E) The Sgd5 aptamer enriches the unstained Toledo cells. (Reproduced from reference (Xu, Phillips et al. 2009) with permission from American Chemical Society)

Finding specific aptamers is an iterative process which requires multiple rounds of selection and amplification. Recently, microfluidic devices have been implemented to discover aptamers (Hybarger, Bynum et al. 2006, Xinhui, Jiangrong et al. 2009) making the selection process rapid, efficient and

automatable. Xinlui et al. Xinhui, Jiangrong et al. 2009) reported using magnetic bead based SELEX process in a microfluidics device for discovering aptamers.
So far, few groups have implemented aptamers in microfluidic devices for enrichment of cancer cells, (Phillips, Xu et al. 2008, Xu, Phillips et al. 2009) and detection of biomolecules (Nguyen, Pei et al. 2009, Nguyen, Pei et al. 2009, Wang, Liu et al. 2010).
An interesting aptamer-based microfluidic device for detection of cancer cells was introduced by Xu et al. (Xu, Phillips et al. 2009) This device selectively captures cells by immobilized DNA-aptamers and yields a 135-fold enrichment of rare cells (Fig. 6-9). Three different leukemia cell types, CCL-119 T-cell (CCRF-CEM human acute lymphoblastic leukemia), Ramos cells (CRL-1596, B-cell, human Burkitt's lymphoma), and Toledo cells (CRL-2631, non-Hodgkin's B-cell lymphoma) were targeted with this device using three different specific aptamers (sgc8, TD05, Sgd5). This device was reported to target and sort cells with 96% purity.

Table 6- 3: Applications of cell sorting in biotechnology (Mattanovich and Borth 2006)

General Aim	Sorting Target	Selected Examples
Physiological research Protein engineering	Viability, vitality, ligand binding	Bacteria, yeast, antibody surface display, peptide surface display
Cellular properties	Enzyme engineering, cell hybridization, cloning, promoter trapping robustness, process related properties	Intra- and extracellular enzymes yeast hybridization, library cloning bacteria, acid tolerance high cell density, low growth rate
Overproduction	Product stained by immunofluorescence autofluorescence of product unspecific staining	Protein, alkaloids, FITC/antibiotic production

6-8 Discussion and future outlook

Microfluidic cell sorting devices have the potential to be used in variety of applications such as preparation of organ transplants (H. and Puchalski 2007),

purification of cell mixtures for diagnostic tests such as cancer (Du, Cheng et al. 2007), umbilical cord blood processing/prenatal blood testing for genetic disorders (Tomas Koblas 2005), tracking tumor cells in the body (Nagrath, Sequist et al. 2007), stem cell purification for regenerative medicine (Guo, SchÄfer et al. 2006, Nichola, Jane et al. 2007, Park, Selvarajah et al. 2007), removal of lymphocytes from transfusion for specialized cell packs (Luban 1994), cell counting such as white blood cells and CD4+ T cell counting (Theera-Umpon and Gader 2002, Chen-Min, Suz-Kai et al. 2007, Xuanhong, Gupta et al. 2009), isolation and detection of pathogenic microorganisms and parasites in food, environment and clinical samples (Rotariu, Ogden et al. 2005) and bacterial identification (Pappas and Wang 2007). (Table 6-3).

Despite these evident potential applications of cell sorting chips, more investigations are needed to develop microfluidic devices to achieve higher selectivity, less separation time and higher cell capture capabilities. New surface patterning and modification approaches combined with more efficient designs, highly selective cell adhesive ligands and effective detection and separation strategies are the main challenges to overcome and to push the technology from R&D laboratories to the market.

Selectivity can be further enhanced by the discovery of new cell adhesive molecules that are inexpensive and easily applicable on microchannel surfaces. Combining nano-patterned surfaces with subsequent coating of the specific cell adhesion molecules can also help achieve higher and more specific selectivity. This is important in designing a microchannel for separating different cell types at different local points of a microchannel. New designs of micfluidics aiming to achieve optimum shear stress and better positioning of the ligands on the surface showed an enhanced separation time and ratio of captured cells. Parallel separation and sorting using a set of microchannels is often used to increase the capture ratio of cells. The design should allow binding of adhesive molecules for each specific cell type on the areas of the channels in which shear stress is optimum for adhesion of target cell type. Optimum flow rate and shear stress not only depend on the cell type but also on the topography and chemistry of the

surface (Plouffe, Kniazeva et al. 2009). Furthermore, the geometry of the microchannels and positioning of the ligands should be taken into consideration according to the optimum shear stress to achieve the best adhesion for each cell type. It should be noticed that the shear stress also affects the functionality of cells and cell membrane receptors. This effect has widely been discussed in the literature under the mechanotransduction topic (Hua, Erickson et al. 1993, Makino, Shin et al. 2007). However the mechanotransduction could be used as an approach in conjunction with surface functionalization techniques to enhance the specificity and selectivity of Lab-on-Chip cell sorting devices.

Detachment of adhered cells for subsequent applications is one of the main issues for adhesion-based microfluidic cell sorting devices. On-chip cell lysis is currently used for devices designed for diagnostic applications, but it is not suitable for applications requiring recovery of viable and functional cells (Plouffe, Brown et al. 2009). As explained in section 3.3.2 a reliable solution to overcome this problem is negative enrichment where undesired cells are captured, while leaving the target cell line, for instance stem cells, in the flow stream (Green and K. 2009).

Achieving high specificity and selectivity is the key point in optimizing and improving adhesion-based cell sorting devices. Current approaches use biomolecules such as proteins, peptides or aptamers to selectivity capture and separate desired cell types as summarized in table 6-4. However, aptamer-based or SELEX technique implemented in microfluidic platforms, remains the reliable and highly specific method, and therefore, the most promising technique for cell research and point of care diagnosis.

Future developments of microfluidic cell sorting devices should combine negative enrichment and aptamer-based techniques to achieve a breakthrough in the field. Negative enrichment will avoid the subsequent detachment of target cells while the use of aptamers will increase the efficiency of separation by capturing target cells with higher selectivity. For high throughput cell separation, the microfluidic platform could be composed of parallel arrays of microchannels, each coated with specific ligands using microfluidic printing. Another promising approach is

modifying each microchannel with different ligands to capture more than one cell type in a single channel. Microfluidic printing, microcontact printing or a combination of these two methods can be used for selectively patterning a single microchannel with different ligands. Implementing of parallel channels with the latter will be very time effective and efficient when the separation of a large population of cells is involved.

A new trend to increase the robustness of cell sorting devices, seeks creating artificial ligands or traps on microchannel surfaces that target cell lines through specific site recognition. This approach, so-called molecular imprinting, allows imprinting desired peptides or aptamers on microchannels surfaces to obtain site specific recognition to initially imprinted ligand (Byrne, Park et al. 2002, Turner, Jeans et al. 2006, Gupta and Kumar 2008). The use of molecularly imprinted ligands or “artificial ligands”, allows for easy, customized production with various template ligands, using common polymers. In addition, imprinted surfaces are selective, robust and applicable under a variety of experimental conditions. They can be mass-produced and therefore the costs associated with the use of biomolecules as templates can be reduced significantly.

As a summary, novel adhesive ligands combined with creative designs will change the trend of adhesion-based cell sorting devices in the future. There is an immediate need to discover and introduce cell specific biomolecules to be used in conjunction with cell separation microfluidic devices. A portable, easy to use and inexpensive adhesion based cell separation microchip can find tremendous applications in early stage diagnosis, blood transfusion and in regenerative medicine for separation of progenitor cells, stem cells and other rare cell types.

Table 6-4: Cell adhesion molecules implemented in microfluidic devices

Cell type	Specific ligand	Optimal Shear stress or Flow rate	Specificity and efficiency of separation	References
CCL-119 T-cell (CCRF-CEM human acute lymphoblastic leukemia)	Sgc8 Aptamer	300 nL/s	>85%	(Shangguan, Li et al. 2006, Xu, Phillips et al. 2009)
CRL-1596, B-cell, human Burkitt's lymphoma), and TD05,	TD05 Aptamer	300 nL/s	>85%	(Shangguan, Li et al. 2006, Xu, Phillips et al. 2009)
Toledo cells (CRL-2631, non-Hodgkin's B-cell lymphoma)	Sgd5 Aptamer	300 nL/s	>85%	(Shangguan, Li et al. 2006, Xu, Phillips et al. 2009)
Mesenchymal stem cells (MSCs)	Aptamer G-8	No Flow	85%>	(Guo, SchÄfer et al. 2006)
Fibroblast	RGDS peptide	1.1 dyn/cm^2	60%-70%	(Kalinina, Gliemann et al. 2008, Green and K. 2009, Plouffe, Brown et al. 2009)
Endothelial cells	REDV peptide fibronectin, Anti-CD34	1.9 dyn/cm^2	60%-90%	(Young, Wheeler et al. 2007)
Smooth muscle cells (SMCs)	VAPG peptide	2.9 dyn/cm^2	83%	(Plouffe, Njoka et al. 2007)
Neurons	IKVAV Peptide	No flow	-	(Rao, Wu et al. 1992, Lu, Bansal et al. 2006)
Osteoblasts	KRSR peptide	No flow	-	(Hasenbein, Andersen et al. 2002)
B lymphoma WEHI-231	DLWYDAV peptide	No flow	-	(Wang, Tu et al. 2005, Suparna Mandal 2007)
Astrocyte	KHIFSDDSSE peptide	No flow	-	(St. John, Kam et al. 1997, Kam, Shain et al. 2002, Lu, Bansal et al. 2006)
Breast cancer cells	Epithelial membrane antigen (EMA) and epithelial growth factor receptor (EGFR)	15 µL/min for 3 minutes	30% cancer cells and less than 5% normal cells captured	(Du, Cheng et al. 2007)
A549 cancer cells	Wheat germ agglutinin (WGA) protein	Stop flow conditions	62% to 74%	(Liu, Guo et al. 2007)
Cervical cancer cells (HCCC)	α6-integrin (antibody)	20 µL/min (1.3mm/s) for 3 minutes	Cancer cell capture>30% , Normal cell capture<5%	(Du, Colls et al. 2006)
Neutrophils	Anti-CD16b	20 µL/min	-	(Hashimoto, Kaji et al. 2009)
Eosinophils	Anti-eosinophil	20 µL/min	-	(Hashimoto, Kaji et al. 2009)
Lung, prostate, pancreatic, breast and colon cancer circulating cells (CTCs)	Anti-epithelial-cell adhesion-molecule (EpCAM), also known as TACSTD1)	0.4 dyn/cm^2, 1-2mL/hr, 460µm/s	50% to 65%	(Nagrath, Sequist et al. 2007)

CD4+ T lymphocyte	anti-CD14, optimum concentration: 75 µg/mL	<0.5 dyn/cm^2	> 80%	(Xuanhong, Gupta et al. 2009)
Platelets	anti-CD36	<0.5 dyn/cm^2	> 80%	(Xuanhong, Gupta et al. 2009)
Type A erythrocytes Type O erythrocytes	Lectin Helix pomatia, Agglutinin (HpA) or Griffonia simplicifolia I (GSI)	No flow	94% 95%	(David, Vijay et al. 2003)
KG1a (acute myeloid leukemia) cells	Nano-particles coated with P-selectin/Fc Chimera, 5 µg/mL	2 dyn/cm^2	70%	(Han, Allio et al. 2009)
Human lymphocyte, MOLT-3	Anti-CD5	0.75 to 1.0 dyn/cm^2	100%, 2.6 min residence time	(Sin, Murthy et al. 2005)
Human lymphocyte cell lines, Raji	Anti-CD19	0.75 to 1.0 dyn/cm^2	75%, 3 min residence time	(Sin, Murthy et al. 2005)
Endothelial progenitor cells, EPC	Anti-CD34, 1010 ligands/mm^2	1.47 dyn/cm^2	54%, 20 fold enrichment	(Plouffe, Kniazeva et al. 2009)
Vascular endothelial cells VEC	Anti-CD31	1.47 dyn/cm^2	53%, 28 fold enrichment	(Plouffe, Kniazeva et al. 2009)
Leukocytes (white blood cells)	Anti-CD16b	1 µL/min	80%	(Hashimoto, Kaji et al. 2009)
Dendritic cells	Uric acid crystals	No flow	-	(Ng, Sharma et al. 2008)

6-9 Acknowledgments

The authors would like to acknowledge National Science and Engineering Research Council of Canada-Collaborative Research program and Discovery program, Genome Canada/ Génome Québec, Le Fonds Québécois de la Recherche sur la Nature et les Technologies-Centre for Biorecognition and Biosensors for their financial support for the development of microfluidic platforms and diagnostic tools.

References

Adam, W. G. and A. H. Daniel (2001). "**Cell separation mediated by differential rolling adhesion**." Biotechnology and Bioengineering **73**(2): 111-124.

Adams, J. D., P. Thevoz, H. Bruus and H. T. Soh (2009). "Integrated acoustic and magnetic separation in microfluidic channels." Applied Physics Letters **95**(25): 254103 (254103 pp.).

Bonner WA, Hulett HR, Sweet RG and H. LA: (1972). "**Fluorescence activated cell sorting.**" Rev Sci Instrum **43**: 404-409.

Buckley, C. D., G. E. Rainger, P. F. Bradfield, G. B. Nash and D. L. Simmons (1998). "**Cell adhesion: more than just glue (Review).**" Molecular Membrane Biology **15**(4): 167-176.

Byrne, M. E., K. Park and N. A. Peppas (2002). "**Molecular imprinting within hydrogels.**" Advanced Drug Delivery Reviews **54**(1): 149-161.

Chang, W. C., L. P. Lee and D. Liepmann (2005). "**Biomimetic technique for adhesion-based collection and separation of cells in a microfluidic channel.**" Lab on a Chip **5**(1): 64-73.

Chen-Min, C., H. Suz-Kai and L. Gwo-Bin (2007). "**Micro flow cytometer chip integrated with micro-pumps/micro-valves for multi-wavelength cell counting and sorting.**" Japanese Journal of Applied Physics, Part 1 (Regular Papers, Short Notes & Review Papers) **46**(5A): 3126-3134.

Chen, Hui W., Colin D. Medley, K. Sefah, D. Shangguan, Z. Tang, L. Meng, Josh E. Smith and W. Tan (2008). "**Molecular Recognition of Small-Cell Lung Cancer Cells Using Aptamers.**" ChemMedChem **3**(6): 991-1001.

Chen, P., X. J. Feng, W. Du and B. F. Liu (2008). "**Microfluidic chips for cell sorting.**" Frontiers in Bioscience **13**: 2464-2483.

Cheung, L. S. L., X. J. Zheng, A. Stopa, J. Schroeder, R. L. Heimark, J. C. Baygents, R. Guzman and Y. Zoharl (2009). **Flow acceleration effect on canser cell deformation abd detachment**, Sorrento, Italy, Institute of Electrical and Electronics Engineers Inc.

Cho, S. H., C. H. Chen, F. S. Tsai, J. M. Godin and Y. H. Lo (2010). "**Human mammalian cell sorting using a highly integrated micro-fabricated fluorescence-activated cell sorter (μFACS).**" Lab on a Chip - Miniaturisation for Chemistry and Biology **10**(12): 1567-1573.

Csordas, A., A. E. Gerdon, J. D. Adams, J. Qian, S. S. Oh, Y. Xiao and H. T. Soh (2010). "**Detection of proteins in serum by micromagnetic aptamer PCR (MAP) technology." Angewandt**e Chemie - International Edition **49**(2): 355-358.

Daniels, D. A., H. Chen, B. J. Hicke, K. M. Swiderek and L. Gold (2003). "**A tenascin-C aptamer identified by tumor cell SELEX: Systematic evolution of ligands by exponential enrichment."** Proceedings of the National Academy of Sciences of the United States of America **100**(26): 15416-15421.

David, D. P., N. Vijay and A. B. Mark (2003). "**Cell affinity separations using magnetically stabilized fluidized beds: Erythrocyte subpopulation fractionation utilizing a lectin-magnetite support."** Biotechnology and Bioengineering **81**(6): 650-665.

Delamarche, E., D. Juncker and H. Schmid (2005). "**Microfluidics for processing surfaces and miniaturizing biological assays**." Advanced Materials **17**(24): 2911-2933.

Deok-Ho, K., A. Haake, S. Yu, A. P. Neild, J. E. Ihm, J. Dual, J. A. Hubbell, J. Byeong-Kwon and B. J. Nelson (2004). **High-throughput cell manipulation using ultrasound fields**, Piscataway, NJ, USA, IEEE.

Di Carlo, D., J. F. Edd, D. Irimia, R. G. Tompkins and M. Toner (2008). "**Equilibrium Separation and Filtration of Particles Using Differential Inertial Focusing.**" Analytical Chemistry **80**(6): 2204-2211.

Di Carlo, D., L. Y. Wu and L. P. Lee (2006). "**Dynamic single cell culture array.**" Lab on a Chip **6**(11): 1445-1449.

Dirican, E. K., O. D. Ozgun, S. Akarsu, K. O. Akin, O. Ercan, M. Ugurlu, C. Camsari, O. Kanyilmaz, A. Kaya and A. Unsal (2008). "**Clinical outcome of magnetic activated cell sorting of non-apoptotic spermatozoa before density gradient centrifugation for assisted reproduction.**" Journal of Assisted Reproduction and Genetics **25**(8): 375-381.

Du, Z., K. H. Cheng, M. W. Vaughn, N. L. Collie and L. S. Gollahon (2007). "**Recognition and capture of breast cancer cells using an antibody-based platform in a microelectromechanical systems device.**" Biomedical Microdevices **9**(1): 35-42.

Du, Z., N. Colls, K. H. Cheng, M. W. Vaughn and L. Gollahon (2006). "**Microfluidic-based diagnostics for cervical cancer cells.**" Biosensors and Bioelectronics **21**(10): 1991-1995.

Ellington, A. D. and J. W. Szostak (1990). "**In vitro selection of RNA molecules that bind specific ligands.**" Nature **346**(6287): 818-818.

Evron, E., W. C. Dooley, C. B. Umbricht, D. Rosenthal, N. Sacchi, E. Gabrielson, A. B. Soito, D. T. Hung, B.-M. Ljung, N. E. Davidson and S. Sukumar (2001). "**Detection of breast cancer cells in ductal lavage fluid by methylation-specific PCR**." The Lancet **357**(9265): 1335-1336.

Fatanat Didar, T., A. Dolatabadi and R. Wüthrich (2008). "**Characterization and modeling of 2D-glass micro-machining by spark-assisted chemical engraving (SACE) with constant velocity.**" Journal of Micromechanics and Microengineering **18**(6): 5016.

Fuqua, S. A. W., C. Wiltschke, Q. X. Zhang, A. Borg, C. G. Castles, W. E. Friedrichs, T. Hopp, S. Hilsenbeck, S. Mohsin, P. O'Connell and D. C. Allred (2000). "**A Hypersensitive Estrogen Receptor-{{alpha}} Mutation in Premalignant Breast Lesions.**" Cancer Res **60**(15): 4026-4029.

Goto, M., T. Tsukahara, K. Sato and T. Kitamori (2008). "**Micro- and nanometer-scale patterned surface in a microchannel for cell culture in microfluidic devices.**" Analytical and Bioanalytical Chemistry **390**(3): 817-823.

Green, J. V. and M. K. (2009). "**Microfluidic enrichment of a target cell type from a heterogenous suspension by adhesion-based negative selection.**" Lab Chip **9**: 2245-2248.

Gristina, R., E. D'Aloia, G. S. Senesi, A. Millella, M. Nardulli, E. Sardella, P. Favia and R. d'Agostino (2009). "I**ncreasing Cell Adhesion on Plasma Deposited Fluorocarbon Coatings by Changing the Surface Topography.**" Journal of Biomedical Materials Research Part B-Applied Biomaterials **88B**(1): 139-149.

Guo, K.-T., R. SchÄfer, A. Paul, A. Gerber, G. Ziemer and H. P. Wendel (2006). "**A New Technique for the Isolation and Surface Immobilization of Mesenchymal Stem Cells from Whole Bone Marrow Using High-Specific DNA Aptamers.**" Stem Cells **24**(10): 2220-2231.

Gupta, R. and A. Kumar (2008). "**Molecular imprinting in sol-gel matrix.**" Biotechnology Advances **26**(6): 533-547.

Gutierrez, E., B. G. Petrich, S. J. Shattil, M. H. Ginsberg, A. Groisman and A. Kasirer-Friede (2008). "**Microfluidic devices for studies of shear-dependent platelet adhesion.**" Lab on a Chip **8**(9): 1486-1495.

H., H. and A. Puchalski (2007). **Systems and methods for identifying organ transplant risk**. U. Patent. US, Renovak Inc. **US Patent 7244555**.

Han, W., B. A. Allio, D. G. Foster and M. R. King (2009). "N**anoparticle Coatings for Enhanced Capture of Flowing Cells in Microtubes.**" ACS Nano **4**(1): 174-180.

Hasenbein, M. E., T. T. Andersen and R. Bizios (2002). "**Micropatterned surfaces modified with select peptides promote exclusive interactions with osteoblasts.**" Biomaterials **23**(19): 3937-3942.

Hashimoto, M., H. Kaji and M. Nishizawa (2009). "**Selective capture of a specific cell type from mixed leucocytes in an electrode-integrated microfluidic device.**" Biosensors and Bioelectronics **24**(9): 2892-2897.

Hengyu, W., K. Jeong-Hwan, Z. Min, T. Steve and K. Jin-Woo (2008). "**Adhesion study of Escherichiacoli cells on nano-/microtextured surfaces in a microfluidic system.**" IEEE Transactions on Nanotechnology **7**(5): 573-579.

Herr, J. K., J. E. Smith, C. D. Medley, D. Shangguan and W. Tan (2006). "**Aptamer-Conjugated Nanoparticles for Selective Collection and Detection of Cancer Cells.**" Analytical Chemistry **78**(9): 2918-2924.

Herzenberg, L. A., R. G. Sweet and A. Herzenberg (1976). "**Fluorescence-activated cell sorting.**" Scientific American **234**(3): 108-116.

Hua, J., L. E. Erickson, Y. Yiin Tian and L. A. Glasgow (1993). "**A review of the effects of shear and interfacial phenomena on cell viability.**" Critical Reviews in Biotechnology **13**(Compendex): 305-328.

Hybarger, G., J. Bynum, R. F. Williams, J. J. Valdes and J. P. Chambers (2006). "**A microfluidic SELEX prototype.**" Analytical and Bioanalytical Chemistry **384**(1): 191-198.

Jian, C., S. Usami and D. Cheng (1997). "**Development of a side-view chamber for studying cell-surface adhesion under flow conditions.**" Annals of Biomedical Engineering **25**(3): 573-580.

Johansson, L., F. Nikolajeff, S. Johansson and S. Thorslund (2009). "**On-chip fluorescence-activated cell sorting by an integrated miniaturized ultrasonic transducer.**" Analytical Chemistry **81**(13): 5188-5196.

Jonas, A. and P. Zemanek (2008). "**Light at work: The use of optical forces for particle manipulation, sorting, and analysis.**" Electrophoresis **29**(24): 4813-4851.

Joong Yull, P., Y. Sung Ju, H. Chang Mo and L. Sang-Hoon (2009). "**Simultaneous generation of chemical concentration and mechanical shear stress gradients using microfluidic osmotic flow comparable to interstitial flow.**" Lab on a Chip **9**(15): 2194-2202.

K**aji, H., M. Hashimoto and M. Nishizawa** (2006). "**On-Demand Patterning of Protein Matrixes Inside a Microfluidic Device.**" Analytical Chemistry **78**(15): 5469-5473.

Kalinina, S., H. Gliemann, M. Lopez-Garcia, A. Petershans, J. Auernheimer, T. Schimmel, M. Bruns, A. Schambony, H. Kessler and D. Wedlich (2008). "**Isothiocyanate-functionalized RGD peptides for tailoring cell-adhesive surface patterns.**" Biomaterials **29**(20): 3004-3013.

Kam, L., W. Shain, J. N. Turner and R. Bizios (2002). "**Selective adhesion of astrocytes to surfaces modified with immobilized peptides.**" Biomaterials **23**(2): 511-515.

Kang, Y. and D. Li (2009). "**Electrokinetic motion of particles and cells in microchannels.**" Microfluidics and Nanofluidics **6**(4): 431-460.

Keon Woo, K., C. Sung Sik, L. Sang Ho, K. Byungkyu, L. Se Na, P. Min Cheol, K. Pilnam, H. Se Yon and K. Y. Suh (2007). "**Label-free, microfluidic separation and enrichment of human breast cancer cells by adhesion difference.**" Lab on a Chip **7**(11): 1461-1468.

Kruger, J., K. Singh, A. O'Neill, C. Jackson, A. Morrison and P. O'Brien (2002). "**Development of a microfluidic device for fluorescence activated cell sorting.**" Journal of Micromechanics and Microengineering **12**(4): 486-494.

Kumar, A. and A. Bhardwaj (2008). "**Methods in cell separation for biomedical application: cryogels as a new tool.**" Biomedical Materials **3**(3): 034008 (034011 pp.).

Kwon, K. W., S. H. Lee, B. Kim, M. C. Park, P. Kim and K. Y. Suh (2007). **Label-free, microfluidic separation of human breast carcinoma and epithelial cells by adhesion difference**, Lyon, France, Inst. of Elec. and Elec. Eng. Computer Society.

Lang, W. (1996). "**Silicon microstructuring technology.**" Materials Science and Engineering R: Reports **17**(1): 1-55.

Liu, Y.-J., S.-S. Guo, Z.-L. Zhang, W.-H. Huang, D. Baigl, M. Xie, Y. Chen and D.-W. Pang (2007). "**A micropillar-integrated smart microfluidic device for specific capture and sorting of cells.**" ELECTROPHORESIS **28**(24): 4713-4722.

Lovchik, R. D., F. Bianco, M. Matteoli and E. Delamarche (2009). "**Controlled deposition of cells in sealed microfluidics using flow velocity boundaries.**" Lab on a Chip **9**(10): 1395-1402.

Lu, H., L. Y. Koo, W. M. Wang, D. A. Lauffenburger, L. G. Griffith and K. F. Jensen (2004). "**Microfluidic shear devices for quantitative analysis of cell adhesion.**" Analytical Chemistry **76**(18): 5257-5264.

Lu, S., A. Bansal, W. Soussou, T. W. Berger and A. Madhukar (2006). "**Receptorâˆ'Ligand-Based Specific Cell Adhesion on Solid Surfaces: Hippocampal Neuronal Cells on Bilinker Functionalized Glass.**" Nano Letters **6**(9): 1977-1981.

Luban, N. L. C. (1994). "**Review of neonatal red cell transfusion practices.**" Blood Reviews **8**(3): 148-153.

M., R., I. R. and Murthy S. (2006). "**Micro- and nanotechnology in cell separation.**" International Journal of Nanomedicine **1**: 3-14.

Makino, A., H. Y. Shin, Y. Komai, S. Fukuda, M. Coughlin, M. Sugihara-Seki and G. W. Schmid-Schonbein (2007). "**Mechanotransduction in leukocyte activation: a review.**" Biorheology **44**(Copyright 2008, The Institution of Engineering and Technology): 221-249.

Manbachi, A., S. Shrivastava, M. Cioffi, C. Bong Geun, M. Moretti, U. Demirci, M. Yliperttula and A. Khademhosseini (2008). "**Microcirculation within grooved substrates regulates cell positioning and cell docking inside microfluidic channels.**" Lab on a Chip **8**(5): 747-754.

Maraldo, D. and R. Mutharasan (2007). "**Optimization of antibody immobilization for sensing using piezoelectrically excited-millimeter-sized cantilever (PEMC) sensors.**" Sensors and Actuators B: Chemical **123**(1): 474-479.

Marek, R., M. Caruso, A. Rostami, J. B. Grinspan and J. D. Sarma (2008). "**Magnetic cell sorting: A fast and effective method of concurrent isolation of high purity viable astrocytes and microglia from neonatal mouse brain tissue.**" Journal of Neuroscience Methods **175**(1): 108-118.

Mattanovich, D. and N. Borth (2006). "**Applications of cell sorting in biotechnology.**" Microbial Cell Factories **5**(1): 12.

Miltenyi S, Muller W, eichel W and R. A (1990). "**High gradient magnetic cell separation with MACS.**" Cytometry **11**: 231-238.

Min-Hsien, W. (2009). "**Simple poly(dimethylsiloxane) surface modification to control cell adhesion.**" Surface and Interface Analysis **41**(1): 11-16.

Morris, K. N., K. B. Jensen, C. M. Julin, M. Weil and L. Gold (1998). "**High affinity ligands from in vitro selection: Complexâ€‰targets.**" Proceedings of the National Academy of Sciences of the United States of America **95**(6): 2902-2907.

Murthy, S. K., A. Sin, R. G. Tompkins and M. Toner (2004). "**Effect of flow and surface conditions on human lymphocyte isolation using microfluidic chambers.**" Langmuir **20**(26): 11649-11655.

Murthy, S. K., M. E. Taslim, D. S. Sokhey, M. Abedi, T. Kniazeva and J. V. Green (2009). "**Effect of channel geometry on cell adhesion in microfluidic devices.**" Lab on a Chip **9**(5): 677-685.

Nagrath, S., L. V. Sequist, S. Maheswaran, D. W. Bell, D. Irimia, L. Ulkus, M. R. Smith, E. L. Kwak, S. Digumarthy, A. Muzikansky, P. Ryan, U. J. Balis, R. G. Tompkins, D. A. Haber and M. Toner (2007). "I**solation of rare circulating tumour cells in cancer patients by microchip technology**." Nature **450**(7173): 1235-U1210.

Nalayanda, D. D., M. Kalukanimuttam and D. W. Schmidtke (2007). "**Micropatterned surfaces for controlling cell adhesion and rolling under flow.**" Biomedical Microdevices **9**(2): 207-214.

Nery, A. A., C. Wrenger and H. Ulrich (2009). "**Recognition of biomarkers and cell-specific molecular signatures: Aptamers as capture agents.**" Journal of Separation Science **32**(10): 1523-1530.

Ng, G., K. Sharma, S. M. Ward, M. D. Desrosiers, L. A. Stephens, W. M. Schoel, T. L. Li, C. A. Lowell, C. C. Ling, M. W. Amrein and Y. Shi (2008). "**Receptor-Independent, Direct Membrane Binding Leads to Cell-Surface Lipid Sorting and Syk Kinase Activation in Dendritic Cells.**" Immunity **29**(5): 807-818.

Nguyen, T., R. Pei, M. Stojanovic and Q. Lin (2009). "**An aptamer-based microfluidic device for thermally controlled affinity extraction.**" Microfluidics and Nanofluidics **6**(4): 479-487.

Nguyen, T. H., R. Pei, C. Qiu, J. Ju, M. Stojanovic and Q. Lin (2009). "**An aptameric microfluidic system for specific purification, enrichment, and mass spectrometric detection of biomolecules**." Journal of Microelectromechanical Systems **18**(6): 1198-1207.

Nichola, C., L. L. Jane and R. K. Michael (2007). "**Investigating the Feasibility of Stem Cell Enrichment Mediated by Immobilized Selectins.**" Biotechnology Progress **23**(6): 1463-1472.

Nilsson, A., F. Petersson, H. Jonsson and T. Laurell (2004). "**Acoustic control of suspended particles in micro fluidic chips.**" Lab on a Chip **4**(2): 131-135.

Nilsson, J., M. Evander, B. Hammarström and T. Laurell (2009). "**Review of cell and particle trapping in microfluidic systems.**" Analytica Chimica Acta **649**(2): 141-157.

Olbrich, K. C., T. T. Andersen, F. A. Blumenstock and R. Bizios (1996). "**Surfaces modified with covalently-immobilized adhesive peptides affect fibroblast population motility.**" Biomaterials **17**(8): 759-764.

Pappas, D. and K. Wang (2007). "**Cellular separations: A review of new challenges in analytical chemistry.**" Analytica Chimica Acta **601**(1): 26-35.

P**ark, P. C., S. Selvarajah, J. Bayani, M. Zielenska and J. A. Squire** (2007). "**Stem cell enrichment approaches.**" Seminars in Cancer Biology **17**(3): 257-264.

Patrito, N., C. McCague, P. R. Norton and N. O. Petersen (2007). "**Spatially controlled cell adhesion via micropatterned surface modification of poly(dimethiylsiloxane).**" Langmuir **23**(2): 715-719.

Phillips, J. A., Y. Xu, Z. Xia, Z. H. Fan and W. Tan (2008). "**Enrichment of Cancer Cells Using Aptamers Immobilized on a Microfluidic Channel.**" Analytical Chemistry **81**(3): 1033-1039.

Plouffe, B. D., T. Kniazeva, J. E. Mayer, Jr., S. K. Murthy and V. L. Sales (2009). "**Development of microfluidics as endothelial progenitor cell capture technology for cardiovascular tissue engineering and diagnostic medicine.**" FASEB J. **23**(10): 3309-3314.

Plouffe, B. D., D. N. Njoka, J. Harris, J. Liao, N. K. Horick, M. Radisic and S. K. Murthy (2007). "**Peptide-mediated selective adhesion of smooth muscle and endothelial cells in microfluidic shear flow.**" Langmuir **23**(9): 5050-5055.

Plouffe, D., M. Brown, R. K.Iyer, M. Radisic and S. Murthy (2009). "**Controlled capture and release of cardiac fibroblasts using peptide-functionalized alginate gels in microfluidic channels.**" Lab Chip **9**: 1507-1510.

Qin, M., S. Hou, L. Wang, X. Feng, R. Wang, Y. Yang, C. Wang, L. Yu, B. Shao and M. Qiao (2007). "**Two methods for glass surface modification and their application in protein immobilization.**" Colloids and Surfaces B: Biointerfaces **60**(2): 243-249.

Rao, Y., X. Wu, J. Gariepy, U. Rutishauser and C. Siu (1992). "**Identification of a peptide sequence involved in homophilic binding in the neural cell adhesion molecule NCAM.**" J. Cell Biol. **118**(4): 937-949.

Rao, Y., X. F. Wu, J. Gariepy, U. Rutishauser and C. H. Siu (1992). "**Identification of a peptide sequence involved in homophilic binding in the neural cell adhesion molecule NCAM.**" J. Cell Biol. **118**(4): 937-949.

Rotariu, O., I. D. Ogden, M. MacRae, L. E. Udrea and N. J. C. Strachan (2005). "**Multiple sample flow through immunomagnetic separator for concentrating pathogenic bacteria."** Physics in Medicine and Biology **50**(12): 2967-2977.

Schena, E. M. (1999). **DNA Microarrays: A Practical Approach.** Oxford, UK, Oxford University Press.

Shaikh-Mohammed, J., M. Li, D. Terala and M. J. McShane (2004). **Integrated Micro/Nano-Fabrication of Cell Culture Scaffolds with Selective Cell Adhesion and Fluorescent Indicators**, San Jose, CA., United states, SPIE.

Shangguan, D., Y. Li, Z. Tang, Z. C. Cao, H. W. Chen, P. Mallikaratchy, K. Sefah, C. J. Yang and W. Tan (2006). "**Aptamers evolved from live cells as effective molecular probes for cancer study.**" Proceedings of the National Academy of Sciences **103**(32): 11838-11843.

Shangguan, D., L. Meng, Z. C. Cao, Z. Xiao, X. Fang, Y. Li, D. Cardona, R. P. Witek, C. Liu and W. Tan (2008). "**Identification of Liver Cancer-Specific Aptamers Using Whole Live Cells.**" Analytical Chemistry **80**(3): 721-728.

Shunichi, U., C. Hsuan-Hsu, Z. Yihua, C. Shu and R. Skalak (1993). "**Design and construction of a linear shear stress flow chamber.**" Annals of Biomedical Engineering **21**(1): 77-83.

Sin, A., S. K. Murthy, A. Revzin, R. G. Tompkins and M. Toner (2005). "**Enrichment using antibody-coated microfluidic chambers in shear flow: Model mixtures of human lymphocytes.**" Biotechnology and Bioengineering **91**(7): 816-826.

St. John, P. M., L. Kam, S. W. Turner, H. G. Craighead, M. Issacson, J. N. Turner and W. Shain (1997). "**Preferential glial cell attachment to microcontact printed surfaces**." Journal of Neuroscience Methods **75**(2): 171-177.

Stefan, M., M. Werner, W. Walter and R. Andreas (1990). "**High gradient magnetic cell separation with MACS.**" Cytometry **11**(2): 231-238.

Stroumpoulis, D., Z. Haining, L. Rubalcava, J. Gliem and M. Tirrell (2007). "**Cell adhesion and growth to peptide-patterned supported lipid membranes.**" Langmuir **23**(7): 3849-3856.

Studer, V., R. Jameson, E. Pellereau, A. Pepin and Y. Chen (2004). **A microfluidic mammalian cell sorter based on fluorescence detection,** Elsevier.

Sun Min, K., L. Sung Hoon and S. Kahp Yang (2008). "**Cell research with physically modified microfluidic channels: a review.**" Lab on a Chip **8**(Copyright 2009, The Institution of Engineering and Technology): 1015-1023.

Suparna Mandal, J. M. R. O. S. E. G. (2007). "**Cytophobic Surface Modification of Microfluidic Arrays for In Situ Parallel Peptide Synthesis and Cell Adhesion Assays.**" Biotechnology Progress **23**(4): 972-978.

Takagi, J., M. Yamada, M. Yasuda and M. Seki (2005). "**Continuous particle separation in a microchannel having asymmetrically arranged multiple branches.**" Lab on a Chip **5**(7): 778-784.

Theera-Umpon, N. and P. D. Gader (2002). "**System-level training of neural networks for counting white blood cells.**" IEEE Transactions on Systems, Man and Cybernetics, Part C (Applications and Reviews) **32**(1): 48-53.

Tomas Koblas, S. M. H., Frantisek Saudek (2005). "**The Application of Umbilical Cord Blood Cells in the Treatment of Diabetes Mellitus.**" Diabetic Perspectives **2(4)**: 228-234.

Tsutsui, H. and C.-M. Ho (2009). "**Cell separation by non-inertial force fields in microfluidic systems.**" Mechanics Research Communications **36**(1): 92-103.

Tuerk C, G. L. (1990). "**Systematic evolution of ligands by exponential enrichment: RNA ligands to bacteriophage T4 DNA polymerase.**" Science **249.**: 505-510.

Turner, N. W., C. W. Jeans, K. R. Brain, C. J. Allender, V. Hlady and D. W. Britt (2006). "**From 3D to 2D: A review of the molecular imprinting of proteins**." Biotechnology Progress **22**(6): 1474-1489.

Ulrich, H., J. E. Ippolito, O. R. PagÃ¡n, V. A. Eterovic, R. M. Hann, H. Shi, J. T. Lis, M. E. Eldefrawi and G. P. Hess (1998). "**In vitro selection of RNA molecules that displace cocaine from the membrane-bound nicotinic acetylcholine receptor.**" Proceedings of the National Academy of Sciences of the United States of America **95**(24): 14051-14056.

Ulrich, H., M. H. Magdesian, M. J. l. M. Alves and W. Colli (2002). "**In Vitro Selection of RNA Aptamers That Bind to Cell Adhesion Receptors of Trypanosoma cruzi and Inhibit Cell Invasion.**" Journal of Biological Chemistry **277**(23): 20756-20762.

Walker, G. M., H. C. Zeringue and D. J. Beebe (2004). "**Microenvironment design considerations for cellular scale studies.**" Lab on a Chip **4**(2): 91-97.

Wang, H., Y. Liu, C. Liu, J. Huang, P. Yang and B. Liu (2010). "**Microfluidic chip-based aptasensor for amplified electrochemical detection of human thrombin.**" Electrochemistry Communications **12**(2): 258-261.

Wang, M. M., E. Tu, D. E. Raymond, J. M. Yang, H. Zhang, N. Hagen, B. Dees, E. M. Mercer, A. H. Forster, I. Kariv, P. J. Marchand and W. F. Butler (2005). "**Microfluidic sorting of mammalian cells by optical force switching.**" Nature Biotechnology **23**(1): 83-87.

Westcott, N. P., B. M. Lamb and M. N. Yousaf (2009). "**Electrochemical and chemical microfluidic gold etching to generate patterned and gradient substrates for cell adhesion and cell migration.**" Analytical Chemistry **81**(9): 3297-3303.

Whitesides, G. M., E. Ostuni, S. Takayama, X. Jiang and D. E. Ingber (2001). "**Soft lithography in biology and biochemistry.**" Annual Review of Biomedical Engineering **3**(1): 335-373.

Wilbur, J. L., A. Kumar, E. Kim and G. M. Whitesides (1994). "**Microfabrication by microcontact printing of self-assembled monolayers.**" Advanced Materials **6**(7-8): 600-604.

Wu, Y., K. Sefah, H. Liu, R. Wang and W. Tan (2010). "**DNA aptamer-micelle as an efficient detection/delivery vehicle toward cancer cells.**" Proceedings of the National Academy of Sciences of the United States of America **107**(1): 5-10.

Wysocki LJ and S. VL (1978). "**Panning' for lymphocytes: A method for cell selection.**" Proc Natl Acad Sci USA **75**: 2844-2848.

Xia, Y. and G. M. Whitesides (1997). "**Extending Microcontact Printing as a Microlithographic Technique.**" Langmuir **13**(7): 2059-2067.

Xinhui, L., Q. Jiangrong, X. Yi, L. Viel, A. E. Gerdon, E. T. Lagally, P. Atzberger, T. M. Tarasow, A. J. Heeger and H. T. Soh (2009). "**Micromagnetic selection of aptamers in microfluidic channels.**" Proceedings of the National Academy of Sciences of the United States of America **106**(9): 2989-2994.

Xu, W. and A. D. Ellington (1996). "**Anti-peptide aptamers recognize amino acid sequence and bind a protein epitope.**" Proceedings of the National Academy of Sciences of the United States of America **93**(15): 7475-7480.

Xu, Y., J. A. Phillips, J. Yan, Q. Li, Z. H. Fan and W. Tan (2009). "**Aptamer-based microfluidic device for enrichment, sorting, and detection of multiple cancer cells.**" Analytical Chemistry **81**(17): 7436-7442.

Xuanhong, C., A. Gupta, C. Chihchen, R. G. Tompkins, W. Rodriguez and M. Toner (2009). "**Enhancing the performance of a point-of-care CD4+ T-cell counting microchip through monocyte depletion for HIV/AIDS diagnostics.**" Lab on a Chip **9**(10): 1357-1364.

Xunli, Z., P. Jones and S. J. Haswell (2008). "**Attachment and detachment of living cells on modified microchannel surfaces in a microfluidic-based lab-on-a-chip system.**" Chemical Engineering Journal: 82-88.

Yamada, M. and M. Seki (2005). "**Hydrodynamic filtration for on-chip particle concentration and classification utilizing microfluidics**." Lab on a Chip **15**: 1233-1239.

Young, E. W. K., A. R. Wheeler and C. A. Simmons (2007). "**Matrix-dependent adhesion of vascular and valvular endothelial cells in microfluidic channels.**" Lab on a Chip **7**(12): 1759-1766.

Yu-Cheng, L. and J. Chun-Ping (2002). "**Mechanism of hydrodynamic separation of biological objects in microchannel devices.**" Lab on a Chip **2**(3): 164-169.

Zhang, J., X. Jia, X. J. Lv, Y. L. Deng and H. Y. Xie (2010). "**Fluorescent quantum dot-labeled aptamer bioprobes specifically targeting mouse liver cancer cells.**" Talanta **81**(1-2): 505-509.

Zhang, X., P. Jones and S. J. Haswell (2007). "**Attachment and detachment of living cells on modified microchannel surfaces in a microfluidic-based lab-on-a-chip system.**" Chemical Engineering Journal **135**(SUPPL. 1): S82-S88.

Zhang, Z. L., C. Crozatier, M. Le Berre and Y. Chen (2005). "**In situ bio-functionalization and cell adhesion in microfluidic devices.**" Microelectronic Engineering **78-79**: 556-562.

Chapter 7. Patterning multiplex protein microarrays in a single microfluidic channel

7-1 Connecting text

Bio-functional detection interfaces are one of the most important and crucial parts of adhesion-based microfluidic devices. Therefore the first step was to produce and embed bio-functional interfaces in LOC chips. In this chapter a combinatorial approach is presented for proper cell-specific probe immobilization inside microfluidic channels with covalent bounds. This approach for producing bio-functional interfaces was further exploited in chapters 8 and 9 to generate multiplex surface gradients of biomolecules and to separate primary and rare cells.

The results of this chapter has been published in this paper:

-Tohid Fatanat Didar, A. Foudeh and M. Tabrizian, (2012), Patterning multiplex protein microarrays in a single microfluidic channel, Analytical Chemistry, 84 (2), 1012-1018.

7-2 Abstract

The development of versatile bio-functional surfaces is a fundamental prerequisite in designing Lab-on-Chip (LOC) devices for applications in biosensing interfaces and micro-bioreactors. The current paper presents a rapid combinatorial approach to create multiplex protein patterns in a single microfluidic channel. This approach consists of coupling micro-contact printing with microfluidic patterning, where micro-contact printing is employed for silanization using (3-Aminopropyl) triethoxysilane (APTES), followed by microfluidic patterning of multiple antibodies. As a result, the biomolecules of choice could be covalently attached to the microchannel surface, thus creating a durable and highly resistant functional interface. Moreover, the experimental procedure was designed to create a microfluidic platform that maintains functionality at high flow rates. The functionalized surfaces were characterized using X-ray photoelectron spectroscopy (XPS) and monitored with fluorescence microscopy at each step of functionalization. To illustrate the possibility of patterning multiple biomolecules along the cross section of a single microfluidic channel, microarrays of five different primary antibodies were patterned onto a single channel and their functionality was evaluated accordingly through a multiplex immunoassay using secondary antibodies specific to each patterned primary antibody. The resulting patterns remained stable at shear stresses of up to 50 dyn/cm^2. The overall findings suggest that the developed multiplex functional interface on a single channel can successfully lead to highly resistant multiplex functional surfaces for high throughput biological assays.

7-3 Introduction

Precise microfluidic control and manipulation of liquids in geometrically-controlled miniaturized channels has proven a useful tool for developing Lab-on-a-Chip (LOC) devices (Whitesides 2006). Among the microfluidic platforms under development, multiplex detection interfaces, created by patterns of different biomarkers or multiple stimuli in a single LOC device, has attracted much attention for high throughput biological applications such as biosensing (Walter, Büssow et al. 2000, Shamansky, Davis et al. 2001, Lee, Lim et al. 2006, Nakajima, Ishino et al. 2006, Fiddes, Chan et al. 2010), micro-bioreactors and cell detection (Saliba, Saias et al. , Takayama, McDonald et al. 1999, Kirby, Wheeler et al. 2003, Khademhosseini, Suh et al. 2004, Patrito, McCague et al. 2006, Didar and Tabrizian 2010, Fricke, Zentis et al. 2011). To develop bio-functional LOC devices, spatial positioning and orientation, as well as binding of functional biomolecules to substrates should be well controlled. Localized and region specific patterning of multiple biomarker microarrays within microfluidic platforms is another important feature of a functional interface for the production of multiplex high-throughput devices (Barbulovic-Nad, Lucente et al. 2006, Wu, Castner et al. 2008).

Despite promising progress in developing functional surfaces in LOC devices, many limitations remain in terms of producing highly resistant devices with durable multiplex detection interfaces using cost effective and straightforward techniques. Several approaches have been introduced to pattern biomarkers on microchannel surfaces (Khademhosseini, Suh et al. 2004, Kaji, Hashimoto et al. 2006, Shi, Yang et al. 2008, Fiddes, Chan et al. 2010, Kim, Choi et al. 2010, Tan, Cipriany et al. 2010, Yin, Tao et al. 2010, Kim, Lee et al. 2011). Among them, microfluidic patterning (Takayama, McDonald et al. 1999) and micro-contact printing (Renault, Bernard et al. 2002) (Kaufmann and Ravoo 2010) are widely used since they are simple and rapid to implement. Microfluidic patterning involves using laminar flow streams to functionalize surfaces, though results are limited to geometrical patterns along the streamlines. This limitation can be overcome by soft lithographic approaches, such as micro-contact printing using

different stamp designs for region specific functionalization (Kaufmann and Ravoo 2010). However, common techniques used to irreversibly bind the microfluidic substrates (e.g. plasma treatment) are destructive to the micro-contact printed patterns. To protect the contact-printed surfaces, a poly(dimethylsiloxane) (PDMS) stamp can be placed on the surface during plasma treatment (Khademhosseini, Suh et al. 2004) or an opaque box of PDMS can be used (Jiang, Xu et al. 2005). These techniques are either time consuming or require additional steps to arrive at an irreversibly sealed microfluidic device.

The robustness of the functionalized interface is another important consideration. Many platforms developed via micro-contact printing rely on physical adsorption of biomolecules to the substrate. Protein patterns formed in this manner tend to detach from surfaces (Rosengren, Pavlovic et al. 2002) and are in turn particularly problematic in microfluidic systems operating under various flow conditions. The efficacy and durability of such patterns may also be altered for long-term applications. Covalent binding using silane solutions, which create active groups on microfluidic substrates for the subsequent attachment of biomolecules, is usually employed to address this limitation. The requirement for air free environments, and the need to work under nitrogen or argon chambers, (Murthy, Sin et al. 2004, Howarter and Youngblood 2006, Mandal, Rouillard et al. 2007, Maraldo and Mutharasan 2007, Hosseinidoust, Van de Ven et al. 2011) reduces the versatility of the silanization technique for the development of time effective interfaces.

For multiplex patterning, robotic printing is the most commonly used technique with which different ligands can be patterned onto a small area. The advantage of this technique resides in patterning different biomarkers onto a small area, though the system is very costly and occupies a large space.

In this work, a dual approach using a combination of micro-contact printing and microfluidic patterning is implemented to create highly resistant multiplex detection interfaces in a microfluidic platform. A protocol for micro-contact printing of (3-Aminopropyl) triethoxysilane (APTES) on glass substrates is introduced as a promising approach for rapid and simple printing of functional

groups to create region specific patterns. Simulation of the flow conditions and diffusion between laminar flow streams containing different concentrations of biomolecules was performed to obtain experimental conditions in which multiplex probes are produced within a single channel. The proposed approach provides the following advantages: i) creates a multiplex detection interface on a single channel for high throughput biological applications; ii) uses silane micro-contact printing to introduce amine functional groups onto the microchannel surface as a means to covalently immobilize the biomolecule of choice, thus overcoming the problems posed by the physical immobilization of biomolecules such as resistance to shear stress; iii) drastically reduces the time and effort required for silane patterning of the surface; iv) results in a microfluidic device capable of withstanding high flow rates through irreversible binding; v) controls the patterning outcome by flow conditions and concentration of the proteins in each flow, in which the patterned probes could posses single or dual antibodies.

7-3 Materials and methods

7-3-1 Reagents and materials

The negative photoresist SU8-2025 was purchased from Microchem Corp (Boston, MA, USA). (3-Aminopropyl) triethoxysilane (APTES), 1-ethyl-3-(3-dimethylaminopropyl) carbodiimide (EDC), N-hydroxysuccinimide (NHS), phosphate buffered saline (PBS), hydrogen peroxide, bovine serum albumin (BSA) and sulfuric acid were purchased from Sigma-Aldrich (Oakville, Ontario, Canada). Sylgard 184 elastomer kit composed of pre-polymer and curing agent of poly(dimethylsiloxane) (PDMS) was purchased from Essex Chemical (Boston, MA). Mouse Anti-CD34, rabbit AntiCD-31 and rat Anti-CD36 primary antibodies, anti-rabbit Cy3 conjugated IgG secondary antibody, anti-rat Cy5 conjugated IgG secondary antibody, and anti-mouse fluorescein isothiocyanate (FITC) conjugated IgG secondary antibody were purchased from Abcam (Cambridge, MA, USA).

7-3-2 Design and fabrication of the microfluidic device

Microfluidic design for channel systems (μFN) and stamps for micro-contact printing were generated using AutoCAD® software (Autodesk Inc., CA, USA). The device consists of seven input microchannels, 100 μm in width and 60 μm in depth merging into a main channel in three different areas (Figures 7-1E and 3-1H). The design was printed on a chrome mask. To fabricate the mold for soft lithography, negative photoresist (SU-8 2025) was spin-coated (at 1500 rpm for 30 seconds) on a silicon wafer and baked to drive off solvent. Photolithography was performed on the wafer using the printed mask to fabricate the mold. The mold was used to create the PDMS platforms. The protocol for creating the irreversibly sealed microfluidic platform is described in the next sections. Once the closed channels were formed, the inlet and outlet tubes were connected. Flow control was achieved using a multi stage syringe pump (Nexus 3000, Chemyx Inc. Stafford, TX). 18G syringe needles (BD, ON, Canada) were cut and used as inlet and outlet connections. Modified pipette tips were used as a support to fix the inlets and outlets by epoxy glue (Figure 7-1H).

7-3-3 Simulation

Simulation of concentration distribution in the device was performed using COMSOL (COMSOL, Inc. Burlington, MA). The Computational Fluid Dynamics (CFD) analysis was first performed to solve the continuity (eq 7-1) and Navier-Stokes (eq 7-2) equations:

$$\nabla . \mathbf{u} = 0 \qquad (7\text{-}1)$$

$$\rho\, \partial \mathbf{u}/\partial \mathbf{t} - \nabla[\eta(\nabla \mathbf{u} + (\nabla \mathbf{u})\,] + \rho(\mathbf{u}.\nabla)\mathbf{u} + \nabla \mathbf{p} = \mathbf{F} \qquad (7\text{-}2)$$

in which η is the dynamic viscosity ρ density, u velocity, p pressure, and F volume force field. Eq (7-2) can be simplified by assuming steady state conditions and volume forces equal to zero. Species diffusion in the solution was then modeled using multi-physics properties of the software. The velocity components from the CFD results were simultaneously implemented for concentration distribution using the convection and diffusion module. Species diffusion in flow conditions was solved according to eq (7-3):

$$\frac{\partial \mathbf{c}}{\partial \mathbf{t}} + \nabla . (-\mathbf{D}\nabla \mathbf{c} + \mathbf{c}\mathbf{u}) = 0 \qquad (7\text{-}3)$$

in which c represents each species concentration and D is the diffusion coefficient (about 1×10^{-11} m^2 s^{-1} for proteins). The geometrical model was generated in AutoCAD software and was imported into COMSOL interface. The fluid inside the channels was assumed to have the properties of water (Newtonian fluid) and a no-slip boundary condition was applied. Inlets and outlets were specified as the entire opening at the beginning and end of each geometry, as opposed to the actual microfluidic device in which inlet holes are in the channel roof. This assumption only changes the flow profile at the inlets and outlets of each channel and has no effect on the velocity/concentration profile within the channels (Green, Kniazeva et al. 2009).

7-3-4 Micro-contact printing of APTES on glass

Different types of PDMS stamps were used for APTES micro-contact printing: flat stamps to create uniform amine groups on the surface and stamps with patterns to create independent bio-functional spots. The PDMS stamp was plasma treated for 1 min using oxygen plasma (60 s, 200 W, 200 mTorr O_2). It was then covered

with 10 µl of 2% APTES solution in ethanol at room temperature. To avoid evaporation of the APTES solution, a cover slip was placed on the stamp for 1 min. After rinsing with 70% ethanol solution for 15 sec and drying under nitrogen gas for 30 sec, the stamp was gently brought into contact with the predetermined areas on glass substrate for 5 sec. Immediately after printing the APTES solution, the plasma treated PDMS substrate (µFN) was brought into contact with the micro-contact printed glass substrate to form the microfluidic device as described in the previous sections. The device was then placed in an oven at 100 ºC for 60 minutes to ensure covalent binding of APTES with glass proceeded through condensation of hydrogen bonded silanol groups (Figure S7-5).

7-3-5 Region specific surface patterning in stop flow conditions

Micro-contact printing and glass surface functionalization were initially performed in stop-flow conditions to optimize the surface functionalization procedure. APTES was contact printed according to the protocol described previously using the desired patterns fabricated on PDMS stamps. The substrate was then cured in an oven at 100ºC for 1 hour. NHS (5 mg/ml) was used along with EDC (2 mg/ml) to crosslink the biomolecules to the amino-silanized patterned surface (Figure S7-5). A 200 µL aliquot of FITC conjugated IgG and Cy3 conjugated IgG secondary antibodies were placed in contact with the surfaces for 60 min at a concentration of 10 µg/ml. After rinsing the surface with PBS, the patterned surfaces were analyzed using a fluorescence microscope (Nikon TE 2000-E).

7-3-6 Surface functionalization procedure using microfluidics

Glass substrates were placed in piranha (H_2O_2:H_2SO_4, 1:3 v/v) solution for 10 min, rinsed extensively with DI water, and dried under a stream of nitrogen. As shown in Figure 7-1, two substrates forming the microfluidic device were plasma treated (60 s, 200 W, 200 mTorr O_2) followed by micro-contact printing of APTES onto the glass substrate. Immediately after micro-contact printing, the glass and patterned PDMS substrates were attached to form an irreversibly sealed microfluidic device. After heat treatment at 100ºC for 1 hour, EDC-NHS solution was flowed into the printed area and incubated over the main channel for 20 minutes to activate the printed amine groups on the glass side of the microfluidic

channel. Separate flow streams containing different antibody solutions were then passed through the input channels (Figure 7-1) and merged into a main channel. The antibodies in each flow stream were covalently bound to the printed amine groups on the surface (Figures 7-1D and 7-1F). Surface functionalization with multiple antibodies using the procedure described above was performed, and functionality of the patterned antibodies was investigated.

7-3-6-1 Multiplex protein functionalization

After micro-contact printing of APTES onto the glass substrate and immediately binding it to the PDMS substrate, an irreversibly sealed microfluidic platform was formed. The PDMS stamp used for this stage is a flat stamp with no pattern and wide enough to cover the main channel area. After connecting the inlets and outlets, the device was washed with a flow of PBS and the printed APTES molecules were activated by EDC-NHS. Laminar flow streams of antibodies, namely Cy3 conjugated IgG to rabbit, Cy5 conjugated IgG to rat, and FITC conjugated IgG to mouse secondary antibodies, were then flowed for one hour through separate input channels and directed to the main channel at a flow rate of 0.5 mm/s. The channel was then rinsed with PBS at a flow rate of 10 cm/s (50 dyn/cm^2).

7-3-6-2 Multiplex protein microarrays in a single channel and immunoassay

To create multiplex protein microarrays and evaluate functionality of the patterned antibody microarrays, two experimental conditions were designed and immunoassays were performed. In the first experiment, each probe contained one functional antibody with five lanes across a single channel's width. The same number of lanes was produced in the second experiment while probes in two of the lanes were patterned with two different functional antibodies. The aim of the first experiment was to demonstrate the capability of the developed technique to produce multiplex protein microarrays with single probe presence at each spot, and the second experiment was designed to show the possibility of producing probes with more than one functional biomolecule at each spot which has recently attracted attention in cell research studies (Cheong, Wang et al. 2009) (Petty, Li et al. 2007).

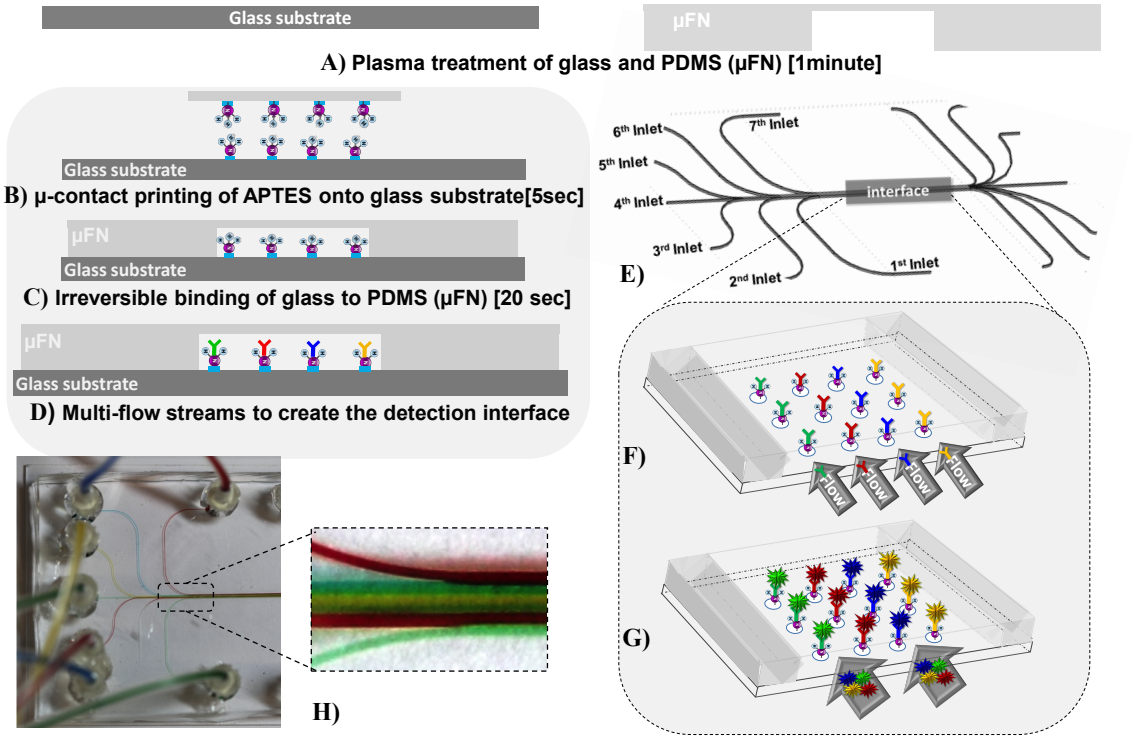

Figure 7-1: Schematic presentation of the experimental procedure, A) Plasma treatment of the glass and PDMS substrates, B) Micro-contact printing of APTES onto glass substrate to create functional amine groups on the surface, C) Forming the irreversibly sealed microfluidic device with the embedded functional amine groups on microchannel surface, D) After heat treatment and activation by EDC-NHS chemistry, biomolecules are covalently attached to the active amine groups present in the printed areas, E) Microfluidic design, F) Multiple laminar flow streams, each one carrying a specific biomarker are passed through the main channel to create multiplex protein patterns along the cross section of the main channel, G) Schematic presentation of a mixture of secondary antibodies specific to the primary antibodies on the surface which is flowed through the channels and incubated for high throughput biomarker assay, H) A picture of the microfluidic device which illustrates the magnified multiple laminar flows in the main channel captured using streams with different colors.

A PDMS stamp with pillars of 25 μm in diameter was used in both experiments to print the APTES solution onto the glass substrate. After forming the microfluidic devices, the cross section of the main channel contained five circular shaped APTES-printed regions. Simulation of the velocity field and concentration distribution was performed prior to the experiments and the results were used to find the optimum experimental conditions for desired patterns. The goal of the first experiment was to pattern protein microarrays in which each probe contains one capture biomolecule (primary antibody). For this purpose, five laminar flow streams containing mouse anti-CD34, rabbit anti-CD31 and rat anti-CD36

primary antibodies were passed through the main channel for 1 hour at a flow rate of 2 mm/s. Concentrations of all primary antibodies were 10 μg/ml in PBS.
The second experiment was designed to pattern lanes of five separate functional spots, along the channel width, three of which possessing one antibody of different types and two others containing two individual concurrent antibodies. For this purpose, the primary antibodies were flowed into the main channel at a flow rate of 1 mm/s and the concentration of the CD 36 antibody in the central flow was increased to 30 μg/ml.
After patterning primary antibodies, the channel surface was washed by flowing PBS (10 cm/s ≈ 50 dyn/cm^2). Following surface treatment with BSA, to avoid non-specific binding, FITC conjugated IgG secondary antibody to mouse, Cy3 conjugated IgG secondary antibody to rabbit and Cy5 conjugated IgG secondary antibody to rat, with a concentration of 5 μg/ml each, were mixed and flowed into the patterned channel. In each experiment, about 200 nl of mixed secondary antibodies were incubated on the surface for 30 minutes in stop-flow to perform a multiplex immunoassay. The surface was then washed with PBS applying the same flow rate used to wash patterned primary antibodies.

7-3-7 Characterization of antibody modified surfaces

Glass discs of 1 cm in diameter were functionalized with antibodies using a flat PDMS stamp. X-ray Photoelectron Spectroscopy (XPS) studies were performed with a VG ESCALAB 3 MKII (VG, Thermo Electron Corporation, UK) on substrates at various stages of functionalization to identify and quantify the elements on the surface at each stage. Samples were irradiated using an MgKα source at a take-off angle of 0^o (i.e., perpendicular); analyzed surface was 2 mm × 3 mm and the depth sampled was ~50-100 Å.

7-3-8 Fluorescence microscopy

An inverted fluorescence microscope (Nikon TE 2000-E) was used to monitor surface functionalization of the microfluidic platform. Antibodies conjugated with three different fluorescent dyes (Cy3, Cy5 and FITC) were used in the experiments and observed through appropriate filters. All images were captured

using a CCD camera (Photometrics CoolSNAP HQ2) and analyzed by MBF_ImageJ (MacBiophotonics, McMaster University).

7-4 Results and discussion

7-4-1 Characterization of functionalized surfaces and chemical patterning of antibodies

Prior to surface patterning of antibodies, the surface of cleaned glass (control), glass micro-contact printed with APTES, and APTES printed glass incubated with antibodies were analyzed by XPS (Figure S7-6). XPS analysis on APTES printed surfaces showed a marked increase in the nitrogen and carbon peaks compared to the control. Increase in carbon and nitrogen percentage was also observed for antibody functionalized surfaces compared to APTES printed glass. The amount of nitrogen and carbon significantly increased at each step of surface functionalization, which was a clear indication of successful surface patterning using the developed protocol for micro-contact printing (Figures S7-6C and S5-6D). The water contact angle of the glass samples was measured before and after cleaning and it was found to decrease from 66^{o} $\pm 0.55^{o}$ to 3.82^{o} $\pm 0.06^{o}$ after cleaning. Following APTES printing, the water contact angle for coated surfaces was found to be 40.2^{o} $\pm 0.14^{o}$.

Figure 7-2A depicts patterning of a glass surface with FITC conjugated IgG antibody. To obtain these patterns, a PDMS stamp with pillar shape features (10 μm in diameter with 70 μm spacing) was used to micro-contact print APTES in stop flow conditions.

Figure 7-2B shows Cy3 conjugated IgG antibody patterns in which separate patterns of either 20×60 μm or 20×20 μm features with 10 μm spacing were created on the surface using another PDMS stamp. The presence of fluorescence spots on both surfaces indicated that micro-contact printing of APTES was successfully implemented to covalently pattern antibodies onto surfaces according to desired micron size features.

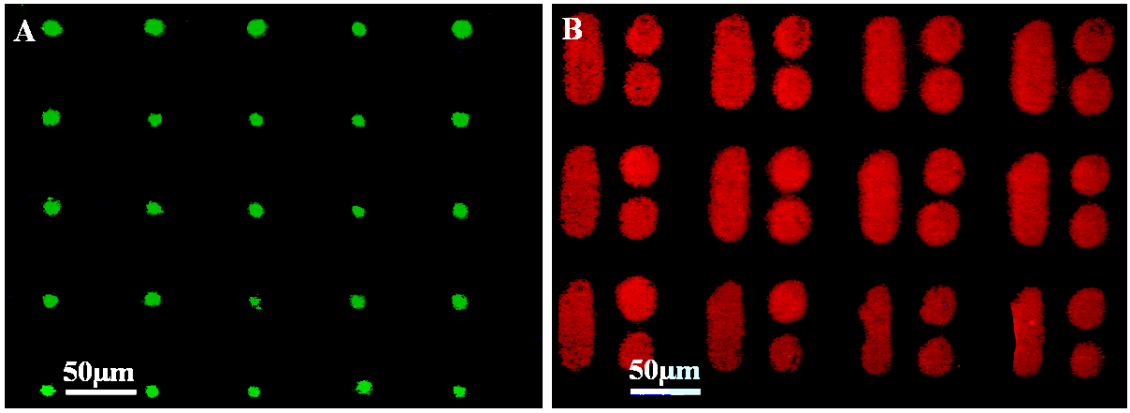

Figure 7-2: Micro-contact printing of APTES and covalently patterning of the antibodies to the printed areas. FITC (A) and Cy3 (B) conjugated IgG antibodies covalently attached to the APTES printed areas.

XPS results, together with fluorescence labeling, confirmed that the developed experimental protocol for printing APTES on glass substrates was effective. Although micro-contact printing of other silanes has already been reported on gold or silicon oxide substrates (Xia, Mrksich et al. 1995, Onclin, Ravoo et al. 2005), the introduced protocol to micro-contact print APTES on glass substrates, is rapid and eliminates the requirement for the stringent controls used in conventional APTES coatings such as air-free reaction chambers. In theory, the proposed technique could be further expanded to chemically attach other biomolecules such as proteins, peptides or aptamers.

7-4-2 Multiplex antibody functionalization

Figure 7-3A represents the microfluidic device functionalized with antibodies through micro-contact printing of APTES and microfluidic patterning of biomolecules. Figure 7-3B shows a cross section of one of the inlet channels, at the boundary of APTES printed area with unprinted glass surface functionalized with Cy3 conjugated antibody at a flow rate of 3 mm/s. As displayed in this figure, after washing the surface with PBS at high flow rates, no non-specific physical adsorption was observed. This is also indicative of strong chemical bonds between the biomolecules and the amine groups in the printed areas.

Figures 7-3C, 3-3D and 3-3E show the fluorescence microscopy images from the surface of the main channel functionalized with FITC, Cy5 and Cy3 conjugated

antibodies, respectively. The superimposed image of the three aforementioned images is shown in figure 7-3F, demonstrating the successful functionalization of the surface with multiple antibodies. Figure 7-3G depicts the normalized fluorescence intensities of the functionalized surface. The microfluidic design consists of multiple inlet branches, which merge to form the main microchannel (Figure 7-1E and Figure 7-3A). These branches join the main channel in different parts along its length, which results in different areas functionalized with three, five and seven antibodies.

These findings address one of the main concerns in using microfluidic patterning, which is controlling the diffusion between laminar flows to functionalize the surface at each area with the desired biomolecules. Although micro-contact printing is a useful tool to selectively activate predetermined areas, manipulation of the laminar flows and the concentration of biomolecules in each stream are also determinant factors important for creating the desired arrays of biomarkers. The velocity of the laminar flow streams affects the amount of diffusion of each antibody to the surrounding streams, (Ismagilov, Stroock et al. 2000, Kamholz and Yager 2001, Walker, Sai et al. 2005, Hu, Gao et al. 2007) and as a result to the microchannel surface (Figure S7-7). Diffusion is more important when flat PDMS stamps are used for APTES printing in which the antibodies covalently attach to the whole area inside the channel. This is important in producing region specific patterns through microfluidic patterning.

As depicted in figure 7-3G, applying a flow rate of 0.5 mm/s resulted in multiplex functionalization of the surface with considerable diffusion, resulting in more than one antibody presence in some spots. Therefore, for experiments requiring individual probes in specific areas, increasing the flow rate could result in lower diffusion and distinguished boundaries between patterned areas. This is illustrated in the next section involving microarray production.

As demonstrated above, surface functionalization could be successfully performed at flow rates up to 3 mm/s. This is one of the main advantages of the proposed method in which diffusion can be controlled by varying flow velocity without altering covalent attachment of the biomolecules.

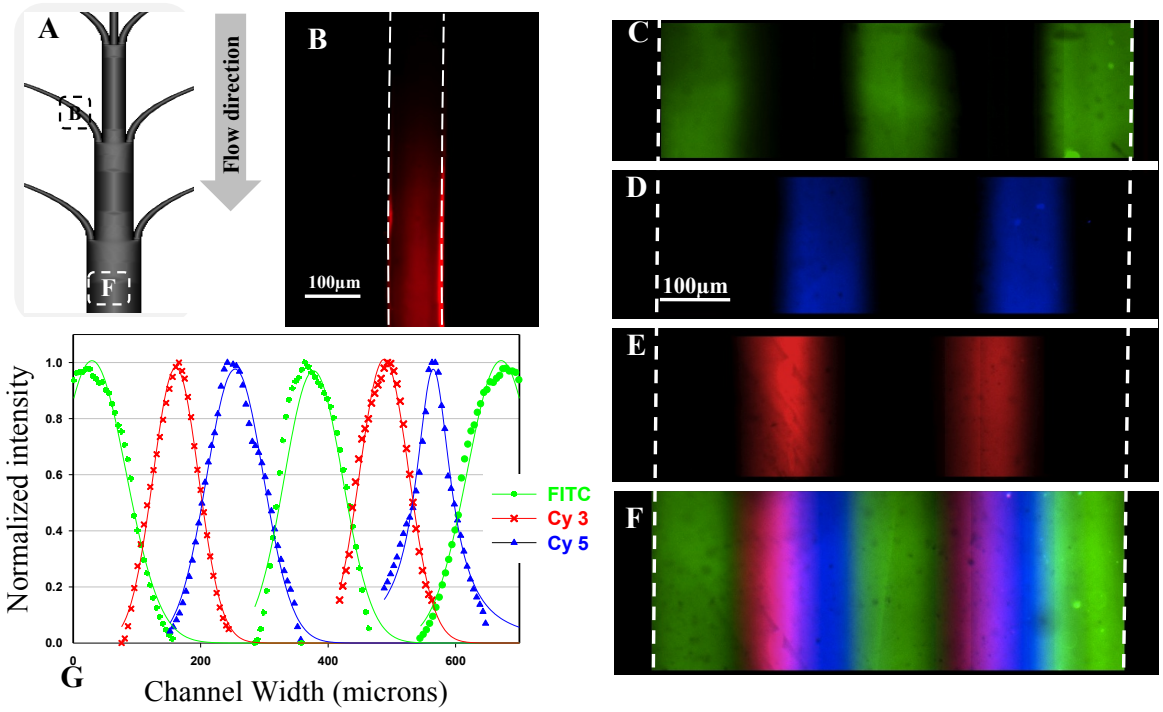

Figure 7-3: Surface functionalization of a single microfluidic channel with multiple antibodies. A) Schematic representation of different areas of the microfluidic device functionalized with antibodies referring to the functionalized surfaces analyzed and shown in figures 7-3B-F, B) Border of micro-contact printing in one of the inlet channels, C,D and E) Fluorescence microscope images after microchannel surface functionalization. Green, red and Blue colors represent FITC, Cy3 and Cy5 conjugated IgG secondary antibodies respectively. F) Superimposed fluorescence microscope image of the channel representing all three antibodies. The white dashed lines represent the microchannel walls. G) Normalized fluorescence intensity of the surface across the channel width shown in figure 7-3F.

Interestingly, the diffusion of biomolecules among fluid streams is not the only parameter that can be controlled through flow rate manipulation. The proposed design could very well provide a stable and robust surface functionalization in which the resulting protein patterns possessed high shear resistance. Stability was demonstrated by washing the surface with PBS under flow rates up to 10 cm/s, corresponding to a shear stress of about 50 dyn/cm^2. Similar devices reported in the literature operated with no more than 1 dyn/cm^2 (Fiddes, Chan et al. 2010). These results also show that even if region specific patterns or multiplexing are not needed, contact printing of APTES onto glass substrates using flat PDMS stamps can be a promising, rapid and simpler alternative to the conventional silanization techniques in microfluidic devices.

7-4-3 Immunoassay in a single channel using multiplex functional protein microarrays

After surface patterning with APTES, multiplex microarrays of primary antibodies were produced and a multiplex immunoassay was performed. Two sets of experiments were designed and performed. Figures 7-4B and 7-4F depict the simulation results for concentration distribution among flow streams for each experiment. The areas highlighted with continuous lines correspond to the APTES-patterned regions where the antibodies in the flow are expected to attach to the surface.

Primary antibodies were patterned on the channel surface as shown in figures 7-4A and 7-4E. Figures 7-4C and 7-4G show fluorescence microscopy images of the surface after performing the multiplex immunoassay using secondary antibodies specific to the patterned primary antibodies. In the second experiment, the higher concentration of CD36 (30 μg/ml versus 10 μg/ml) in the central flow stream ensures adequate diffusion of this antibody to the neighboring streams, thus creating columns of probes with dual antibodies in two of the arrays as quantified by fluorescent intensity measurement (Figure 7-4H).

The multiplex immunoassay results show that the patterned antibodies were functional and that the developed interface can be employed as a multiplex detection interface for high throughput applications using very small sample volumes. Using three different fluorescent dyes conjugated to secondary antibodies, it was possible to show the ability of patterning and detecting five different antibodies across a single channel width with single or dual probe presence at each patterned spot. Such a multiplexed biomarker microarray, with each lane containing a single probe, would be advantageous for high throughput biosensing and point of care diagnosis applications. Indeed, one of the main applications of the developed chip will be simultaneous detection of several biomarkers in complex samples such as blood or serum. In addition, the surface patterned with more than one biomolecule in some spots, as illustrated in the

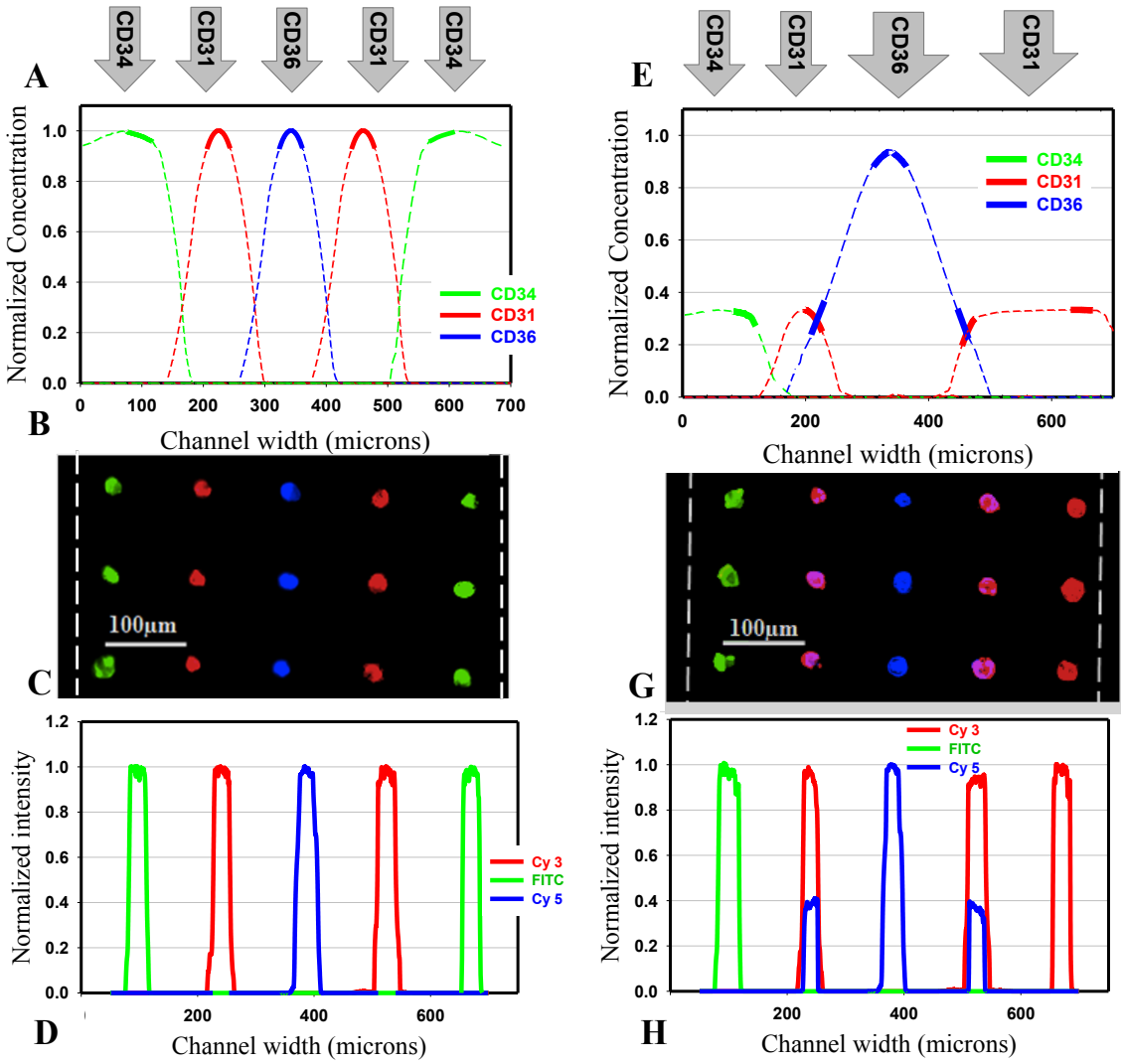

Figure 7-4: Patterning multiplex protein microarrays with strong covalent bonds and high throughput biomarker assay. A and E) Schematic representation of laminar flows containing different primary antibody solutions to create the detection interface. B and F) Simulation results for concentration distribution inside the flow streams. The areas shown with continuous solid lines correspond to the areas patterned with APTES and thus the antibodies in the flow are expected to attach to the surface at these spots. C and G) Superimposed fluorescence microscope images of the surfaces showing the multiplex immunoassay results. The white dashed lines represent the microchannel walls, D and H) Fluorescence intensities obtained from C and G in which fluorescently conjugated secondary antibodies are detected by their specific primary antibodies on the surface.

second experiment, could be beneficial for some biological applications such as studying cell response to multiple stimuli (Cheong, Wang et al. 2009) (Petty, Li et al. 2007).

The developed microfluidic chip can also be used in applications where high shear stress is required such as adhesion based sorting of lymphocytes on the

developed detection interface and investigating their behavior under high shear forces.

7-5 Conclusions

A versatile technique for multiplex protein patterning in a microfluidic platform was introduced. This approach consisted in silanization using micro-contact printing of APTES onto glass surface followed by microfluidic patterning of multiple antibodies. This led to covalent chemical attachment of different proteins onto a single microchannel surface, resistant under shear stresses of up to 50 dyn/cm^2, also allowing operation and manipulation of the microfluidic device at high flow rates. Since the created patterns were across a single microchannel, confining various analytes to a small surface area in the solution, a multiplex whole immunoassay could be performed using very small sample volumes. This also reduced the number of sensing signals required to be captured for analysis compared to multiple channel devices. Although the proof of concept is shown for antibodies, the versatility and robustness of the approach allows for creating desired patterns of functional biomolecules such as proteins, peptides and aptamers for various applications in multiplex biosensing and whole bioassay systems as well as for cell sorting or cell response to multiple stimuli by simply changing the PDMS stamp design, flow rates and concentrations of biomolecules.

7-6 Supporting Information

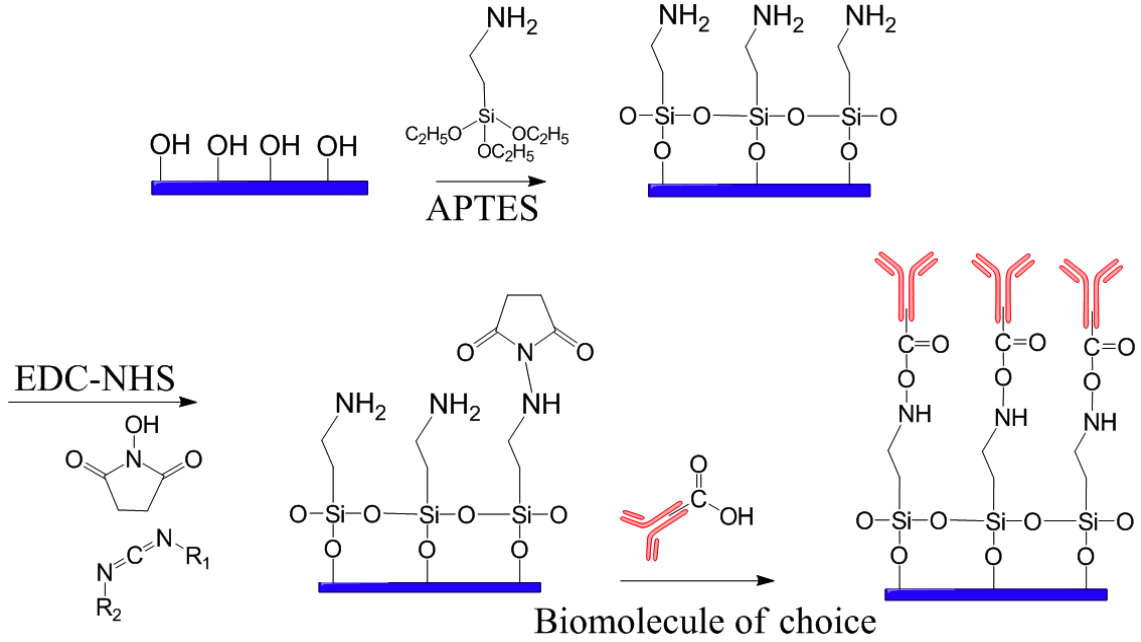

Figure S7-5: Schematic representation of different steps for glass surface functionalization with antibodies using APTES. First APTES reacts with the available OH- groups on the glass surface using micro-contact printing technique. This is followed by activation through EDC-NHS chemistry. The biomolecules (antibodies in this study) can then covalently attach to the activated APTES coated sites.

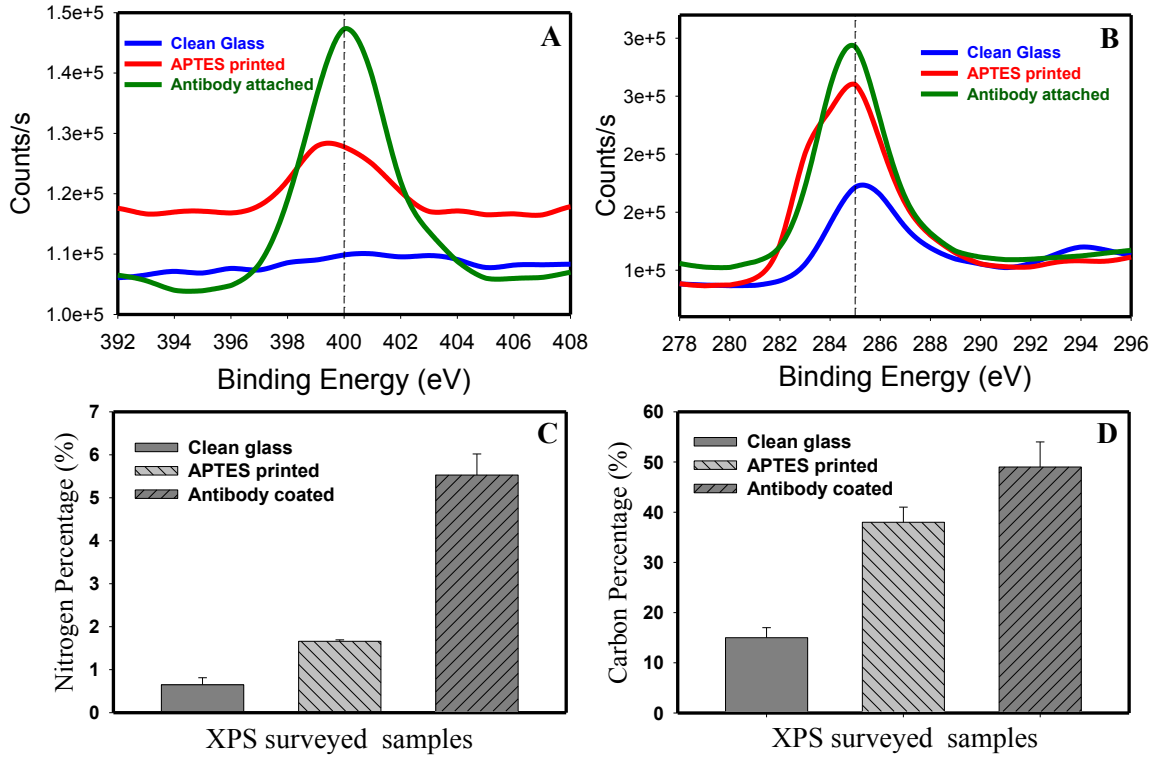

Figure S7-6: XPS analysis results of antibody-functionalized surfaces created by micro-contact printing of APTES. A and B) Overlay of XPS scan for different samples (Cleaned glass, APTES printed and antibody attached). Dashed lines in A and B represent the nitrogen and carbon peaks respectively. C and D) Depict the percentage of nitrogen and carbon on the surface of analyzed samples respectively. Error bars represent standard deviation for three different samples.

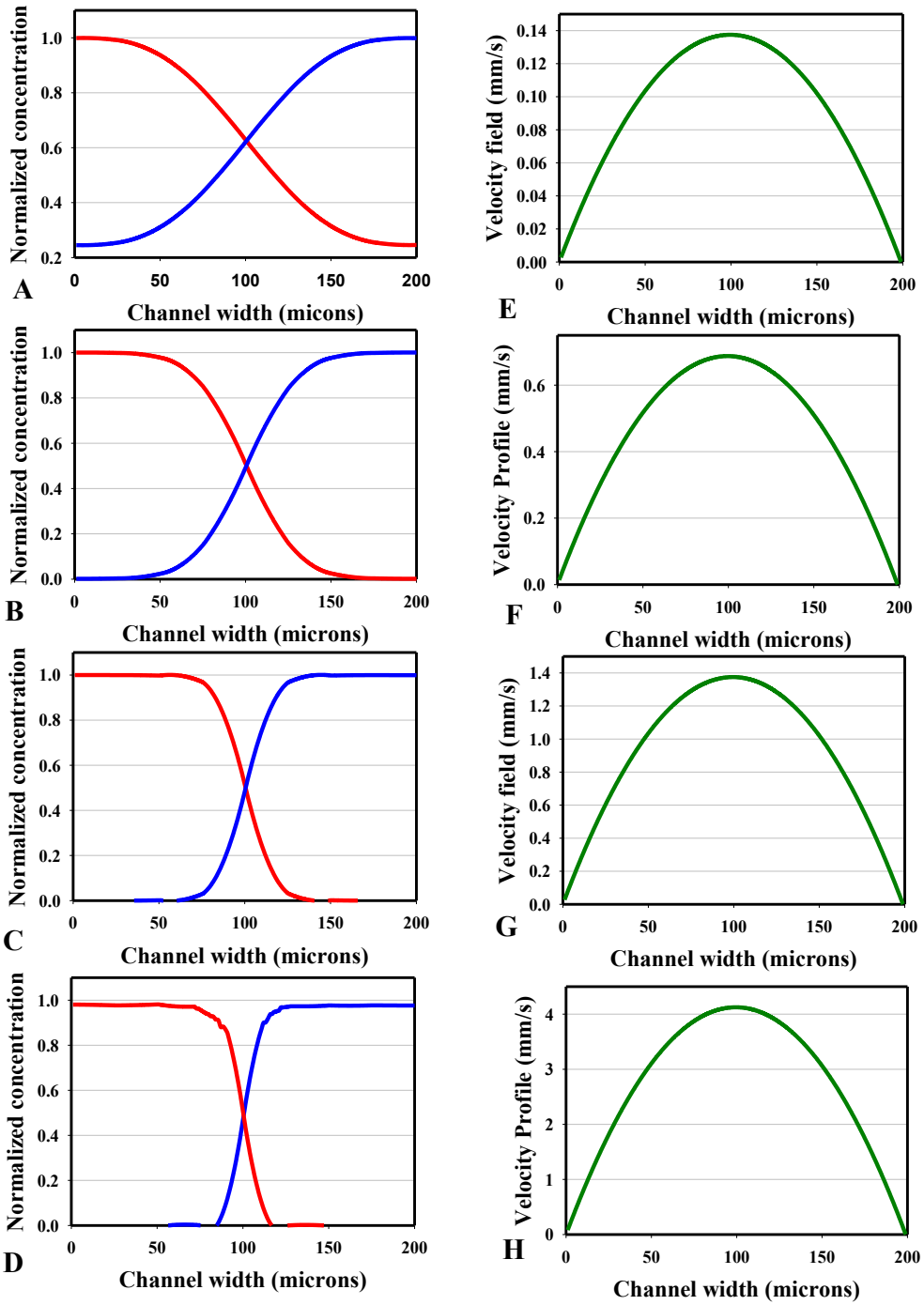

Figure S7-7: The effect of flow velocity on diffusion of antibodies between laminar flows. A to C depicts normalized concentration distribution across a microchnnels width in which two laminar flow streams pass through the channel applying 0.1 mm/s, 0.5 mm/s, 1 mm/s and 3 mm/s flow rates respectively. Figures E to H show the velocity field for applied flow rates. As shown in these figures increasing the flow rates decreases the diffusion between laminar flows.

Shear stress estimation

We performed computational fluid dynamics (CFD) modeling on the system. The simulation results also include shear stress calculations at different areas of the device. Shear stress can also be estimated using simplified Navier Stokes equations as follows:

The steady flow of an incompressible Newtonian fluid between two parallel flat plates is generally known as Hele-Shaw flow. Using Hele-Shaw flow approximation the pressure, p, is related to the velocity U by:

$$\nabla P = -\frac{12\eta}{h^2} U$$

where η is the dynamic viscosity and h channel depth . The wall shear stress, for the same geometry is then defined as (Detailed information can be found in: Annals of Biomedical Engineering, Vol. 21, pp. 77-83, 1993):

$$_{w} = \frac{6\_}{h} U$$

7-7 Acknowledgments

The authors would like to acknowledge National Science and Engineering Research Council of Canada-Collaborative Research program and Discovery program, Genome Canada/Génome Québec, NanoQuébec and Le Fonds Québécois de la Recherche sur la Nature et les Technologies-Centre for Biorecognition and Biosensors for their financial support.

References

Barbulovic-Nad, I., M. Lucente, Y. Sun, M. Zhang, A. R. Wheeler and M. Bussmann (2006). "**Bio-Microarray Fabrication Techniques—A Review.**" Critical Reviews in Biotechnology **26**(4): 237-259.

Cheong, R., C. J. Wang and A. Levchenko (2009). "**High Content Cell Screening in a Microfluidic Device.**" Molecular & Cellular Proteomics **8**(3): 433-442.

Didar, T. F. and M. Tabrizian (2010). "**Adhesion based detection, sorting and enrichment of cells in microfluidic Lab-on-Chip devices.**" Lab on a Chip **10**(22): 3043-3053.

Fiddes, L. K., H. K. C. Chan, B. Lau, E. Kumacheva and A. R. Wheeler (2010). "**Durable, region-specific protein patterning in microfluidic channels.**" Biomaterials **31**(2): 315-320.

Fricke, R., P. D. Zentis, L. T. Rajappa, B. Hofmann, M. Banzet, A. Offenhäusser and S. H. Meffert (2011). "**Axon guidance of rat cortical neurons by microcontact printed gradients.**" Biomaterials **32**(8): 2070-2076.

Green, J. V., T. Kniazeva, M. Abedi, D. S. Sokhey, M. E. Taslim and S. K. Murthy (2009). "**Effect of channel geometry on cell adhesion in microfluidic devices.**" Lab on a Chip **9**(5): 677-685.

Hosseinidoust, Z., T. G. M. Van de Ven and N. Tufenkji (2011). "**Bacterial Capture Efficiency and Antimicrobial Activity of Phage-Functionalized Model Surfaces.**" Langmuir: null-null.

Howarter, J. A. and J. P. Youngblood (2006). "**Optimization of Silica Silanization by 3-Aminopropyltriethoxysilane.**" Langmuir **22**(26): 11142-11147.

Hu, G., Y. Gao and D. Li (2007). "**Modeling micropatterned antigen–antibody binding kinetics in a microfluidic chip."** Biosensors and Bioelectronics **22**(7): 1403-1409.

Ismagilov, R. F., A. D. Stroock, P. J. A. Kenis, G. Whitesides and H. A. Stone (2000). "**Experimental and theoretical scaling laws for transverse diffusive broadening in two-phase laminar flows in microchannels.**" Applied Physics Letters **76**(17): 2376-2378.

Jiang, X., Q. Xu, S. K. W. Dertinger, A. D. Stroock, T.-m. Fu and G. M. Whitesides (2005). "**A General Method for Patterning Gradients of Biomolecules on Surfaces Using Microfluidic Networks.**" Analytical Chemistry **77**(8): 2338-2347.

Kaji, H., M. Hashimoto and M. Nishizawa (2006). "**On-Demand Patterning of Protein Matrixes Inside a Microfluidic Device.**" Analytical Chemistry **78**(15): 5469-5473.

Kamholz, A. E. and P. Yager (2001). "**Theoretical Analysis of Molecular Diffusion in Pressure-Driven Laminar Flow in Microfluidic Channels.**" Biophysical Journal **80**(1): 155-160.

Kaufmann, T. and B. J. Ravoo (2010). "**Stamps, inks and substrates: polymers in microcontact printing.**" Polymer Chemistry **1**(4): 371-387.

Khademhosseini, A., K. Y. Suh, S. Jon, G. Eng, J. Yeh, G.-J. Chen and R. Langer (2004). "**A Soft Lithographic Approach To Fabricate Patterned Microfluidic Channels**." Analytical Chemistry **76**(13): 3675-3681.

Kim, D. J., J. M. Lee, J.-G. Park and B. G. Chung (2011). "**A self-assembled monolayer-based micropatterned array for controlling cell adhesion and protein adsorption.**" Biotechnology and Bioengineering **108**(5): 1194-1202.

Kim, M., J.-C. Choi, H.-R. Jung, J. S. Katz, M.-G. Kim and J. Doh (2010). "**Addressable Micropatterning of Multiple Proteins and Cells by Microscope Projection Photolithography Based on a Protein Friendly Photoresist.**" Langmuir **26**(14): 12112-12118.

Kirby, B. J., A. R. Wheeler, R. N. Zare, J. A. Fruetel and T. J. Shepodd (2003). "**Programmable modification of cell adhesion and zeta potential in silica microchips.**" Lab on a Chip **3**(1): 5-10.

Lee, N. Y., J. R. Lim and Y. S. Kim (2006). "**Selective patterning and immobilization of biomolecules within precisely-defined micro-reservoirs.**" Biosensors and Bioelectronics **21**(11): 2188-2193.

Mandal, S., J. M. Rouillard, O. Srivannavit and E. Gulari (2007). "**Cytophobic Surface Modification of Microfluidic Arrays for In Situ Parallel Peptide Synthesis and Cell Adhesion Assays.**" Biotechnology Progress **23**(4): 972-978.

Maraldo, D. and R. Mutharasan (2007). "**Optimization of antibody immobilization for sensing using piezoelectrically excited-millimeter-sized cantilever (PEMC) sensors.**" Sensors and Actuators B: Chemical **123**(1): 474-479.

Murthy, S. K., A. Sin, R. G. Tompkins and M. Toner (2004). "**Effect of flow and surface conditions on human lymphocyte isolation using microfluidic chambers.**" Langmuir **20**(26): 11649-11655.

Nakajima, H., S. Ishino, H. Masuda, T. Nakagama, T. Shimosaka and K. Uchiyama (2006). "**Photochemical immobilization of protein on the inner wall of a microchannel and Its application in a glucose sensor.**" Analytica Chimica Acta **562**(1): 103-109.

Onclin, S., B. J. Ravoo and D. N. Reinhoudt (2005). "**Engineering Silicon Oxide Surfaces Using Self-Assembled Monolayers.**" Angewandte Chemie International Edition **44**(39): 6282-6304.

Patrito, N., C. McCague, S. Chiang, P. R. Norton and N. O. Petersen (2006). "**Photolithographically Patterned Surface Modification of Poly(dimethylsiloxane) via UV-Initiated Graft Polymerization of Acrylates.**" Langmuir **22**(8): 3453-3455.

Petty, R. T., H.-W. Li, J. H. Maduram, R. Ismagilov and M. Mrksich (2007). "**Attachment of Cells to Islands Presenting Gradients of Adhesion Ligands.**" Journal of the American Chemical Society **129**(29): 8966-8967.

Renault, J. P., A. Bernard, D. Juncker, B. Michel, H. R. Bosshard and E. Delamarche (2002). "**Fabricating Microarrays of Functional Proteins Using Affinity Contact Printing.**" Angewandte Chemie International Edition **41**(13): 2320-2323.

Rosengren, Å., E. Pavlovic, S. Oscarsson, A. Krajewski, A. Ravaglioli and A. Piancastelli (2002). **"Plasma protein adsorption pattern on characterized ceramic biomaterials.**" Biomaterials **23**(4): 1237-1247.

Saliba, A. E., L. Saias, E. Psychari, N. Minc, D. Simon, F. C. Bidard, C. Mathiot, J. Y. Pierga, V. Fraisier, J. Salamero, V. Saada, F. Farace, P. Vielh, L. Malaquin and J. L. Viovy "**Microfluidic sorting and multimodal typing of cancer cells in self-assembled magnetic arrays.**" Proceedings of the National Academy of Sciences of the United States of America **107**(33): 14524-14529.

Shamansky, L. M., C. B. Davis, J. K. Stuart and W. G. Kuhr (2001). "**Immobilization and detection of DNA on microfluidic chips**." Talanta **55**(5): 909-918.

Shi, J., T. Yang and P. S. Cremer (2008). **"Multiplexing Ligand−Receptor Binding Measurements by Chemically Patterning Microfluidic Channels.**" Analytical Chemistry **80**(15): 6078-6084.

Takayama, S., J. C. McDonald, E. Ostuni, M. N. Liang, P. J. A. Kenis, R. F. Ismagilov and G. M. Whitesides (1999). **"Patterning cells and their environments using multiple laminar fluid flows in capillary networks.**" Proceedings of the National Academy of Sciences of the United States of America **96**(10): 5545-5548.

Tan, C. P., B. R. Cipriany, D. M. Lin and H. G. Craighead (2010). "**Nanoscale Resolution, Multicomponent Biomolecular Arrays Generated By Aligned Printing With Parylene Peel-Off.**" Nano Letters **10**(2): 719-725.

Walker, G. M., J. Sai, A. Richmond, M. Stremler, C. Y. Chung and J. P. Wikswo (2005). **"Effects of flow and diffusion on chemotaxis studies in a microfabricated gradient generator."** Lab on a Chip **5**(6): 611-618.

Walter, G., K. Büssow, D. Cahill, A. Lueking and H. Lehrach (2000). "**Protein arrays for gene expression and molecular interaction screening."** Current Opinion in Microbiology **3**(3): 298-302.

Whitesides, G. M. (2006). "**The origins and the future of microfluidics.**" Nature **442**(7101): 368-373.

Wu, P., D. G. Castner and D. W. Grainger (2008). "**Diagnostic devices as biomaterials: a review of nucleic acid and protein microarray surface performance issues."** Journal of Biomaterials Science, Polymer Edition **19**(6): 725-753.

Xia, Y., M. Mrksich, E. Kim and G. M. Whitesides (1995). **"Microcontact Printing of Octadecylsiloxane on the Surface of Silicon Dioxide and Its Application in Microfabrication.**" Journal of the American Chemical Society **117**(37): 9576-9577.

Yin, Z., S.-C. Tao, R. Cheong, H. Zhu and A. Levchenko (2010). "**An integrated micro-electro-fluidic and protein arraying system for parallel analysis of cell responses to controlled microenvironments.**" Integrative Biology **2**(9): 416-423.

Chapter 8. Generating multiplex gradients of biomolecules for controlling cellular adhesion in parallel microfluidic channels

8-1 Connecting text

Producing covalent multiplex biomarker arrays was successfully demonstrated in chapter 7. Herein, the same chip with a new design was used to produce multiplex gradients of biomolecules. The originality of the work relies on the microfluidic gradient generators in parallel channels to mimic critical aspects of *in vivo* environments at micro/nano scale. In addition to a variety of applications and advantages, specifically for cell sorting, the developed chip can be used to discover new cell-specific markers and study the degree of adhesion of target cells based on the biomarker density immobilized on the surface.

These results of this chapter has been published in the following article:

- Tohid Fatanat Didar and M. Tabrizian, (2012), Generating multiplex gradients of biomolecules for controlling cellular adhesion in parallel microfluidic channels, Lab on Chip, 12, 4363-4371.

8-2 Abstract

Here we present a microfluidic platform to generate multiplex gradients of biomolecules within parallel microfluidic channels, in which a range of multiplex concentration gradients with different profile shapes are simultaneously produced. Nonlinear polynominal gradients were also generated using this device. The gradient generation principle is based on implementing parrallel channels with each providing a different hydrodynamic resistantance. The generated biomolecule gradients were then covalently functionalized onto the microchannel surfaces. Surface gradients along the channel width was a result of covalent attachment of biomolecules to the surface, which remained functional under high shear stresses (50 dyn/cm^2). An IgG antibody conjugated to three different fluorescence dyes (FITC, Cy5 and Cy3) was used to demonstrate the resulting multiplex concentration gradients of biomolecules. The device enabled generation of gradients with up to three different biomolecules in each channel with varying concentration profiles. We were also able to produce 2-dimensional gradients in which biomolecules were distributed along the length and width of the channel. To demonstrate the applicibility of the developed design, three different multiplex concentration gradients of REDV and KRSR peptides were patterned along the width of three parallel channels and adhesion of primary human umbilical vein endothelial cell (HUVEC) in each channel was subsequently investigated using a single chip.

8-3 Introduction

Over the past decade, engineering tools have increasingly been applied to design and develop in vitro platforms to mimic important aspects of cellular microenvironments. This includes quantitative and reproducible characterization of cellular responses to chemical gradients (Keenan and Folch 2008). Significant advances in this regard were first made through conventional assays such as the Boyden chamber (Boyden 1962). Recently, lab-on-a-chip (LOC) devices have opened new avenues for in vitro study of biological samples through creating gradients of biomolecules based on microfluidic principles. Forming multiple simultaneous gradients with highly resistant surface bonds in a simple and straightforward set-up, while maintaining a small device footprint, are important factors in designing microfluidic gradient-based devices for high throughput applications.

Several recent reports have implemented gradient-based microfluidic platforms to study biological phenomena such as cancer cell migration under the influence of well-defined chemokine and growth factor gradients (Saadi, Wang et al. 2006, Mosadegh, Saadi et al. 2008, Kim, Kim et al. 2010), quantitative relationship between directional guiding cues and chemotaxis of immune cells (Li Jeon, Baskaran et al. 2002), stem cell differentiation due to spatial and temporal distribution of cytokines and growth factors (Chung, Flanagan et al. 2005), angiogenesis (Barkefors, Thorslund et al. 2009), selective cell adhesion and spreading (Guarnieri, De Capua et al. 2010, Lamb, Park et al. 2010, Millet, Stewart et al. 2010) and microorganism response to surrounding chemical gradients (Breslauer, Lee et al. 2006).

Diffusion and convection are the two principle methods used to generate gradients of biomolecules in microfluidic devices (Keenan and Folch 2008, Cooksey, Sip et al. 2009, Bhattacharjee, Li et al. 2010, Cate, Sip et al. 2010, Kim, Kim et al. 2010). The first systematic microfluidic-based gradient device was introduced by Jeon et al. (Jeon, Dertinger et al. 2000). This tree-like design repetitively mixes and splits solutions of different concentrations, until several laminar flows, each possessing a percentage of the initial concentration,

converge within a single channel. A stable gradient is then generated through diffusion between converging laminar flows perpendicular to the flow direction. Subsequently, Whithesides et al. (Jeon, Dertinger et al. 2000, Dertinger, Chiu et al. 2001, Jiang, Xu et al. 2005) reported on different configurations of this basic design to create gradients in microfluidic channels. Theoretical modelling and simulation of this design and similar devices are also available in the literature (Ismagilov, Stroock et al. 2000, Kamholz and Yager 2001, Holden, Kumar et al. 2003, Kang, Zongxing et al. 2008). Several studies have since modified this design to create more precise, rapid and well-controlled gradient profiles (Irimia, Liu et al. 2006, Campbell and Groisman 2007, Chung and Choo 2010, Kim, Kim et al. 2010, Bui, Li et al. 2011, Yeh, Chen et al. 2011). However, the tree-like platform contains a series of microfluidic channels specifically dedicated to gradient generation which results in a big device footprint - thus minimizing the space available for experiments (Campbell and Groisman 2007). Irimia et al (Irimia, Geba et al. 2006) also reported a microfluidic design to generate desired non-linear concentration gradient profiles based on parallel linear shape barriers on the flow direction. Recently Selimovic et al. (Selimović, Sim et al. 2011) proposed a simpler design using asymmetric channels with two inlets to address some limitations of the tree-like design and successfully generated gradients of one biomolecule.

The tree like design was implemented to generate multiplex gradients of two different biomolecules (Jiang, Xu et al. 2005). Multiplex concentration profiles of biomolecules was also reported using a scanning microfluidic probe in open volumes (Olofsson, Bridle et al. 2005).

Many gradient dependent biological applications such as cell adhesion or cell migration experiments require bio-functional and stable surface gradients. To produce surface gradients, most devices rely on physical adsorption of biomolecules onto surfaces. Adsorbed biomolecules, however, tend to detach unpredictably and are particularly problematic in microfluidic systems operating under flow. Physical adsorption can also cause random orientation of biomolecules and alter their bio-functionality. To address this limitation, covalent

binding using silane solutions are employed. This method creates active groups on microfluidic substrates for subsequent attachment of biomolecules. However, stringent experimental conditions are required that in turn reduce the versatility of the silanization for the development of time effective interfaces in microfluidic devices.

Herein, we introduce a microfluidic platform for generating multiplex concentration gradients of biomolecules based on hydrodynamic resistances. The microfluidic design generates simultaneous multiplex concentration gradients of several biomolecules with varying concentration gradient slopes in up to seven parallel channels. The main advantage of such a device is the ability to perform high throughput gradient-dependent experiments in parallel channels with multiplex gradients in each channel. Furthermore, nonlinear polynomial (parabolic) gradients could also be produced using this design. The other important feature of this design is observing 2-dimensional gradients in which concentration gradients could be produced along both the length (800 μm) and width (600 μm) of the channel.

To produce highly resistant covalently bounded surface gradients, amine functional groups were immobilized on the target microchannel surface using micro-contact printing. Micro-contact printing of amino silanes not only drastically reduces the time and effort required for silane patterning of the surface; but also produces a homogenous monolayer of functional amine groups on the microchannel surface. This results in producing covalently bounded homogenous surface concentration gradients of biomolecules.

Solutions of IgG antibody conjugated with three different fluorescent dyes were used to demonstrate the produced surface gradients. The antibody attachment to the surface was achieved through chemically stable and robust bonds, which remain stable under high shear stress. Using this device, different multiplex concentration gradients of REDV and KRSR peptides, along the width of three parallel channels, were produced to investigate primary human umbilical vein endothelial cell (HUVEC) adhesion. This allowed us to perform three different cell adhesion experiments simultaneously using a single microfluidic chip.

8-4 Materials and methods

8-4-1 Materials

The negative photoresist SU8-25 was purchased from Microchem Corp (Boston, MA). (3-Aminopropyl) triethoxysilane (APTES), 1-ethyl-3-(3-dimethylaminopropyl) carbodiimide (EDC), N-hydroxysuccinimide (NHS), phosphate buffered saline (PBS), hydrogen peroxide and sulfuric acid were purchased from Sigma-Aldrich. Sylgard 184 elastomer kit composed of pre-polymer and curing agent of poly(dimethylsiloxane) (PDMS) was purchased from Essex Chemical (Boston, MA). Cy3, Cy5 and fluorescein isothiocyanate (FITC) conjugated IgG antibody was purchased from Abcam (Cambridge, MA). Arg-Glu-Asp-Val (REDV) and KRSR (Lysine-Arginine-Serine-Arginine) peptides were purchased from CHI SCIENTIFIC (Maynard, Massachusetts). Primary Human Umbilical Vein Endothelial Cells (HUVEC) were purchased from Invitrogen. Cell media 200 (M-200-500) supplement with low serum growth supplement (LSSG), and PS 1% were bought from Invitrogen.

8-4-2 Design and fabrication of the microfluidic chip

The microfluidic design consists of seven inlet channels, which merge to compose a main channel (Figure 8-1a). The main channel then feeds seven separate parallel channels named "target channels" in which the gradients are generated. These target channels were 100 μm wide and their height was 60 μm. Standard soft lithography using polydimethylsiloxane (PDMS) was employed to create microfluidic channels (μFN) followed by fabrication of the chip through irreversible binding of a flat glass slide to the PDMS substrate. The microfluidic channel system was designed in AutoCAD® software (Autodesk Inc., CA, USA) and printed on a chrome mask. To fabricate the mold for soft lithography, negative photoresist (SU8-25) was spin-coated (at 1500 rpm for 30 seconds) on a silicon wafer and baked to drive off solvent. Standard photolithography was performed on the wafer using the printed mask to fabricate the mold. The PDMS pre-polymer was prepared according to the protocol provided by the supplier and soft lithography was performed to fabricate the microfluidic channels on the PDMS substrate. After peeling the PDMS layer off the mold, holes were punched

to form ports for inlets and outlets. Oxygen plasma bonding was used to achieve irreversible binding of the PDMS substrate. The protocol for combinatorial micro-contact printing and creating the irreversible microfluidic platform is described in next sections. Once the closed channels were formed, the inlet and outlet tubes were connected (Fig S8-1). Flow control was achieved using a multi stage syringe pump (Nexus 3000, Chemyx Inc.).

8-4-3 Theory

From the electronic-hydrodynamic analogy, the hydrodynamic resistance (Rh) of a microchannel in a laminar incompressible steady state flow can be defined as:

$$Rh=\Delta P/Q \quad (8\text{-}1)$$

in which Q is the flow rate and ΔP ∇P is the pressure drop along the channel length. For a microchannel of length L, hydrodynamic diameter Dh and cross section area A, the hydrodynamic resistance can be defined as:

$$\mathbf{R_h = \frac{(f\ Re)\mu L}{2D_h^2 A}} \quad (8\text{-}2)$$

in which μ, f and Re are dynamic viscosity, friction factor and Reynolds number respectively. Using eqn 6-1 and assuming the flow rate at each channel to be the product of channel cross section area and average velocity, the hydrodynamic resistance of a straight channel with rectangular cross section (w: width and h: hight, assuming w~h) can be calculated as: (Beebe, Mensing et al. 2002, Oh, Lee et al. 2012)

$$R_h = \frac{12\mu L}{w h^3}\left[1 - \frac{h}{w}\left(\frac{192}{\pi^5}\sum_{(n=1,3,5)}^{\infty}\left[\frac{1}{n^5}\tanh\left(\frac{n\pi w}{2h}\right)\right]\right)\right]^{-1} \quad (8\text{-}3)$$

Therefore in straight microchannels (in a laminar, steady and incompressible flow) the hydrodynamic resistance depends only on the microchannel geometry (eqn 6-3).

For curved microchannels, different empirical equations have been proposed (Yang, Zhang et al. 2005, Chu, Teng et al. 2010). These empirical equations suggest that friction factor and therefore hydrodynamic resistance in curved channels depend on both geometry and Re number. In this case, calculating the hydrodynamic resistance becomes more complicated for curved channels. The target channels designed for multiplex gradient generation in this work (Figure 8-1a) consist of both curved and straight sections. Therefore simulation of the velocity field was performed to optimize the hydrodynamic resistances in each channel prior to device fabrication and predicted flow rates were later verified by experiment.

8-4-4 Computational Fluid Dynamics (CFD) analysis

Full scale simulation of the experimental setup was performed using a 3D model of the microfluidic design. The governing equations used for computational fluid dynamic (CFD) analysis were as follows:

$$\nabla[\eta(\nabla \mathbf{u} + (\nabla \mathbf{u})^{T}] + \rho(\mathbf{u}.\nabla)\mathbf{u} + \nabla p = 0 \qquad (8\text{-}4)$$

$$\nabla . \mathbf{u} = 0 \qquad (8\text{-}5)$$

Eqns (6-4) and (6-5) represent the Navier-Stokes and continuity equations respectively assuming incompressible steady state conditions. u is the velocity vector, p is pressure, η is the dynamic viscosity and ρ is liquid density. CFD analysis was performed using COMSOL (COMSOL Inc., Burlington, MA) software. Simulations were performed using a 12-core computer with 24GB of memory running a Linux operating system. The geometrical model was generated in AutoCAD and imported into COMSOL interface. Mesh density was designed to be finer at the areas targeted for gradient generation. Iterations were performed until the residual sums for velocity components reached values < 10^{-9}.

The fluid inside the channels was assumed to be Newtonian, with the physical properties of water. The applied boundary conditions were as following:

(1) inlet boundary conditions:

$$u_i = u_0 \ , i = 1, 2, 3, \dots, 7$$

(2) wall boundary conditions:

$u_w = 0$

(3) Outlet boundary conditions:

$P_o=0$

in which u_0 is equal to Q/A, where Q is the applied flow rate and A is cross section of the inlet channels. Inlets and outlets were specified as the entire opening at the beginning and end of each geometry, as opposed to the experimental platform in which holes are in the channel roof.

8-4-5 Rapid generation of covalent surface gradients

8-4-5-1 Micro-contact printing of amine groups

Detailed information about covalent surface functionalization using micro-contact printing protocol has been explained elsewhere (Didar, Foudeh et al. 2011). Briefly, flat PDMS stamps were used to micro-contact print APTES onto the glass substrates in the areas which form the target microchannels. The PDMS stamp was plasma treated for 1 min using oxygen plasma (60 s, 200 W, 200 mTorr O2). It was then covered with 10 µl of 2% APTES solution in ethanol at room temperature. To avoid evaporation of the APTES solution, a cover slip was placed on the stamp for 1 min. After rinsing with 70% ethanol solution for 15 sec and drying under nitrogen gas for 30 sec, the stamp was gently brought into contact with the predetermined areas on glass substrate for 5 sec. Immediately after printing the APTES solution, the plasma treated PDMS substrate (µFN) was brought into contact with the micro-contact printed glass substrate to form the microfluidic device (Figure 8-1b).

The device was then placed in an oven at 100 ºC for 60 min to ensure that the covalent binding of APTES with glass proceeded through condensation of hydrogen bonded silanol groups (Smith and Chen 2008).

8-4-5-2 Device assembly and covalent surface functionalization

Glass substrates were placed in piranha (H2O2:H2SO4, 1:3 v/v) solution for 10 min, rinsed extensively with deionized water, and dried under a nitrogen stream. Two substrates forming the microfluidic device (PDMS and glass) were plasma treated followed by micro-contact printing of (APTES) onto the glass substrate (Figure 8-1b). Immediately after microcontact printing, the glass and PDMS substrates were attached to form an irreversible microfluidic device. The platform was then placed in an oven at 100ºC for 60 min. N-hydroxysuccinimide (NHS) was used along with 1-ethyl-3-(3-dimethylaminopropyl) carbodiimide (EDC) to crosslink the biomolecules to the amino-silainized patterned surface. EDC (2 mg/ml) and NHS (5 mg/ml), dissolved in PBS, were incubated over the main channel for 20 min to activate the printed amine groups on the glass side of the microfluidic channel. After creating active amine groups on the surface, laminar flow streams of biomolecules were passed through the device to create solution gradients followed by covalent attachment of the biomolecules onto the channel surface.

For multiplex gradient generation, Cy3 conjugated IgG was introduced from inlets 1, 5 and 7, Cy5 conjugated IgG from 3rd and 6th inlets and FITC conjugated IgG from 2nd and 5th inlets. Concentration of antibody solutions was 10 µg/ml except for the 7th inlet which was 20 µg/ml. In addition, outlet of the 3rd target channel was pressurized to block the flow through this channel and create the highest hydrodynamic resistance at this channel. The aforementioned laminar flow streams were applied at a flow rate of 1 mm/s for 60 min. The channels were then rinsed with PBS at a flow rate of 10 cm/s (50 dyn/cm2) at each inlet channel.

8-4-6 Fluorescence microscopy

Generated concentration gradient profiles at each target channel were captured using an inverted fluorescence microscope (Nikon TE 2000-U). IgG Antibody conjugated with Cy3, Cy5 and FITC fluorescent dyes were observed through appropriate filters. All images were recorded using a CCD camera (Photometrics CoolSNAP HQ2) coupled to an optical microscope. Images were analyzed using ImageJ (MacBiophotonics) software.

8-4-7 Cell culture and cell adhesion onto multiplex peptide gradients

Cell adhesion experiments were conducted using primary human umbilical vein endothelial cells (HUVEC). Cells were cultured in 200 (M-200-500) media with low serum growth supplement (LSSG), and 1% PS. Cells were grown in a humidified incubator at 37 °C and supplemented with 5% CO_2 for 5 days and then trypsinized with 0.25% trypsin-EDTA (Gibco, USA) and used in the experiments. Cell suspensions were centrifuged at 200 g and then re-suspended in media to a concentration of 1×10^5 cells/ml.

Three different multiplex surface gradient profiles of REDV and KRSR peptides were produced in three of the target channels to investigate HUVECs adhesion to different gradient profiles under flow conditions. After generating surface gradients, outlets of the target channels were used as inlets to ensure that an equal number of cells with equal flow rates are passed through each channel. Target channel`s surfaces were washed by flowing sterile PBS. BSA was then passed through the channels and incubated for 30min to avoid nonspecific cell adhesion. Cells were then introduced into the channels at a flow rate of 0.25 µl/min for 40 min. Finally, channel surfaces were rinsed by flowing cell media.

8-5 Results and discussion

8-5-1 Gradient generation principle and CFD analysis

Concentration gradients of biomolecules were generated within parallel channels by varying hydrodynamic resistances. First, laminar flows containing solutions of different biomolecules are introduced through seven inlet channels. These inlet channels merge to compose a main channel. The main channel then feeds seven separate parallel channels labelled as "target channels" in which gradients are generated. In this design, hydrodynamic resistances were generated through embedded curves and differences in the lengths of channels. Figure S8-7 shows the effect of curved sections embedded in the design. In this figure, simulation results for flow rates in the proposed design are compared to a design consisting of straight target channels while maintaining the same length.

Imposed differences in hydrodynamic resistances of target channels result in different flow rates through each target channel. This provides control over the distribution of biomolecules into the target channels. To enhance the distribution of biomolecules, one or several target channels are pressurized to impose the highest possible hydrodynamic resistance. This generates a much higher velocity component perpendicular to the flow direction (in Y direction) facing the blocked channel. As such, no gradients are generated in the blocked channel. Interestingly, hydrodynamic resistances of target channels can be adjusted to produce 2-dimensional gradients in the main channel prior to entering the target channels in both X and Y directions.

It is well acknowledged that diffusion of biomolecules between different laminar flow streams occurs within the main channel at the onset of the gradient generation process. It is important to outline however, that this effect is later offset by advection forces (attributed to the action of Y-component of the velocity vector), which is the dominant part of the design that leads to several different gradient profiles on the same device.

To produce surface concentration gradients, functionalization is not affected by increasing flow rates up to 3 mm/s (Didar, Foudeh et al. 2011). The biomolecules are covalently attached to the surface through activated amine groups, thus yielding gradients of biomolecules in each target channel. Depending on the inlets, the biomolecule concentration, and associated flow rates, gradients of 1-3 biomolecules of choice with different concentration profiles can be generated in the target channels.

Figure 8-1c shows simulation results for the velocity field in which an average flow rate of 1 mm/s was applied at each of the inlets. The outlet of the 3rd target channel has been pressurized to stop the flow through this channel. This figure illustrates how the velocity in the main channel is altered as the flow approaches the target channels. Figure 8-1d represents the Y-component of the velocity vector. After entering the target channels, the velocity profile changes into the well-known parabolic shape as expected. Further from the target channels, the Y-

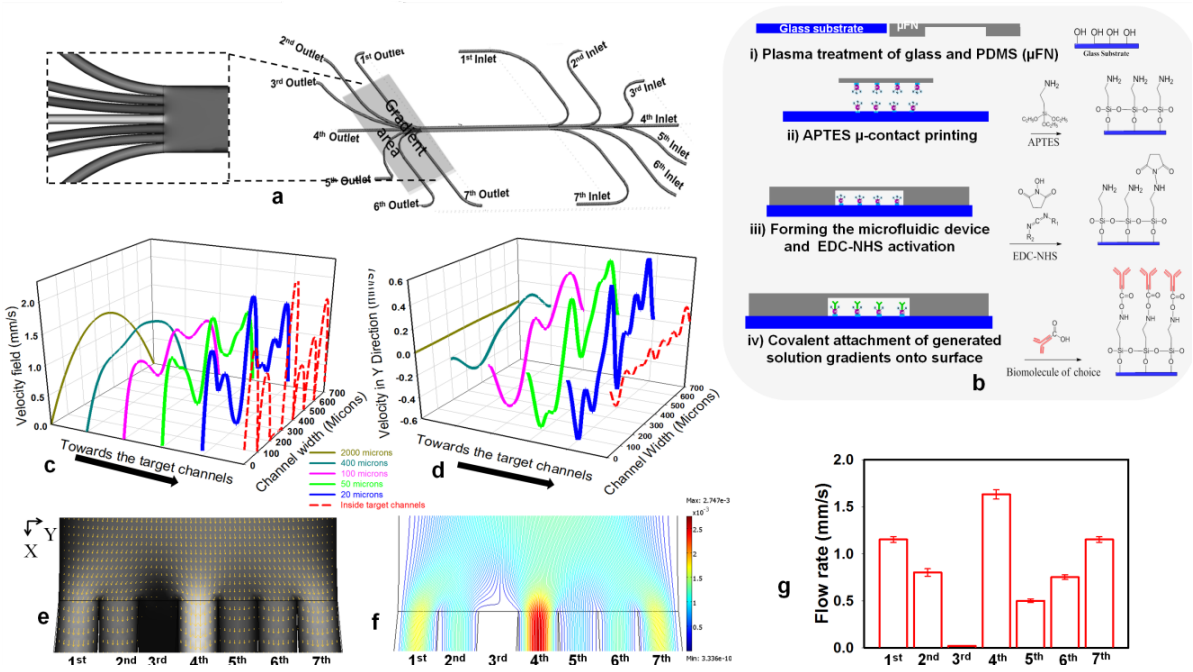

Figure 8-1: a) Schematic representation of the microfluidic design for gradient generation. The device consists of seven inlet channels and seven parallel channels named as "target channels" for gradient generation as shown in the magnified image. b) Schematic presentation of the surface functionalization and device assembly: glass and PDMS substrates are plasma treated and APTES is micro-contact printed on to the glass substrate. Immediately after micro-contact printing, the glass substrate is attached to the plasma treated PDMS (μFN) to form an irreversibly sealed microfluidic device, this is followed by activating the amine groups through EDC-NHS chemistry and biomolecules distributed in the flow are covalently attached onto the surface. c) Simulation results for the velocity field as the flow moves downstream in the main channel and enters the target channels. Velocity profile plotted in red dashed line represents the flow inside the target channels. d) Simulation results for the Y-component of the velocity field shown in part a, different velocity magnitudes in the Y direction contributes to the creation of gradients with different rates in the target channels. e) Simulation of the velocity field before entering the target channels, direction and length of the velocity arrows are proportional to the velocity field at each point. f) Simulation results for streamlines distribution into the target channels. g) Depicts experimental results for the flow rates through each target channel measured by collecting the amount of liquid exiting form each target channel referring to simulation results for the velocity profiles shown in red dashed line in c. Error bars represent standard deviation of three different experiments.

component of the velocity vector is zero and as the flow moves towards the target channels, it becomes more pronounced. In this region, Y-velocity varies depending on each channel it is facing, which in turn changes the flow direction, thus orienting the flow to the target channels (See ESI† Movie S8-1).

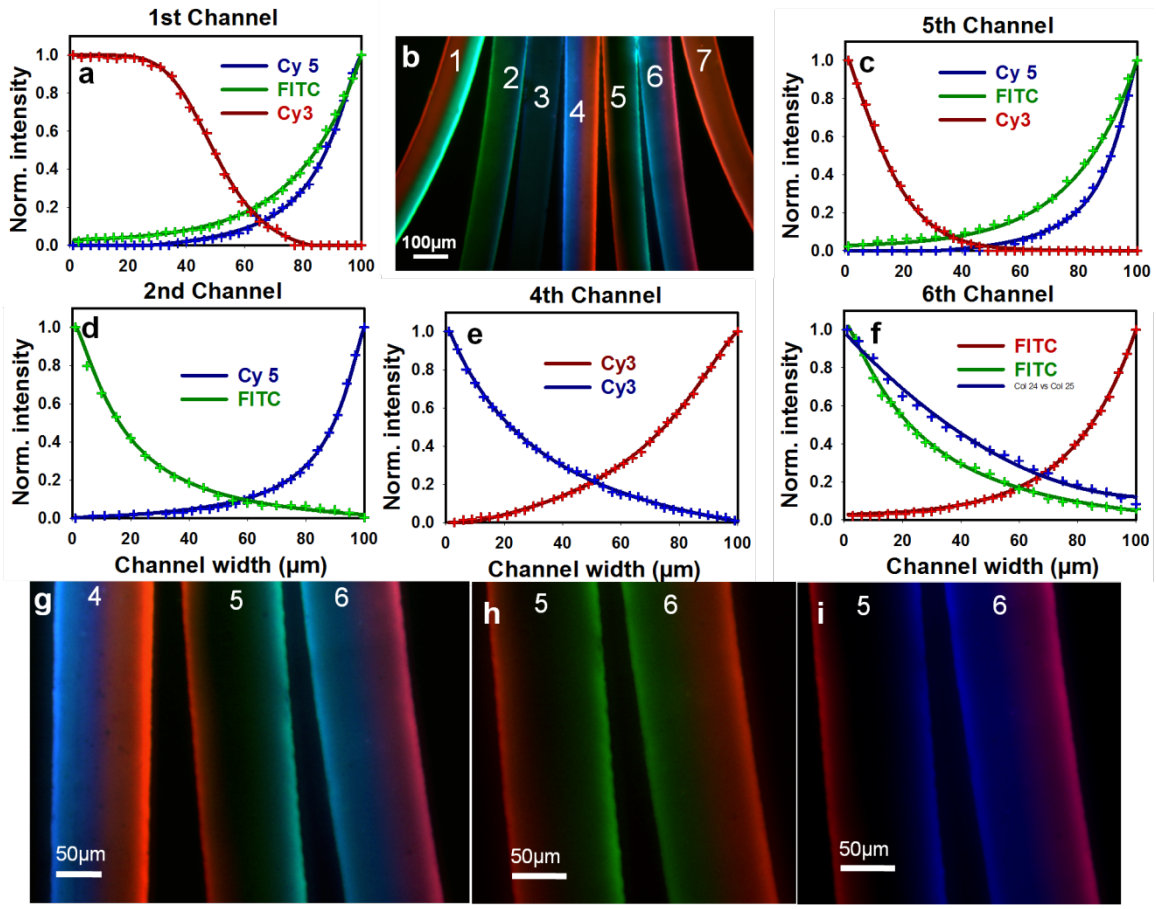

Figure 8-2: Multiplex surface concentration gradients produced in the target channels with different concentrations and different gradient rates. a,c,d, e and f) show fluorescent intensities of patterned gradients of antibodies in target channels. b) Superimposed fluorescence microscopy image, g) magnified fluorescence image of channels 4, 5 and 6, h and i) Magnified fluorescence images of the 5th and 6th channels patterned with FITC-Cy3 and Cy5-Cy3 conjugated IgG antibody respectively.

After entering the target channels, the Y-velocity decreases inside all seven channels. Figure 8-1e represents the overall flow velocity vectors in which the length of the arrows is proportional to the magnitude of the velocity vector. Figure 8-1f shows the density and distribution of the streamlines at the entrance of the target channels. It is clear that streamlines are much denser in the channels with lower resistance, leading to higher concentrations of biomolecules in these channels. In addition, the measured experimental results for the flow rate in each of the target channels, corresponded well to the predicted results by simulation (figure 8-1g). Based on the simulation results and experimental measurements, relative hydrodynamic resistances of each target channel can be determined

(Supporting information eqn S8-1, eqn S8-2 and Table S8-1). Applying different experimental conditions (flow rate, concentration of biomolecules and hydrodynamic resistances, desired combination of fixed multiplex gradient profiles in all or some of the target channels can be achieved.

8-5-2 Multiplex surface gradients

Figure 8-2b shows the superimposed flourescence microscopy image of generated multiplex surface concentration gradients. Cy5, FITC and Cy3 conjugated IgG antibodies were used for this purpose. The normalized fluorescence intensity across the widths of five selected target channels is presented in figures 8-2a-f. It should be noted that the fluorescence intensity of each dye has been normalized independently for each channel. Four target channels (1st, 4th, 5th and 6th) contain patterned gradients of three different antibodies. Magnified superimposed fluorescence microscopy images for the 4th, 5th and 6th channels are shown in figure 8-2g. Figures 8-2h and 8-2i depict 5th and 6th channels containing FITC-Cy3 and Cy5-Cy3 conjugated IgG respectively.

Analysis of fluorescence intensities obtained for FITC, Cy5 and Cy3 conjugated antibodies in each of the target channels was performed (Figure 8-3). Fluorescence intensities in target channels were calculated from a single image captured for each fluorescence dye in order to be able to compare intensities in different channels. As shown in figure 8-3, different gradient slopes of each antibody can be produced using parallel channels with varying hydrodynamic resistances. Each target channel provides a different maximum concentration of each antibody (shown with fitted polynomial gray lines in figure 8-3). These results clearly indicate the possibility of patterning each of the target channels with multiple biomolecules while obtaining different concentration gradient profiles.

One of the most important advantages of this microfluidic design is the ability to achieve simultaneous multiplex gradient profiles and concentration ranges in separate parallel channels, as opposed to the previously proposed designs in which only one concentration profile could be obtained at a specific time. This is

beneficial in performing high throughput gradient dependent experiments where different concentration ranges and profile slopes are required. The multiplex surface gradients, produced via covalent chemical bounds, remained stable under high shear stresses. This provides an important advantage especially for applications where high shear stress is required. The procedure used for forming the irreversibly sealed microfluidic device also underlied operation of the chip at high flow rates.

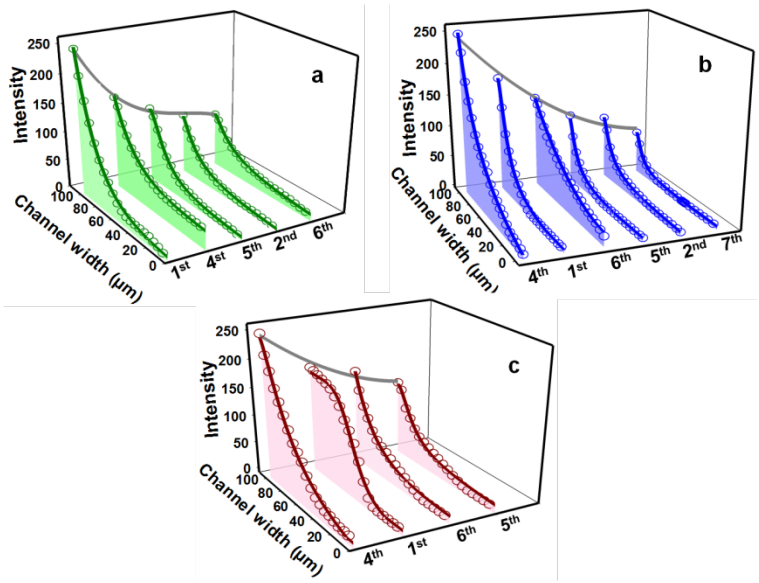

Figure 8-3: Analysis of generated surface gradients shown in figure 8-2. Gradient profiles and intensities of FITC, Cy5 and Cy3 conjugated IgG antibody in selected target channels has been shown in a, b and c respectively. The fitted polynomial line in gray color, shows variations in the maximum concentration of each dye in different target channels.

8-5-3 Nonlinear and 2-Dimensional concentration gradients

Although generating multiplex gradients with different profile slopes and concentrations in target channels would be beneficial, particularly for high throughput applications, nonlinear concentration profiles are often required.

The proposed design successfully demonstrates the ability to produce different profile shapes of surface concentration gradients. Figure 8-4 shows three different gradient profiles obtained for Cy5 conjugated antibody. Figure 8-4a was obtained by applying the same hydrodynamic resistances applied in the previous section.

Different experimental conditions can be applied to produce parabolic shape gradients. Two experiments are presented in which polynomial concentration profiles of Cy5 conjugated IgG were generated. For this purpose, the 2nd, 3rd, 5th and 6th channels were blocked. In the first experiment (figures 6-4b and 6-4e), the Cy5 conjugated antibody solution was introduced from the 4th inlet; while in the second experiment, it was introduced through the 3rd and 5th inlets (figures 8-4c and 8-4f).

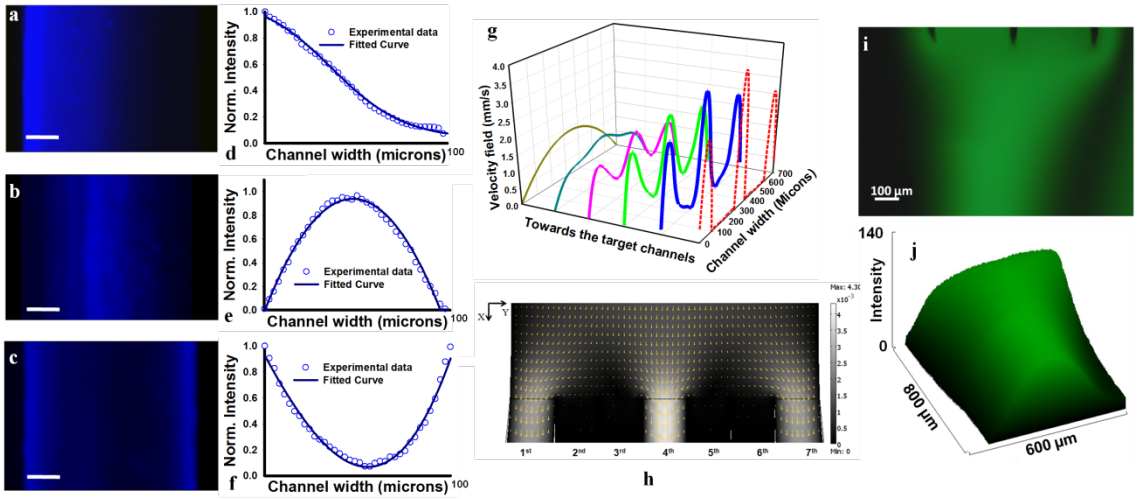

Figure 8-4: Different gradient profiles of Cy5 conjugated IgG obtained in the 4th channel by applying different experimental conditions: a) applying the experimental conditions explained in the previous section, b) Cy5 conjugated antibody was introduced form the 4th inlet applying the experimental conditions shown in g and h. c) Cy5 conjugated IgG was introduced from the 3rd and 6th inlets applying the same resistances in part b. d-f) shows the fluorescence intensities for a, b and c respectively. The fitted curves represent R2>0.98, g and h) represent simulation results for the velocity field applied in parts b and c, i) shows generating 2-dimensional gradients before the flow enters the target channels. This could be achieved by blocking the two channels in the middle, while the channel in the right side has a lower resistance compared to the channel at the left side of the figure. j) 3-D fluorescence intensity of the surface shown in i which clearly indicates 2-Dimentional gradients in an area of 800 µm in 600 µm before the flow enters the target channels. The image was produced using image J software.

In both experiments, buffer was introduced from the other remaining channels. Results clearly show the possibility of obtaining polynomial (parabolic) gradient profiles by applying simple changes to the experimental conditions.

Distribution of the biomolecules prior to entering the target channels is also of interest. The flow distribution just before entering the target channels can also be manipulated and controlled by adjusting the resistances of these channels. This leads to generation of biomolecule gradients in more than one direction within the

main channel (figure 8-4i). We report this observation as 2-dimensional gradient formation. Figures 8-4i-j show the resulting 2-dimensional solution gradient of FITC conjugated-IgG antibodies that are generated before entering the target channels.

In this figure, the right channel has a lower resistance compared to the left one, while the two channels in the middle have been pressurized and blocked. This variable resistance resulted in gradients of FITC conjugated-IgG antibodies in both the length and width of the main channel prior to entering the target channels (figure 8-4j). Applying equal resistances in both left and right channels in this figure resulted in equal distribution of biomolecules (Fig S8-8). Although we reported generation of 2-dimenstional biomolecule gradients, the proposed design may be simply manipulated and modified using the introduced principles in order to address specific applications depending on the area and profile shape needed.

8-5-4 Cell adhesion on multiplex peptide gradients

Three different multiplex surface gradients of REDV and KRSR peptides were generated along the cross section of three target channels. HUVEC adhesion onto these respective surfaces was subsequently investigated. Cells adhered across the width of the channels in response to the concentration of REDV peptide. In addition, under the same experimental conditions and parameters, the cells did not respond to the KRSR surface gradients (figure 8-5). HUVEC cells did not also adhere to the surfaces functionalized only with KRSR peptide gradient without the presence of REDV peptide. Moreover, HUVEC adhesion was also investigated on generated REDV surface gradients in the main channel (figure 8-5j-l). Time lapse imaging of the cells for several hours after attachment showed that the cells remained viable (See ESI† Movie S8-2) and proliferated (See ESI† Movie S8-3). It is important to note that cell adhesion density is directly proportional to REDV peptide surface concentration (figure 8-5). Endothelial cells were previously reported to attach onto surfaces functionalized with REDV peptide (Massia and Hubbell 1992, Plouffe, Njoka et al. 2007, Didar and Tabrizian 2010).

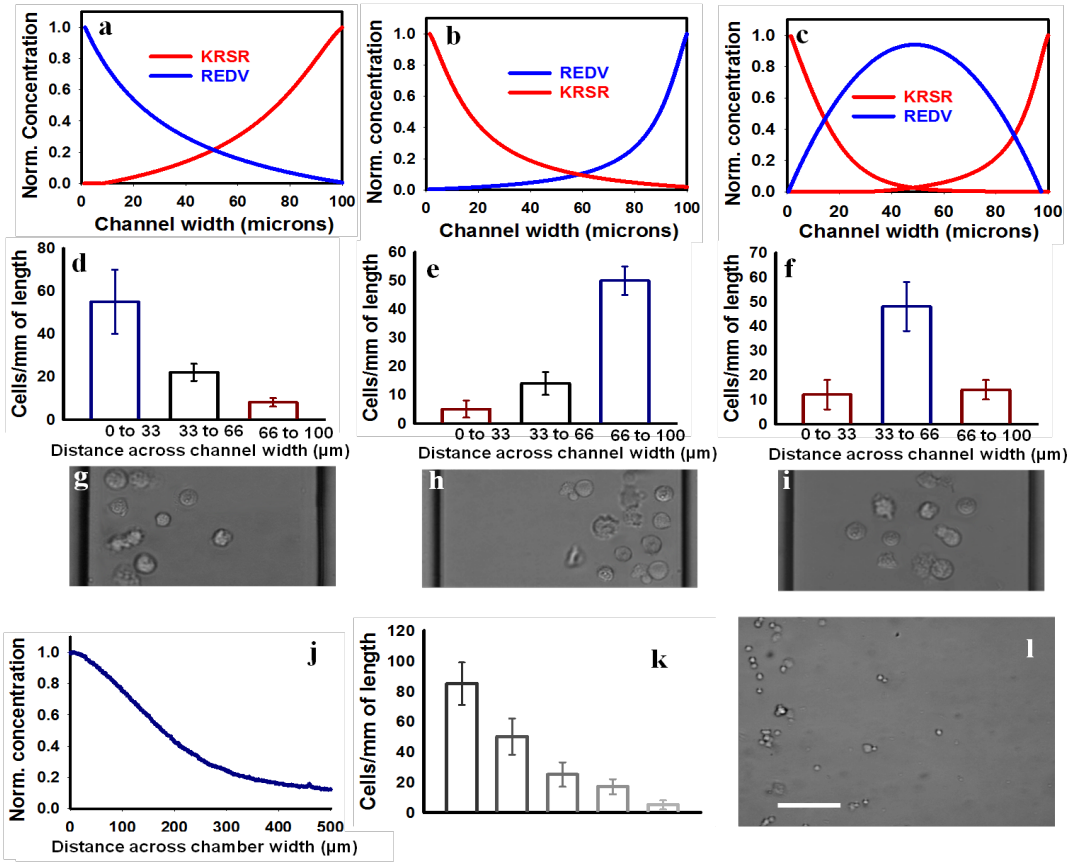

Figure 8-5: HUVECs adhesion on multiplex gradients of REDV and KRSR peptides. a, b and c) show the generated surface concentration gradients of REDV and KRSR peptides within three parallel channels. d, e and f) represent HUVECs adhesion across the width of three parallel channels. Error bars represent standard deviation of analyzing 5 different images for each channel. g, h and i) representative optical microscope images of HUVECs adhesion corresponding to d, e and f respectively. j) Shows the generated REDV concentration gradient across the width of the main channel. k) shows cell adhesion onto REDV peptide gradient shown in j, l) represents the optical microscope image of HUVECs adhesion shown in k. Scale bar is 100 μm.

Our results are not only in full accordance with the literature, but also demonstrate the degree of HUVEC adhesion through variation of REDV peptide concentration under flow conditions, as well as the presence of surface gradients of KRSR peptide. The introduced method may also be implemented for selective and controlled cell patterning at specific areas across the channels width.

8-6 Conclusion

These results indicate that the microfluidic chip can be implemented to investigate cell adhesion on multiplex peptide surface gradients. The developed

design can further be used for in vitro biological applications requiring concentration gradients of multiplex biomolecules such as selective cell adhesion and cell sorting. Furthermore, implementing such a design can be applied to investigations of cellular response to gradients of multiplex stimuli on the surface or in suspension to study migration, differentiation, proliferation or screening against different drug dosages.

A novel approach for performing high throughput studies requiring gradients of various chemical agents for cellular analysis is presented. This was addressed by the innovative design of a chip in which different microchannels provide different concentrations and varying distributions of multiple biomolecules. Our results showed that this microfluidic design provides highly resistant and durable gradients of multiple biomolecules in parallel microfluidic channels, each containing different concentrations and gradient slopes by employing different hydrodynamic resistances. Covalent chemical surface gradients were also produced through micro-contact printing of amine groups onto glass substrates prior to assembling the microfluidic device. These surface concentration gradients remained stable and functional under high shear stresses. To illustrate the versatility of the design, the same IgG antibodies, conjugated to three different fluorescence dyes, were employed. Multiplex gradients were generated simultaneously in parallel microchannels, each possessing a different concentration and gradient slope, thus providing an interface for high throughput analysis of gradient dependent biological processes. To further demonstrate the capabilities of the design, multiplex surface gradients of REDV and KRSR peptides were produced in three parallel channels and HUVECs adhesion was investigated. HUVECs responded favourably to REDV concentration gradients while displaying poor cell adhesion onto KRSR gradients within the same channel. The proposed approach is straightforward, rapid, reliable, cost effective and consumes less reagents. It could facilitate future developments in the field of integrated biosensor or lab-on-a-chip devices. Such technologies are anticipated to become routine analytical tools to study adhesion based cell sorting and

patterning, as well as in the development of inexpensive methods for screening clinical, environmental and food samples.

8-7 Supporting Information

Figure S8-6: Photograph of the microfluidic device connected to the syringe pump.

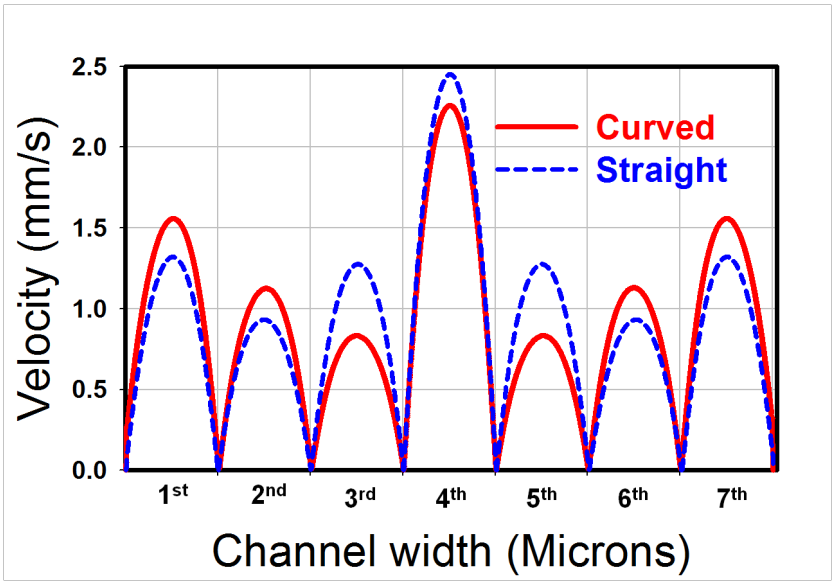

Figure S8-7: Simulation results for flow rates in the proposed design with embedded curves (red) compared to a design consisting of straight target channels while maintaining the same length (dashed blue).

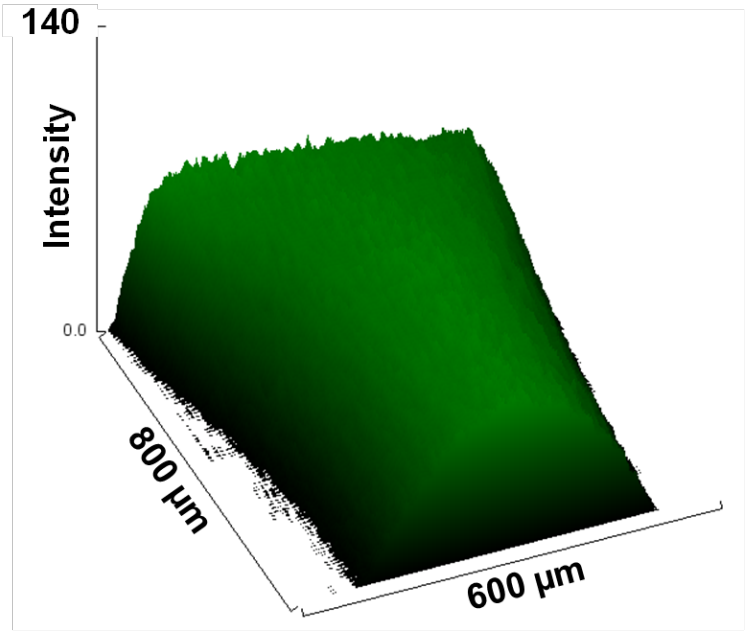

Figure S8-8: 3D fluorescence intensity profile prior to entering the target channels shown in figure 8-4i, applying equal resistances in both left and right channels. As shown here equal resistances has resulted in equal distribution of biomolecules.

Calculating relative hydrodynamic resistances of target channels

Assuming the flow rate in the main channel to be Qm, hydrodynamic resistances of the target channels to be Ri (i=1,2,3,...7) and the flow rate at each target channel to be Qi (i=1,2,3,...,7), then the total flow rate Qm is:

$$Q_m = ?_{i=1}^{7} Q_i = ?_{i=1}^{7} \frac{?\_p_i}{R_i} = ?\_p\, ?_{i=1}^{7} \frac{1}{R_i} \quad \text{(S8-1)}$$

Flow rate in each channel, Qi is the product of average velocity and channel cross section. Based on the numerical simulation results, Assuming the average velocity in channel 4 to be V4, then the relative average velocity in the other channels was calculated to be:

$$\begin{cases} V_{1=}0.7V_4 \\ V_{2=}0.5V_4 \\ V_{3=}0 \\ V_{5=}0.3V_4 \\ V_{6=}0.5V_4 \\ V_{7=}0.7V_4 \end{cases} \quad \text{(S8-2)}$$

Assuming equal pressure drop for all target channels except the 3rd channel which has been pressurized, the relative hydrodynamic resistances of each target channel can be determined. For this purpose the hydrodynamic resistance of the 4th channel was assumed to be 1, then the relative hydrodynamic resistances of the target channels compared to the fourth channel was calculated as shown in table S8-1. These results were also confirmed by measuring the flow rates at each target channel (Figure 8-1g). The measured flow rates correspond to the relative velocities as shown in eqn S6-2.

Table S8-1: Relative hydrodynamic resistances of target channels

Channel No.	1st	2nd	3rd	4th	5th	6th	7th
Resistance	1.4	2	∞	1	3.3	2	1.4

Table S8-2: Description of the peptides used for gradient generation

Peptide Name	Description	Modification for flourecence
KRSR	Lysine-Arginine-Serine-Arginine N-terminus- Free amine	N-terminus- Free amine C-terminus- 5'-FAM
REDV	Arg-Glu-Asp-Val N-terminus- Free amine	N-terminus- Free amine C-terminus- Rhodamin (red)

8-8 Acknowledgment

The authors would like to acknowledge National Science and Engineering Research Council of Canada (NSERC)-Collaborative Research program, NSERC-CREATE, Nano-Quebec, Genome Canada/ Génome Québec. T.F. Didar would like to thank the faculty of medicine at McGill and Fonds de recherche du Quebec - Nature et technologies (FQRNT) for their financial´ support. The

authors would like to acknowledge Prof. D. Juncker for providing access to micro-contact printing and microscopy facilities. The authors would also like to thank S. G. Ricoult for scientific discussions and J. Daoud and K. Bowey for comments on the manuscript.

References

Barkefors, I., S. Thorslund, F. Nikolajeff and J. Kreuger (2009). "**A fluidic device to study directional angiogenesis in complex tissue and organ culture models.**" Lab on a Chip **9**(4): 529-535.

Beebe, D. J., G. A. Mensing and G. M. Walker (2002). "**Physics and applications of microfluididcs in biology**." Annual Review of Biomedical Engineering **4**(1): 261-286.

Bhattacharjee, N., N. Li, T. M. Keenan and A. Folch (2010). "**A neuron-benign microfluidic gradient generator for studying the response of mammalian neurons towards axon guidance factors.**" Integrative Biology **2**(11-12): 669-679.

Boyden, S. (1962). "**The chemotactic effect of mixtures of antibody and antigen on polymorphonuclear leucocytes.**" J. Exp. Med. **115**(3): 453–466.

Breslauer, D. N., P. J. Lee and L. P. Lee (2006). "**Microfluidics-based systems biology.**" Molecular BioSystems **2**(2): 97-112.

Bui, M.-P. N., C. A. Li, K. N. Han, J. Choo, E. K. Lee and G. H. Seong (2011). "**Enzyme Kinetic Measurements Using a Droplet-Based Microfluidic System with a Concentration Gradient.**" Analytical Chemistry **83**(5): 1603-1608.

Campbell, K. and A. Groisman (2007). "**Generation of complex concentration profiles in microchannels in a logarithmically small number of steps.**" Lab on a Chip **7**(2): 264-272.

Cate, D. M., C. G. Sip and A. Folch (2010). "**A microfluidic platform for generation of sharp gradients in open-access culture.**" Biomicrofluidics **4**(Copyright 2011, The Institution of Engineering and Technology): 044105 (044110 pp.).

Chu, J.-C., J.-T. Teng and R. Greif (2010). "**Experimental and numerical study on the flow characteristics in curved rectangular microchannels.**" Applied Thermal Engineering **30**(13): 1558-1566.

Chung, B. G. and J. Choo (2010). "**Microfluidic gradient platforms for controlling cellular behavior.**" ELECTROPHORESIS **31**(18): 3014-3027.

Chung, B. G., L. A. Flanagan, S. W. Rhee, P. H. Schwartz, A. P. Lee, E. S. Monuki and N. L. Jeon (2005). "**Human neural stem cell growth and differentiation in a gradient-generating microfluidic device.**" Lab on a Chip **5**(4): 401-406.

Cooksey, G. A., C. G. Sip and A. Folch (2009). "**A multi-purpose microfluidic perfusion system with combinatorial choice of inputs, mixtures, gradient patterns, and flow rates.**" Lab on a Chip **9**(3): 417-426.

Dertinger, S. K. W., D. T. Chiu, N. L. Jeon and G. M. Whitesides (2001). "**Generation of Gradients Having Complex Shapes Using Microfluidic Networks.**" Analytical Chemistry **73**(6): 1240-1246.

Didar, T. F., A. M. Foudeh and M. Tabrizian (2011). "**Patterning Multiplex Protein Microarrays in a Single Microfluidic Channel.**" Analytical Chemistry.

Didar, T. F. and M. Tabrizian (2010). "**Adhesion based detection, sorting and enrichment of cells in microfluidic Lab-on-Chip devices.**" Lab on a Chip **10**(22): 3043-3053.

Guarnieri, D., A. De Capua, M. Ventre, A. Borzacchiello, C. Pedone, D. Marasco, M. Ruvo and P. A. Netti (2010). "**Covalently immobilized RGD gradient on PEG hydrogel scaffold influences cell migration parameters.**" Acta Biomaterialia **6**(7): 2532-2539.

Holden, M. A., S. Kumar, E. T. Castellana, A. Beskok and P. S. Cremer (2003). "**Generating fixed concentration arrays in a microfluidic device.**" Sensors and Actuators B: Chemical **92**(1-2): 199-207.

Irimia, D., D. A. Geba and M. Toner (2006). "**Universal Microfluidic Gradient Generator.**" Analytical Chemistry **78**(10): 3472-3477.

Irimia, D., S.-Y. Liu, W. G. Tharp, A. Samadani, M. Toner and M. C. Poznansky (2006). "**Microfluidic system for measuring neutrophil migratory responses to fast switches of chemical gradients.**" Lab on a Chip **6**(2): 191-198.

Ismagilov, R. F., A. D. Stroock, P. J. A. Kenis, G. Whitesides and H. A. Stone (2000). "**Experimental and theoretical scaling laws for transverse diffusive broadening in two-phase laminar flows in microchannels.**" Applied Physics Letters **76**(17): 2376-2378.

Jeon, N. L., S. K. W. Dertinger, D. T. Chiu, I. S. Choi, A. D. Stroock and G. M. Whitesides (2000). "**Generation of Solution and Surface Gradients Using Microfluidic Systems.**" Langmuir **16**(22): 8311-8316.

Jiang, X., Q. Xu, S. K. W. Dertinger, A. D. Stroock, T.-m. Fu and G. M. Whitesides (2005). "**A General Method for Patterning Gradients of Biomolecules on Surfaces Using Microfluidic Networks.**" Analytical Chemistry **77**(8): 2338-2347.

Kamholz, A. E. and P. Yager (2001). "**Theoretical Analysis of Molecular Diffusion in Pressure-Driven Laminar Flow in Microfluidic Channels.**" Biophysical Journal **80**(1): 155-160.

Kang, S., W. Zongxing and J. Xingyu (2008). "**Modular microfluidics for gradient generation.**" Lab on a Chip **8**(Copyright 2009, The Institution of Engineering and Technology): 1536-1543.

Keenan, T. M. and A. Folch (2008). "**Biomolecular gradients in cell culture systems.**" Lab on a Chip **8**(1): 34-57.

Kim, S., H. J. Kim and N. L. Jeon (2010). "**Biological applications of microfluidic gradient devices.**" Integrative Biology **2**(11-12): 584-603.

Lamb, B. M., S. Park and M. N. Yousaf (2010). "**Microfluidic Permeation Printing of Self-Assembled Monolayer Gradients on Surfaces for Chemoselective Ligand Immobilization Applied to Cell Adhesion and Polarization.**" Langmuir **26**(15): 12817-12823.

Li Jeon, N., H. Baskaran, S. K. W. Dertinger, G. M. Whitesides, L. Van De Water and M. Toner (2002). "**Neutrophil chemotaxis in linear and complex gradients of interleukin-8 formed in a microfabricated device.**" Nat Biotech **20**(8): 826-830.

Massia, S. and J. Hubbell (1992). "**Vascular endothelial cell adhesion and spreading promoted by the peptide REDV of the IIICS region of plasma fibronectin is mediated by integrin alpha 4 beta 1**." J. Biol. Chem. **267**(20): 14019-14026.

Millet, L. J., M. E. Stewart, R. G. Nuzzo and M. U. Gillette (2010). "**Guiding neuron development with planar surface gradients of substrate cues deposited using microfluidic devices.**" Lab on a Chip **10**(12): 1525-1535.

Mosadegh, B., W. Saadi, S.-J. Wang and N. L. Jeon (2008). "**Epidermal growth factor promotes breast cancer cell chemotaxis in CXCL12 gradients.**" Biotechnology and Bioengineering **100**(6): 1205-1213.

Oh, K. W., K. Lee, B. Ahn and E. P. Furlani (2012). "**Design of pressure-driven microfluidic networks using electric circuit analogy.**" Lab on a Chip.

Olofsson, J., H. Bridle, J. Sinclair, D. Granfeldt, E. Sahlin and O. Orwar (2005). "**A chemical waveform synthesizer.**" Proceedings of the National Academy of Sciences of the United States of America **102**(23): 8097-8102.

Plouffe, B. D., D. N. Njoka, J. Harris, J. Liao, N. K. Horick, M. Radisic and S. K. Murthy (2007). "**Peptide-mediated selective adhesion of smooth muscle and endothelial cells in microfluidic shear flow.**" Langmuir **23**(9): 5050-5055.

Saadi, W., S.-J. Wang, F. Lin and N. Jeon (2006). "**A parallel-gradient microfluidic chamber for quantitative analysis of breast cancer cell chemotaxis.**" Biomedical Microdevices **8**(2): 109-118.

Selimović, S. e., W. Y. Sim, S. B. Kim, Y. H. Jang, W. G. Lee, M. Khabiry, H. Bae, S. **Jambovane, J. W. Hong and A. Khademhosseini** (2011). "**Generating Nonlinear Concentration Gradients in Microfluidic Devices for Cell Studies.**" Analytical Chemistry **83**(6): 2020-2028.

Smith, E. A. and W. Chen (2008). "**How to prevent the loss of surface functionality derived from aminosilanes.**" Langmuir **24**(21): 12405-12409.

Yang, W.-h., J.-z. Zhang and H.-e. Cheng (2005). "**The study of flow characteristics of curved microchannel.**" Applied Thermal Engineering **25**(13): 1894-1907.

Yeh, C.-H., C.-H. Chen and Y.-C. Lin (2011). "**Use of a gradient-generating microfluidic device to rapidly determine a suitable glucose concentration for cell viability test.**" Microfluidics and Nanofluidics **10**(5): 1011-1018.

Chapter 9. A miniaturized platform for rapid and simultaneous separation, patterning and in vitro culture of primary cells

9-1 Connecting text

In chapters 7 and 8 producing bio-functional interfaces in the form of microarrays and surface gradients were demonstrated. This chapter implements the micro-contact printing approach developed in the previous chapters to separate target primary cells. In the context, the capability of adhesion-based approach for separation, patterning and *in vitro* culture of oligodendrocyte progenitor cells and cardiomyocytes from brain and heart tissues respectively is demonstrated. This chapter addresses the second main goal of the project for implementing label-free techniques for cell separation. In addition to cell separation, the developed platform was shown to be useful for subsequent applications to study separated cells *in vitro.*

The research contributions of this chapter are as following:

Patent: Tohid Fatanat Didar, K. Bowey and M. Tabrizian, Universal microchip for detection separation, isolation and controlled attachment and spreading of rare and primary cells, (June 2013).

Journal paper: Tohid Fatanat Didar, Kristen Bowey and Maryam Tabrizian, (2013), A miniaturized platform for rapid and simultaneous separation, patterning and *in vitro* culture of primary cells, Advanced Healthcare Materials, Accepted.

9-2 Abstract

Given that current cell isolation techniques are expensive, time consuming, yield low isolation purities, and/or alter target cell properties, we have developed a versatile, cost effective and easy-to-operate microchip with the capability to simultaneously separate, capture, pattern and culture rare and primary cells in vitro. The platform is based on target cell adhesion onto the micro-fabricated interfaces produced by micro-contact printing of cell-specific antibodies. Results showed over 95% separation efficiency in less than 10 min for the separation of oligodendrocyte progenitor cells (OPCs) and cardiomyocytes from rat brain and heart mixtures respectively. Target cell attachment and single cell spreading could be precisely controlled based on the designed patterns. Both cell types could maintain their biofunctionality. Indeed, isolated OPCs could proliferate and differentiate into mature oligodendrocytes, while isolated cardiomyocytes retained their contractile properties on the separation platform. Successful separation of two dissimilar cell types present in varying concentrations in their respective cell mixtures and demonstration of their integrity after separation opens new avenues for time and cost effective sorting of various cell types using the developed miniaturized platform.

9-2 Introduction

The separation of a homogenous population of cells from a mixed cell system is critical to the success of many clinical diagnostic tests and to a significant faction of fundamental medical research. In cell separation, physical (e.g. density, size) or affinity-based (e.g. electric, magnetic) properties can be exploited to separate target cells from mixtures derived from primary biological tissues. However, conventional cell separation techniques, such as filtration, centrifugation, and sedimentation can be time consuming and problematic in terms of reproducibility. Equally, differences in physical properties such as size or density may not be sufficient among cell types to yield efficient separation. Cell sorting techniques can further be divided into label-free and pre-processed techniques (Didar and Tabrizian 2010). Fluorescence activated cell sorting (FACS) (Herzenberg, Sweet et al. 1976) and magnetic activated cell sorting (MACS) (Marek, Caruso et al. 2008) are two commercialized examples of pre-processed techniques. Though highly efficient, these methods typically require costly equipment and complex procedures that may alter cellular properties, restricting target cell use in subsequent applications. In addition these methods require using significant amount of cell-specific biomarkers which are often quite expensive.

Among label-free techniques, adhesion-based separation can be used to sort cells with simliar physical properties, though separation efficiencies may be significantly reduced. However, if appropriate methods are implemented to produce an adhesion-based platform, the resultant separation method is not only label-free, but also highly specific to the target cell population. Therefore, the key to adhesion-based cell separation lies in both the method for producing a platform with embedded bio-functional interfaces and in the specificity of the immobilized biomolecule to the target cell population (Didar and Tabrizian 2010).

A bio-functional capture interface is fundamental to the success of an adhesion-based separation platform. Recently, miniaturized platforms with embedded bio-functional interfaces have opened new avenues for a variety of biological applications such as biosensing, microbioreactors, cell detection, sorting, and in vitro culture (Nagrath, Sequist et al. 2007, Plouffe, Kniazeva et al. 2009, Legeay,

Coudreuse et al. 2010, Esch, Post et al. 2011). Most bio-functional miniaturized interfaces are produced by engineering surfaces to immobilize biomarkers or multiple stimuli onto substrates4 (Didar, Foudeh et al. 2011).

Several approaches have been proposed to pattern biomarkers onto miniaturized surfaces (Mandal, Rouillard et al. 2007, Jang and Liu 2009, Fiddes, Chan et al. 2010, Kim, Choi et al. 2010). Among them, micro-contact printing (Graber, Zieziulewicz et al. 2003, Quist, Pavlovic et al. 2005, Kaufmann and Ravoo 2010) is of particular interest since it is rapid and user friendly. Although micro-contact printing has previously been used to pattern extracellular matrix (ECM) biomolecules with the aim of guiding cell adhesion and growth, it has thus far not been used to separate cells from a heterogeneous mixture.

Here, we present a method to develop miniaturized, bio-functional interfaces for highly specific detection, separation and guided attachment of target cells from primary mixtures with differing physical properties and initial concentrations. The proof of concept was demonstrated by separating two cell types, namely oligodendrocyte progenitor cells (OPCs) with a population of 5-10% in rat brain tissues and cardiomyocytes representing 50-60% of total cells in rat heart tissues. Both cell types have limited proliferative potential in vitro and OPC maturation, in particular, is thought to be limited by the inability to obtain pure cell populations. OPCs and cardiomyocytes are frequently used as cell models for in vitro and preclinical investigations of various diseases. For instance, OPCs play an important role in both initiation and treatment of numerous central nervous system (CNS) diseases. They are involved in the myelinating glial cells in the CNS, critical to facilitating the rapid conduction of neuronal action potentials and supporting axonal survival (Chen, Balasubramaniyan et al. 2007). Isolated OPCs are commonly used as a tool in myelin repair research and to study oligodendrocyte development, function and axon–oligodendroglial interactions. Several methods have been developed to separate rat OPCs from the CNS, such as FAC(Sim, McClain et al. 2011), MACS (Cizkova, Cizek et al. 2009), and shaking methods based on the differential adherent properties of glial cells. However, in addition to specialized laboratory requirements with high costs,

these methods require multiple time consuming steps to reach a degree of OPC purity over 90% and often alter target cells properties for subsequent applications.

In the same way, *in vitro* cultured cardiomyocytes are used in many cardiovascular research models to study morphological, biochemical and electrophysiological characteristics of the myocardium. In particular, cardiomyocyte contraction, myocardial ischemia, hypoxia and drug toxicity can be studied with isolated cells. Cardiomyocytes form about 50% of initial cell mixtures derived from primary heart tissue (Banerjee, Fuseler et al. 2007). However, achieving high yields of cells capable of contracting at high pacing rates and surviving β-adrenergic stimulation after separation is challenging using current isolation methods. Specifically, cardiomyocyte isolation techniques based on mechanical separation can damage cardiomyocyte membranes and membrane-bound receptors.

Simple methods for the isolation and purification of workable quantities of OPCs and cardiomyocytes would thusly be useful in the fields of both neural and cardiac research. To implement adhesion-based cell sorting, separation, and patterning, A2B5 and PDGFα progenitor markers expressed at the early stage of OPC maturation (Sim, McClain et al. 2011) and signal-regulatory protein alpha (SIRPA) (Dubois, Craft et al. 2011) were used as adhesion molecules to specifically identify OPC and cardiomyocytes, respectively. The introduced method based on micro-contact printing significantly reduces the use of expensive cell-specific biomarkers compared to FACs and MACs due to the fact that only 10 µl (20 µg/ml) of cell-specific biomolecule solution is sufficient to produce the bio-functional interface by micro-contact printing. In addition to rapid cell separation, the developed microchip was also used to guide the attachment and spreading of single target cells directly within the platform.

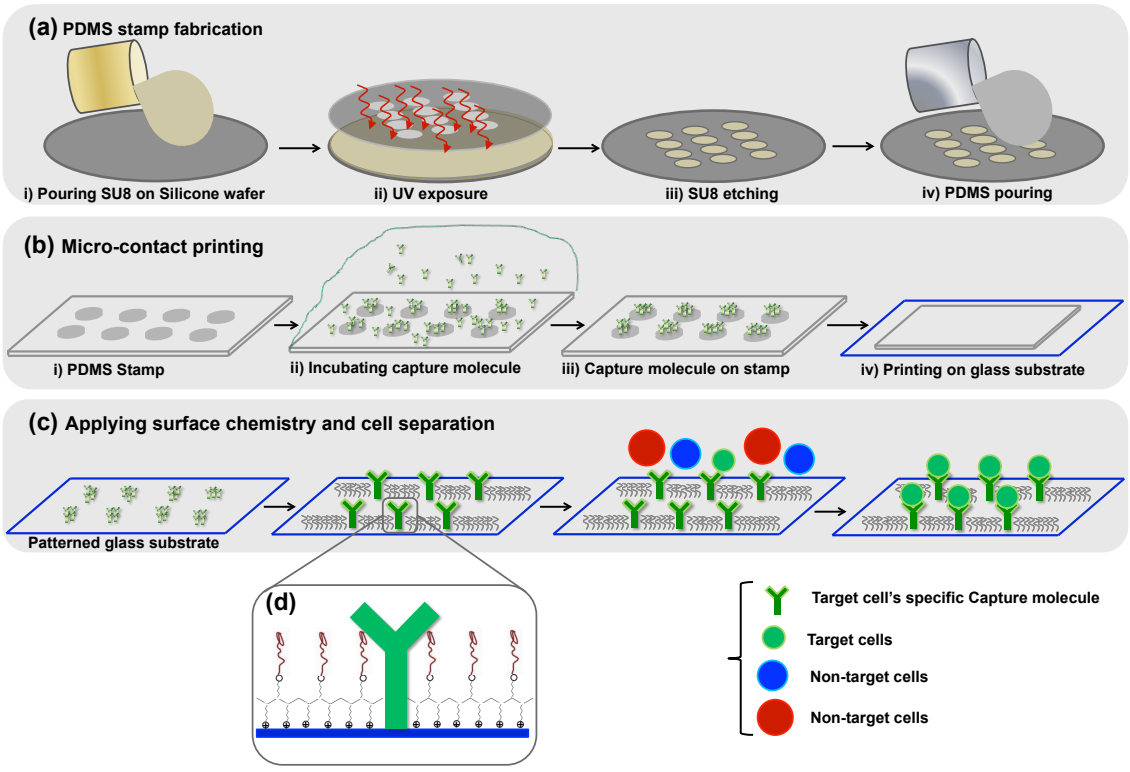

Figure 9-1: Scheme of the fabrication process to produce the cell separation platform. (a) Represents photolithography and soft lithography steps to fabricate the PDMS stamps. First a silicon wafer was coated with SU8 photoresist and was patterned according to the desired design in a clean room using a chrome mask. After fabricating the SU-8 based mold, soft lithography was implemented to produce PDMS stamps using the fabricated mold. (b) Shows the micro-contact printing procedure where the target cell's specific antibodies were incubated with the PDMS stamp and printed onto a glass substrate. (c) Represents the target cell's separation using the produced platform. Primary cell mixtures from isolated rat brain or heart were placed in contact with the patterned substrate. Target cells were allowed to attach to the antibodies patterned on the surface over a brief incubation period, after which the surface was washed with media to remove unbound cells. (d) Represents applied surface chemistry to avoid non-specific cell adhesion. 2% PLL-g-PEG solution was used for this purpose.

9-3 Results

9-3-1 Design and fabrication of the platform

Three steps were followed to fabricate the multi-purpose adhesion based separation and patterning platform (Figure 9-1): design and fabrication of the PDMS stamps, immobilizing and patterning of cell-specific biomolecules onto capture substrates using micro-contact printing, and applying proper surface chemistry to avoid non-specific cell adhesion.

First, desired stamp patterns were printed on a chrome mask followed by fabrication of a silicon-based mold with SU-8 photoresist patterns through standard photolithography in a clean room. Soft lithography was then implemented to produce PDMS stamps using the fabricated mold. The fabricated stamps were used to micro-contact print target cell-specific antibodies onto a glass substrate. Finally, patterned surfaces were coated with a 2% PLL(20 kDa)-PEG(2 kDa) solution to avoid non-specific cell attachment. Primary cell mixtures were placed in contact with the patterned substrate. Target cells were allowed to attach to antibodies patterned on the surface over a brief incubation period (10 min), after which the surface was washed with cell media to remove unbound cells.

9-3-2 Assessment of surfaces bio-functionality

To investigate the bio-functionality of the developed interfaces, immunoassays were performed on the platforms patterned with target cell-specific antibodies. The patterned target cell specific primary antibodies Cy5-anti-rabbit and FITC-anti-mouse secondary antibodies were detected by applying fluorescently labeled secondary antibodies specific to each primary antibody (Figure 9-2). Results indicated successful micro-contact printing of the antibodies and demonstrated functionality after patterning and applying the appropriate surface chemistry. To determine bio-functionality of the patterned surfaces for long-term cell culture, platforms patterned with A2B5 and PDGFα primary antibodies specific to OPCs were maintained in a cell culture incubator (37ºC, 5% CO2). After 2 weeks, the samples were stained with fluorescently labeled secondary antibodies specific to A2B5 and PDGFα. Results indicated that the bio-functionality of patterns antibodies was preserved.

9-3-3 Evaluation of target cell initial concentration

Primary culture flasks of mixed cells were trypsinized (0.25% trypsin for 10 min) and diluted to a concentration of 4×10^5 cells/ml. Cells were then cultured on tissue culture treated petri dishes and incubated for 24 h. To identify the OPCs population, immunocytochemsitry was performed (Supplementary Figure 9-1).

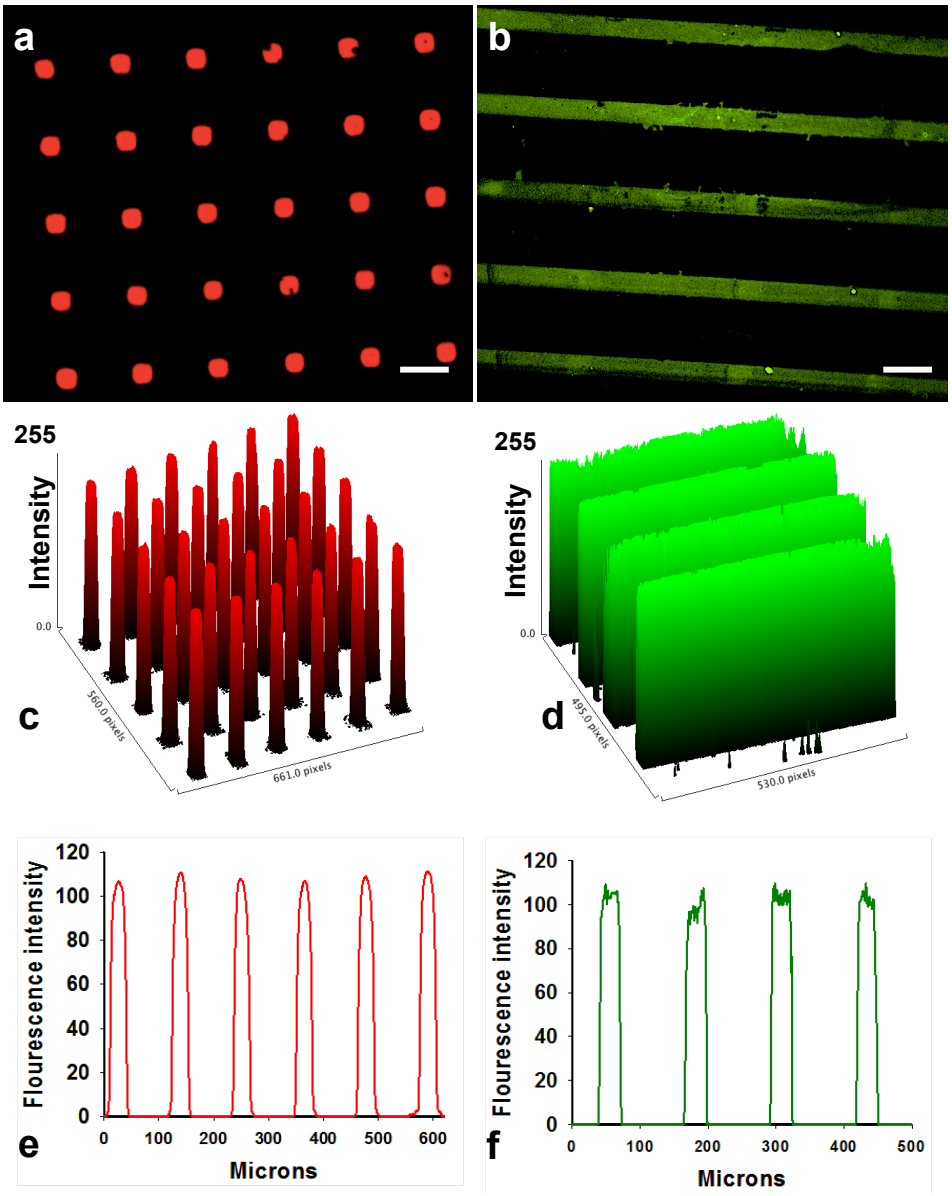

Figure 9-2: Investigation of bio-functionality of produced capture interfaces. Cy5-anti-rabbit (a) and FITC-anti-mouse (b) secondary antibodies were used to visualize patterned primary antibodies. Patterned interfaces remained bio-functional after two weeks in cell culture conditions. Scale bars represent 50 µm. (c) and (d) 3D graphs showing quantitative analysis of fluorescence intensities obtained from (a) and (b). (e) and (f) represent 2D fluorescence intensities of the bio-functional interfaces. 3D and 2D fluorescence intensities were obtained using Image J software.

Results showed that OPCs comprised 7±1% (n=4) of the initial primary cell cultures' concentration. This corresponds to previously reported OPC populations in initial mixtures (5-10%) (Cizkova, Cizek et al. 2009, Sim, McClain et al. 2011). Cardiomyocytes also form 50-60% of the initial cell mixture, as detailed in the literature (Banerjee, Fuseler et al. 2007).

9-3-4 Primary cells separation

Target cell separation was first performed using a flat PDMS stamp to micro-contact print cell specific antibodies. Anti-A2B5 and anti-PDGFα primary antibodies were used to separate OPCs and an anti-SIRPA primary antibody was used for separation of cardiomyocytes. Primary cell mixtures with a concentration of 5×10^7 cells/ml were introduced to the micro-patterned platform. A 10 min incubation time was sufficient to capture cells on the patterned interfaces (data not shown).

For OPC separation, 7±2% of the initial cells were captured on the patterned surfaces, while no cells attached to the control platform (Figs. 9-3a-d). Figure 9-3m depicts the initial concentration of glial mixed cells introduced onto the platform and the number of captured cells on the patterned interfaces. Captured cells on the patterned surfaces were cultured in vitro to investigate their viability, as well as their ability to proliferate and differentiate. To determine the purity of OPCs after separation, they were cultured for 48 h on the separation platform and immunocytochemistry was performed to determine the OPC population (Figs. 9-3e-h). As shown in Figs. 9-3e and 9-2k, captured cells displayed typical bipolar or tri-polar OPC morphology. Using PDGFα patterned interfaces; a 95% OPC enriched population was obtained (Figure 9-3n).

To demonstrate the universality of the developed interface for various cell types and concentration ranges, the same technique was applied for adhesion-based separation of cardiomyocytes from rat heart tissue. The primary cell mixture included cardiac fibroblasts, vascular smooth muscle cells, red blood cells, and cardiomyocytes. The initial cell mixture, control platform, and separated cells after 2 days in culture are shown in Figs. 9-3p-s. Immunocytochemistry results using a cadiomyocyte specific marker (Cardiac Troponin I), showed greater than 99% cardiomyocyte population on the capture interface (Figs. 9-3o).

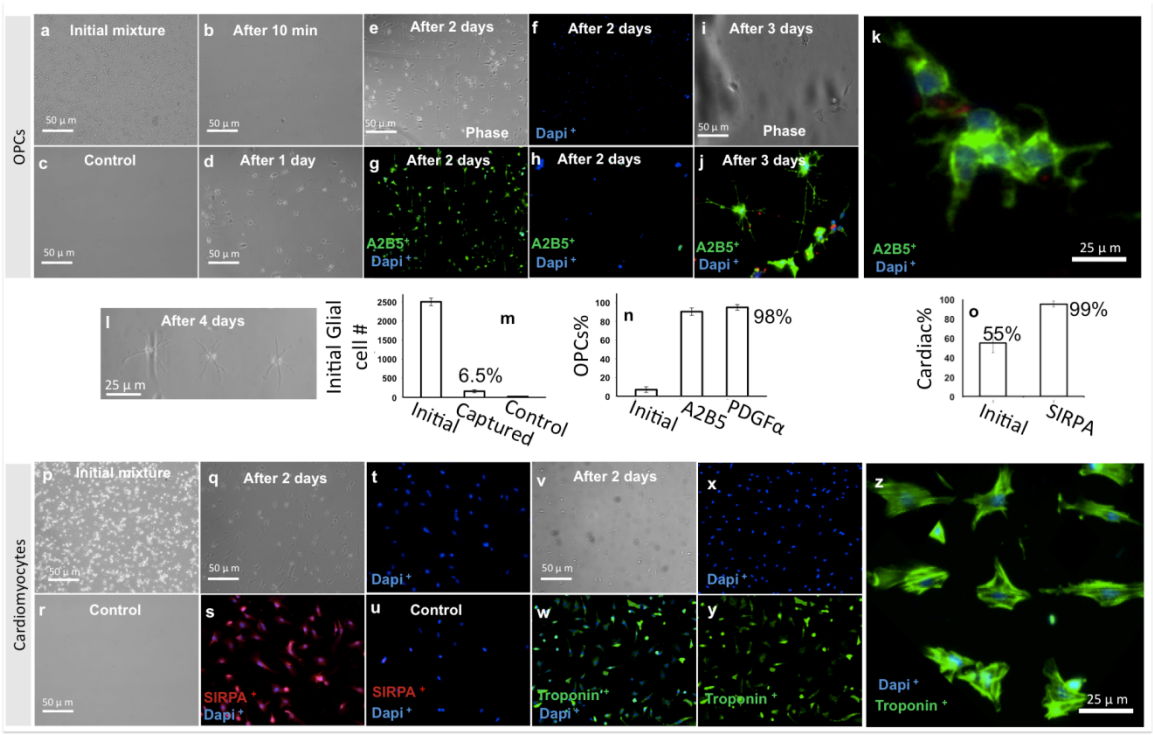

Figure 9-3: Separation of OPCs and cardiomyocytes: a, b, c and c) representative optical microscopy images of a platform patterned with PDGFα primary antibodies after incubation with initial cell mixture (a), 10 min after washing (b) and one after one day *in vitro* culture (d). c) showing no cell adhesion after washing of the control surface without antibody blocked for non-specific adhesion, e-h) fluorescence microscope images of immunocytochemistry results for OPCs separation using PDGFα antibody and dapi staining i-j) optical microscope and immunocytochemistry results of separated OPCs after 3 days *in vitro* culture inside the platform. k) optical microscope image of OPCs after 4 days *in vitro* culture inside the platform shwoing cells spreading and differentiation into mature oligodendrocytes, l) initial number of introduced cells into the platform and captured cells after incubation and washing, h) purity of OPCs after separation using A2B5 and PDGFα antibodies determined by imuunocytochemistry. Error bars represent standard deviations of five separate experiments. n) initial concentration of cells extracted form heart tissue incubated on the platform, o-w) images demonstrating results for cardiomyocytes separation stained with SIRPA, anti-cardiac troponin dapi, and l) immunocytochemistry results showed greater than 99% cardiomyocyte purity (n=3).

9-3-5 Simultaneous separation and precise patterning of target primary cells

Next, the possibility of simultaneous separation and patterning of target cells was investigated. PDMS stamps with varying patterns were used to produce surfaces with OPC- and cardiomyocyte-specific antibodies. Both cell types responded to antibody patterns on the surface (Figure 9-4, Supplementary Movie S9-1 for OPC separation, and Supplementary Movie S9-2 for cardiomyocyte separation).

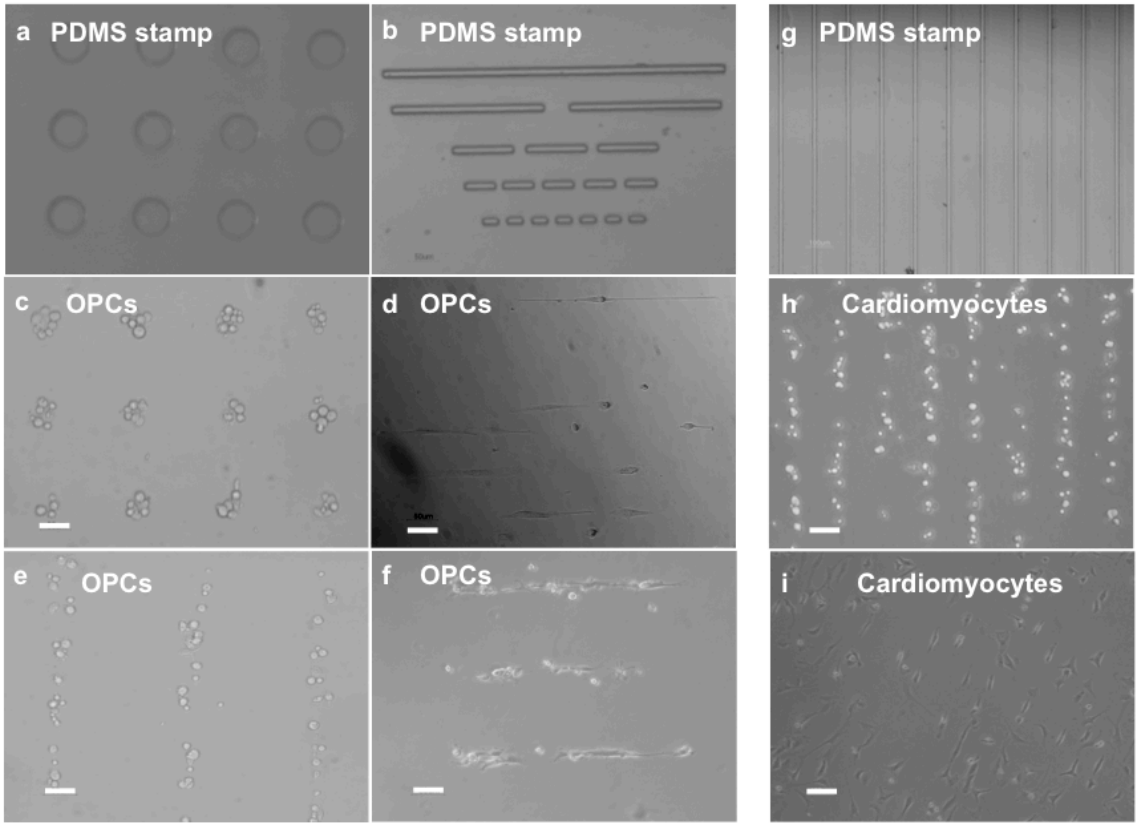

Figure 9-4: a and b) optical microscope images of two of the stamps used to micro-contact print OPC specific antibodies. c and d) are separated OPCs captured on the interfaces produced using stamps shown in a and b respectively. As shown in d, single OPCs spreading was controlled by the length of the linear antibody pattern embedded in the design of the stamp shown in b. e and f) represent other OPC patterns produced using desired stamp designs. g) optical microscope image of one of the stamps used to micro-contact print cardiomyocyte specific antibodies, h) separated cardiomyocytes captured on the interfaces produced using stamps shown in g, i) separated and patterned cardiomyocytes after 2 days *in vitro* culture inside the platform. Scale bars represent 50 μm.

Single target primary cell spreading could also be controlled based on the geometry of the patterned cell specific antibody. As shown in Figure 9-4d, OPCs spread along the length of the patterned antibodies printed with the stamp seen in Figure 9-4b. It was therefore possible to isolate cells that comprised roughly 7% and 50% of the total cell population in a mixture, as well as control individual cell morphology and spreading. Time laps imaging of patterned cells confirmed their attachment and spreading on the patterned surface over the course of several hours.

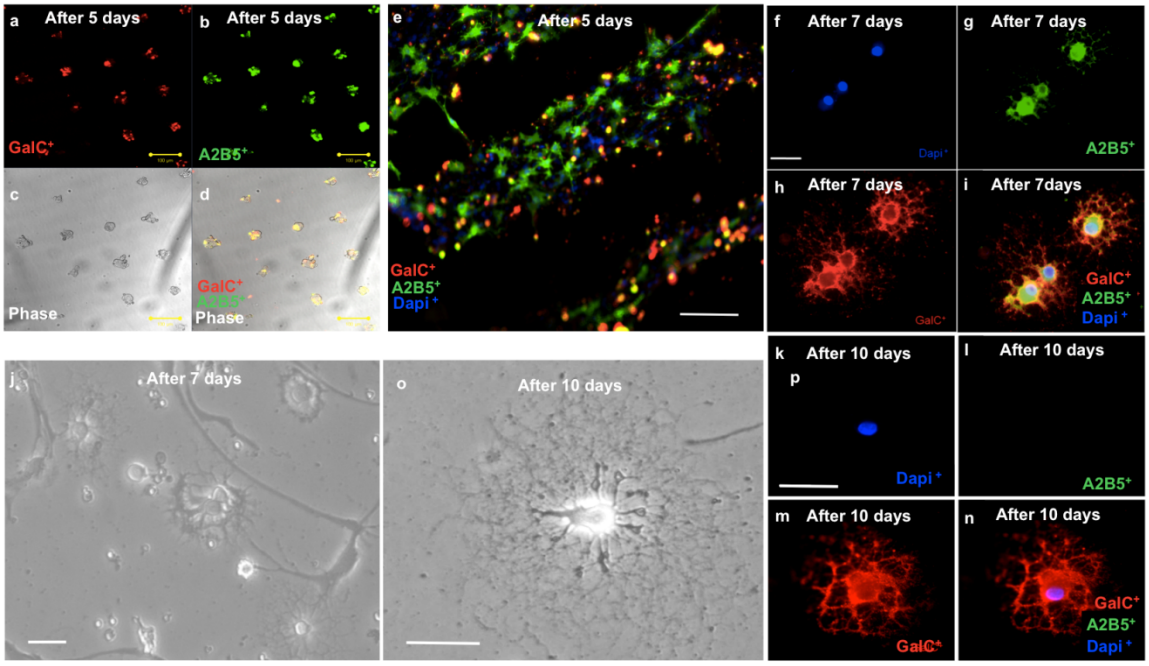

Figure 9-5: Immunocytochemistry results showing differentiation of separated OPCs. a, b, c and d) flourescence microscope images of patterned cells after 5 days in culture. Cells stained against A2B5 (oligodendrocyte progenitor marker) and GalC (mature oligodendrocyte marker), e) flourescence microscope image of captured cells on virtual micro-channels after 5 days in culture, f, g, h and i) differentiated mature oligodendrocytes after 7 days in culture, and k-n) after 10 days showing OPCs differentiation to mature oligodendrocytes since cells express only mature oligodendrocyte marker. Scale bars represent 100 µm.

9-3-6 In vitro culture, viability and differentiation of separated primary cells inside the platform

OPCs have limited proliferative potential in vitro, requiring strict conditions for growth (Mekhail, Almazan et al. 2012). To demonstrate the capability of the developed bio-interface for OPC proliferation and differentiation, fluorescence imaging was performed over several days with appropriate markers (A2B5 for OPCs and GalC for mature oligodendrocytes). Results showed that separated OPCs can proliferate on the platform (Movie S9-3) and fluorescence micrographs demonstrated that patterned cells were viable and differentiated *in vitro* (Figure 9-5).

Separated cells were cultured for up to 10 days and then stained with PDGFα and GalC to investigate in situ OPC population and differentiation to mature oligodendrocytes. After 5 days, cells expressed GalC, mature oligodendrocyte

marker, as shown in Figure 9-5a-e. After 10 days in culture, only the mature oligodendrocyte marker was expressed, which was consistent with mature oligodendrocytes morphology presented in Figure 9-5 f-n.

9-4 Conclusion

Given that conventional cell isolation techniques can be expensive, time consuming, non-specific, yield low isolation purities, and/or damage cells, we propose an alternative adhesion-based multi-purpose micro-fabricated platform that can rapidly separate target cell populations with proven functionality at high efficiencies. To demonstrate the versatility of this methodology, separation was performed with two cell types, OPCs and cardiomyocytes. These cells were selected based on their dissimilar physical properties and concentration scenarios, where OPCs make up less than 7% of the total cell population in extracted rat tissues and cardiomyocytes make up more than 50% in rat heart tissues. The separation time was as rapid as 10 min, with a reproducible degree of purity greater than 95% for both cell types. The platform was shown to be suitable for in vitro proliferation and differentiation of primary cell types over 10 days. The ability to culture cells directly on the platform confers significant advantages compared to FACS and MACS techniques, since cells can be utilizated directly for further investigation, improving practicality and decreasing costs. In addition, the introduced method significantly reduces the use of expensive primary antibodies compared to FACs and MACs due to implementing micro-contact printing where only 10 µl (20 µg/ml) of cell-specific biomolecule solution is sufficient to produce the bio-functional interface. Overall, we have shown that we can simultaneously separate target cells from a mixed population, localize the cells to a site of interest, enable long-term culture, and control single cell morphology on the patterned surface using our unique and straightforward approach.

Notably, the ability to control single cell spreading on the interface could be beneficial for studies that involve crosstalk between cells. For instance, the set-up can be used to investigate the interactions and myeliniating properties of OPCs in a co-culture with neurons, where a single neuron and OPC can be

brought into contact with each other. This is a desirable area of research due to the complexity involved in the myelination and re-myelination processes after spinal cord injuries. In the same way, control over single cell morphology may be relevant to the study of myocardial cell morphology and contractile properties in specific conditions and well-controlled patterns.

The need for a marketable device that is cost-effective, fabricated with a small footprint, and capable of separating different cell types at a high efficiency in a short period of time is increasingly becoming apparent in the context of first principles and diagnostic research. The fabrication method detailed herein produces a device that satisfies all of these requirements. We have demonstrated that our platform can separate two dissimilar primary cells from a mixture by patterning cell-specific biomarkers on the platform and simultaneously position the cells for in vitro co-culture and subsequent studies.

9-5 Experimental

Materials: The negative photoresist SU8-2025, Sylgard 184 elastomer kit composed of pre-polymer and curing agent of poly(dimethylsiloxane) (PDMS) were purchased from Microchem Corp (Boston, MA, USA) and Essex Chemical (Boston, MA), respectively. A2B5 mouse, PDGFα rabbit, GalC rat primary antibodies, FITC conjugated IgG mouse, and Cy3 conjugated IgG1 secondary antibodies were obtained from Invitrogen. Signal-regulatory protein alpha (SIRPA) was purchased from Santa Cruz biotechnology, Inc.

Fabrication of PDMS stamps: PDMS stamp designs for micro-contact printing were generated using AutoCAD® software (Autodesk Inc., CA, USA) and printed on a chrome mask. A 5-inch silicon wafer was used to fabricate the mold for soft lithography. After cleaning with 10% hydrofluoric acid for 10 s, the SU-8 2015 negative photo-resist was spin-coated at 1500 rpm for 30 s onto the wafer. Soft bake was performed on the SU-8 coated wafer at 95 ºC for 5 min. Photolithography was carried out on the wafer using the printed mask. After UV exposure through the mask, post baking was achieved at 65 ºC for 3 min and at 95 ºC for 6 min. The features were then developed in SU-8-developer for 5-10 min. The mold was rinsed with isopropyl alcohol, and hard baked at 150 ºC for 30

min followed by silanization. To prevent undesired PDMS residue adhesion after curing, a drop of trichloro(1,1,2,2-perfluorooctyl)silane was placed in a glass vial and incubated for 2 h with the mold in a desiccator under vacuum.

Soft lithography was used to produce PDMS platforms (Figure 9-1). PDMS base and curing agents were mixed in a 10 to 1 weight ratio, and poured onto the fabricated mold. After degassing under vacuum, it was placed at 80 ºC for 4 h. Cured PDMS containing the desired patterns was then peeled off and cut for micro-contact printing.

Micro-contact printing: Different PDMS stamp designs were used to micro-contact print target cell-specific biomolecules onto glass substrates. Glass substrates (bio-functional interface substrates) were placed in piranha (H2O2:H2SO4, 1:3 v/v) solution for 10 min, rinsed extensively with DI water, and dried under nitrogen. The PDMS stamps were exposed to UV light for 20 min and rinsed with 70% ethanol. Each PDMS stamp was covered with 15 µl of target cell specific antibodies (20 µg/ml) at room temperature. A plasma treated cover slip (60 s, 200 W, 200 mTorr O_2) was placed on the stamp for 10 min, to help spread the antibody solution and prevent evaporation. After rinsing with PBS and distilled water and drying under nitrogen, the stamp was gently brought into contact with the glass substrate for 60 s. The micro-contact printed surfaces can be stored at 4 ºC for up to 4 weeks.

Surface modification to avoid non-specific adhesion: After patterning the interface surface with the cell-specific antibody, surface modification was performed to avoid nonspecific binding. For this purpose, micro-contact printed glass substrates were covered with 2% PLL(20 kDa)-PEG(2 kDa) solution for 30 min. The surfaces were then washed twice with sterile PBS.

Brain tissue extraction and culture: Using a protocol approved by McGill University Animal Care Ethic Committee, OPC mixed primary cultures were prepared from brains of newborn Sprague-Dawley rats. The meninges and blood vessels were removed from the cerebral hemispheres in Ham’s F-12 medium. The tissues were gently forced through a 230-µm nylon mesh. Dissociated cells were then gravity-filtered through a 100-µm nylon mesh. This second filtrate was

centrifuged for 7 min at 1000 rpm, and the pellet was re-suspended in DMEM supplemented with 12.5% fetal calf serum, 50 units/ml penicillin, and 50 µg/ml streptomycin. Cells were plated on poly-L-ornithine precoated 80-cm2 flasks and incubated at 37 °C with 5% CO_2. The mixed cell flasks were then used for subsequent separation experiments.

Heart tissue extraction and culture: Mixed heart cultures were obtained from newborn Sprague-Dawley rats using a protocol approved by McGill University Animal Care Ethic Committee. To release the cells, hearts were minced into small fragments and placed in a 50 µg/mL trypsin solution in calcium- and magnesium-free Hank's Balanced Salt Solution. After overnight incubation at 4 ºC, trypsin inhibitor was added to tissue fragments, which were subsequently warmed to 37 ºC. Collagenase was added to the mixture and incubated at 37 ºC for 45 min, under gentle rotation. Finally, to release the cells tissue fragments were triturated. Large fragments were allowed to settle and all experiments were performed using the mixed culture using the supernatant. Cells were cultured in DMEM containing 4.5 g/L glucose supplemented with 10% fetal bovine serum and 100 units/mL pen-strep.

Immunocytochemistry: To identify OPCs, cells were live stained by incubating with media containing A2B5 (50 µg/ml) for 30 min at 37 ºC. To identify differentiated OPCs, GalC (50 µg/ml) was also added to the cell media. Next, the cells were washed with media and fixed using 4% paraformaldehyde in PBS for 30 min at room temperature, then incubated with 10% goat serum for 20 min. After washing with sterile PBS, secondary antibodies (anti-mouse FITC-IgG1, anti-rabbit Cy3-IgG3) at a concentration of 100 µg/ml, were incubated with the fixed cells for 45 min. The cells were then washed twice with PBS. Next, nucleus stain (DAPI 1:1000) in PBS was applied for 15 min. The cells were then rinsed 3X with sterile PBS and observed using fluorescence microscopy. Separated cells were incubated with the secondary antibody only as a control. A negative control was also performed by similarly staining NIH 3T3 fibroblasts.

The same method was used to stain separated cardiomyocytes against SIRPA mouse and Troponin I rabbit primary antibody (20 µg/ml) followed by surface

blocking and staining with Cy3 conjugated anti-mouse and FITC conjugated anti-rabbit IgG secondary antibody (100 µg/ml).

An inverted fluorescence microscope (Nikon TE 2000-E) was used to monitor surface functionalization and immunocytochemistry. Antibodies conjugated with three different fluorescent dyes (Cy3, FITC and DAPI) were used in the experiments and observed through appropriate filters. All images were captured using a CCD camera (Photometrics CoolSNAP HQ2) and analyzed by MBF_ImageJ (MacBiophotonics, McMaster University).

9-6 Supporting Information

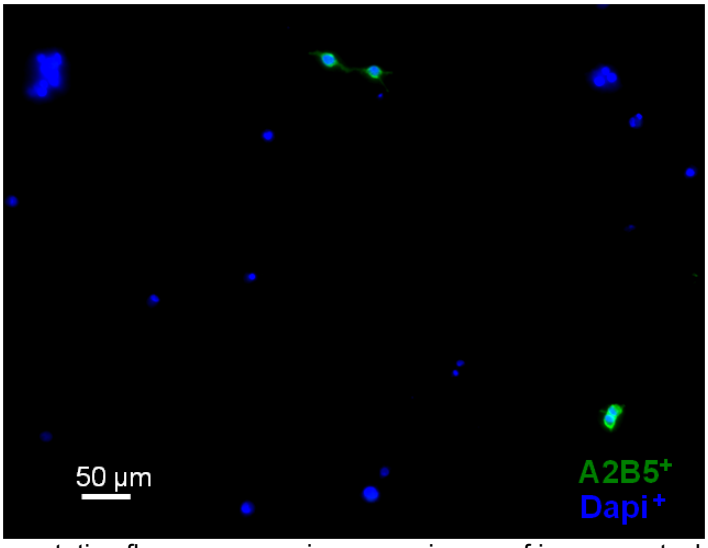

Figure S9-6: Representative fluorescence microscope image of immunocytochemistry results on the initial mixed primary cells to determine OPCs initial concentration. A2B5 positive cells (green fluorescence) were identified as OPCs.

9-7 Acknowledgements

The authors would like to acknowledge National Science and Engineering Research Council of Canada (NSERC)-Discovery, NSERC-Vanier scholarship to K. Bowey, NSERC-CREATE for Integrated Sensor Systems (ISS), Nano-Québec, Genome Canada/Génome Québec. T.F.D. would like to thank the Faculty of Medicine at McGill and Fonds de Recherche du Quebec - Nature et Technologies (FQRNT) for financial support. The authors would like to thank

Prof. D. Juncker for providing access to microscopy facilities, Mr Mina Mekhail for his technical advices on the principle and basic of oligodendrocyte function as well as Marcio Dipaula for his assistance with the cell isolation experiments.

References

Banerjee, I., J. W. Fuseler, R. L. Price, T. K. Borg and T. A. Baudino (2007). "**Determination of cell types and numbers during cardiac development in the neonatal and adult rat and mouse.**" Am J Physiol Heart Circ Physiol **293**(3): H1883-1891.

Chen, Y., V. Balasubramaniyan, J. Peng, E. C. Hurlock, M. Tallquist, J. Li and Q. R. Lu (2007). "**Isolation and culture of rat and mouse oligodendrocyte precursor cells.**" Nat. Protocols **2**(5): 1044-1051.

Cizkova, D., M. Cizek, M. Nagyova, L. Slovinska, I. Novotna, S. Jergova, J. Radonak, J. Hlucilova and I. Vanicky (2009). "**Enrichment of rat oligodendrocyte progenitor cells by magnetic cell sorting.**" Journal of Neuroscience Methods **184**(1): 88-94.

Didar, T. F., A. M. Foudeh and M. Tabrizian (2011). "**Patterning Multiplex Protein Microarrays in a Single Microfluidic Channel.**" Analytical Chemistry.

Didar, T. F. and M. Tabrizian (2010). "**Adhesion based detection, sorting and enrichment of cells in microfluidic Lab-on-Chip devices.**" Lab on a Chip **10**(22): 3043-3053.

Dubois, N. C., A. M. Craft, P. Sharma, D. A. Elliott, E. G. Stanley, A. G. Elefanty, A. Gramolini and G. Keller (2011). "**SIRPA is a specific cell-surface marker for isolating cardiomyocytes derived from human pluripotent stem cells.**" Nat Biotech **29**(11): 1011-1018.

Esch, M. B., D. J. Post, M. L. Shuler and T. Stokol (2011). "**Characterization of in vitro endothelial linings grown within microfluidic channels.**" Tissue Engineering - Part A **17**(23-24): 2965-2971.

Fiddes, L. K., H. K. C. Chan, B. Lau, E. Kumacheva and A. R. Wheeler (2010). "**Durable, region-specific protein patterning in microfluidic channels.**" Biomaterials **31**(2): 315-320.

Graber, D. J., T. J. Zieziulewicz, D. A. Lawrence, W. Shain and J. N. Turner (2003). "**Antigen Binding Specificity of Antibodies Patterned by Microcontact Printing.**" Langmuir **19**(13): 5431-5434.

Herzenberg, L. A., R. G. Sweet and A. Herzenberg (1976). "**Fluorescence-activated cell sorting.**" Scientific American **234**(3): 108-116.

Jang, L.-S. and H.-J. Liu (2009). "**Fabrication of protein chips based on 3-aminopropyltriethoxysilane as a monolayer.**" Biomedical Microdevices **11**(2): 331-338.

Kaufmann, T. and B. J. Ravoo (2010). "**Stamps, inks and substrates: polymers in microcontact printing.**" Polymer Chemistry **1**(4): 371-387.

Kim, M., J.-C. Choi, H.-R. Jung, J. S. Katz, M.-G. Kim and J. Doh (2010). "**Addressable Micropatterning of Multiple Proteins and Cells by Microscope Projection Photolithography Based on a Protein Friendly Photoresist.**" Langmuir **26**(14): 12112-12118.

Legeay, G., A. Coudreuse, F. Poncin-Epaillard, J. M. Herry and M. N. Bellon-Fontaine (2010). "**Surface engineering and cell adhesion.**" Journal of Adhesion Science and Technology **24**(13-14): 2301-2322.

Mandal, S., J. M. Rouillard, O. Srivannavit and E. Gulari (2007). "**Cytophobic Surface Modification of Microfluidic Arrays for In Situ Parallel Peptide Synthesis and Cell Adhesion Assays.**" Biotechnology Progress **23**(4): 972-978.

Marek, R., M. Caruso, A. Rostami, J. B. Grinspan and J. D. Sarma (2008). "**Magnetic cell sorting: A fast and effective method of concurrent isolation of high purity viable astrocytes and microglia from neonatal mouse brain tissue.**" Journal of Neuroscience Methods **175**(1): 108-118.

Mekhail, M., G. Almazan and M. Tabrizian (2012). "**Oligodendrocyte-protection and remyelination post-spinal cord injuries: a review.**" Prog Neurobiol **96**(3): 322-339.

Nagrath, S., L. V. Sequist, S. Maheswaran, D. W. Bell, D. Irimia, L. Ulkus, M. R. Smith, E. L. Kwak, S. Digumarthy, A. Muzikansky, P. Ryan, U. J. Balis, R. G. Tompkins, D. A. Haber and M. Toner (2007). "**Isolation of rare circulating tumour cells in cancer patients by microchip technology.**" Nature **450**(7173): 1235-U1210.

Plouffe, B. D., T. Kniazeva, J. E. Mayer, Jr., S. K. Murthy and V. L. Sales (2009). "**Development of microfluidics as endothelial progenitor cell capture technology for cardiovascular tissue engineering and diagnostic medicine.**" FASEB J. **23**(10): 3309-3314.

Quist, A. P., E. Pavlovic and S. Oscarsson (2005). "**Recent advances in microcontact printing.**" Analytical and Bioanalytical Chemistry **381**(3): 591-600.

Sim, F. J., C. R. McClain, S. J. Schanz, T. L. Protack, M. S. Windrem and S. A. Goldman (2011). "**CD140a identifies a population of highly myelinogenic, migration-competent and efficiently engrafting human oligodendrocyte progenitor cells.**" Nat Biotech **29**(10): 934-941.

Chapter 10. General discussion

In this dissertation, size-based and adhesion-based cell separation technologies were successfully implemented in novel LOC devices with four main prerequisites formulated in the thesis hypothesis. These prerequisites for the devices were label-free, high throughput, high separation efficiency and cost effectiveness for mass production. As for the investigated target cells for each device, they have been selected according to thesis criteria to allow for proper evaluation of the device functionality, or chosen among primary and rare cells that are difficult to obtain with a pure population with high efficiency using standard techniques without altering the target cell properties. We could meet all these criteria during this doctoral thesis and successfully separated selected target cells from a cell mixture with high efficiency using the developed devices. A detailed list of accomplishments, addressing the objectives of this doctoral work is discussed below.

Objective 1: Development of a LOC device for size-based cell separation

The fulfillment of this research objective was stated in chapters 4 and 5. These manuscript-based chapters report on a novel multilayered, fully thermoplastic elastomeric-based microfluidic device for high-throughput size-based separation of micro/nano particles and cells.

In chapter 4, the design and fabrication process of fluidic and pneumatic layers of the device using hot-embossing lithography were detailed. Commercially available polycarbonate membranes could successfully be sandwiched between two fluidic layers coupled with an embedded peristaltic micro-pump. The use of thermoplastic elastomers allowed fabricating a multilayered chip with embedded micropumping mechanism using hot-embossing lithography. As such, the device can be mass-produced and be commercially viable. Most importantly, the coupled peristaltic micropump could avoid particle clogging and membrane blocking to address the major limitations of previous developed size-based particle and cell separation techniques. Separation of micro and nano size particles was confirmed and separation efficiency greater than 99% was

achieved. The operating flow rate of up to 100 µl/min allowed for high throughput sorting and separation of particles, which is again a significant advantage compared to previously reported microchips.

In chapter 5, we successfully demonstrated the application of this chip for separation of primary rare cells. In a case study, a mixed primary cell cultures from rat brain tissue were used to separate and enrich oligodendrocyte progenitor cells (OPCs). Results showed over 99% pure OPC populations after their separation from an initial population of around 7% in the cell mixture. Although in this chapter we report on the OPCs separation, the device can be used for other applications such as mixing biological samples through generating turbulence.

Objective 2: Development of a chip for adhesion-based cell separation

The second main objective of this thesis was to develop LOC devices with embedded bio-functional interfaces for adhesion-based separation of cells. The development of these bio-functional interfaces for targeted cell recognition was the most challenging part of developing adhesion-based microchips. A combinatorial approach consisting of micro-contact printing at the first step and microfluidic patterning at the second step were used to achieve covalent attachment of multiplex microarrays of biomarkers. As detailed in Chapter 7, a multiplex immunoassay inside a single microfluidic channel was accomplished. Such a device can be very useful for simultaneous detection of several biological elements in complex samples such as blood or serum. It could also be very beneficial in applications where high shear stress is required such as adhesion of lymphocytes on the developed interface and investigating their behavior under high shear forces.

In further pursuit of the second objective of this thesis, a novel microfluidic device was designed to induce different hydrodynamic resistances in parallel microfluidic channels in order to generate concentration gradients of several biomolecules in every microfluidic channel. The aim was to achieve multiplex gradients of biomarkers for investigation of gradient-dependent adhesion of cells to varying biomarker concentrations. As a proof of concept, the degree of adhesion of

human umbilical vein endothelial cells on multiplex gradients of peptides was demonstrated (Chapter 8). This design-based gradient generator platform features the time and cost effectiveness. It significantly decreases the complexity of gradient dependent experiments while providing a powerful tool for high-throughput multiplex experiments or to discover cell-specific adhesive biomolecules when cell sorting is the application of interest.

Indeed, the knowledge gained during the development of bio-functional interfaces, led to the development of a universal adhesion-based cell separation chip in order to address the last and ultimate goal of this thesis. For this purpose, bio-functional interfaces for targeted cell recognition, was employed to develop the required LOC device. In chapter 9, we showed highly efficient sorting (95%-100%) of rare primary oligodendrocyte progenitor cells (OPCs) from rat brain cell mixture in less than 10 min using this platform. To determine its applicability for a wide range of target cell concentrations, the primary cardiomyocytes from heart tissue with an abundancy of almost 10 times higher compared to OPCs, in the crude heart cell mixture, were separated with over 95% separation efficiency.

Furthermore, we investigated the high specificity of bio-interface towards the target cell by creation of specific antibody-patterns on chip surface. Using a single platform, OPCs and cardiomyocytes could again be captured and separated with high efficiency from the rat brain and heart cell mixtures. More interestingly, cells could be cultured on patterned surface over 10 days in the view of their use for further investigation, thus providing significant advantages compared to FACS and MACS techniques in terms of practicality and cost.

Simultaneously separating target cells, localizing the desired cell population on the site of interest along with controlling single cell's morphology and culturing them on a patterned surface would be beneficial for a variety of applications such as primary cells co-culture to investigate fundamental aspects of cell-cell interactions as well as cell therapy and/or new drug testing.

Chapter 11. Limitations, future prospective and general conclusion

11-1 Limitations and future prospective:

For size-based separation, the current chip is capable of separating only one cell type from a mixture based on its size. The design can be modified to separate three different cell types by integrating another membrane into the design. This will require more complex fabrication and assembly processes. In addition, it will be challenging to control the flow by using one embedded peristaltic micro pump specially for generating turbulent flow across the second membrane. To address this issue, another pneumatic layer might be required to introduce a second pumping option into the design.

Furthermore, to reduce separation time; several parallel designs can be integrated into a single chip. This requires changes in the microfluidic design and also more instrumentation to support multiple pumping systems

As for the adhesion-based separation, the developed chips were all made of PDMS-Glass substrates. This limits commercial applications of these platforms. Employing other materials to fabricate adhesion-based devices such as TPEs, as was the case for our size-based separation platforms, would push these devices furthermore towards their mass production. However functionalization, patterning and biocompatibility of any new material should first be investigated.

As a part of objective 2, the developed chip to generate multiplex gradients would also be of particular interest to study the degree of adhesion of different cell types to multiplex biomolecule gradients, which could lead to discovery of new cell-specific markers. This chip can also be implemented to study the effect of different drug concentrations on cells for applications such as cancer treatment or antibiotic susceptibility.

In addition, the adhesion-based chip can be further modified to simultaneously separate more than one type of target primary cells from a mixture. This can be achieved by patterning more than one cell-specific biomarker. For instance for

our particular interest, neurons and OPCs from brain tissue can be simultaneously separated and patterned in desired areas for subsequent *in vitro* co-culture. Modifications can also be made to produce bio-functional interfaces with minimum non-specific adhesion for separation of target cells from whole blood. However, in case of targeting more than three cell types on a single interface, the implementation of micro-contact printing will be extremely challenging and other technologies should be explored. Combined micro-contact printing and microfluidic patterning that we described in chapter 7 was one of the possibilities to address this limitation. Nevertheless, the introduced procedure will require precise flow control and more time compared to micro-contact printing.

For post-separation applications, the set-up introduced in chapter 9, can easily be applied to study the interactions and myeliniating properties of OPCs in a co-culture with neurons in which specific parts of a single neuron and OPC can be brought into contact with each other. For separated cardiomyocytes, the control of single cell's morphology is particularly interesting in studying of myocardial cell morphology and contractile properties under desired and well-controlled morphological patterns.

Finally the size-based separation chip can be further integrated with the adhesion-based approach to capture or separate the cells with the same size or to culture the target cells on the same platform.

It should also be noted that although compared to FACS machine, the developed size-based and adhesion based chips provide many advantages over FACS, FACS still remains a powerful technique for sorting cells at a rate of 10,000 cells/second.

11-2 General conclusion

The two generations of cell sorting platforms, size-based or adhesion-based, will open new avenues for obtaining and culturing pure/enriched pluripotent, progenitor or primary cells. The possibility of generating concentration gradients of bio-factors would ensure preservation of cell phenotyping, proliferation, migration and differentiation *in vitro*. Conversely, patterning cells and localizing the desired cell population on the site of interest, controlling single cell's

morphology and spreading on the interface, and culturing them on a single platform would be extremely beneficial for a variety of fundamental cell studies such as primary cells co-culture to investigate and assist the crosstalk between cells. In addition, for drug toxicology, discovery and testing, gradients of novel drugs can be applied onto the separated cells inside the platform to study the effect of different drug dosages.

Overall the achievements in this thesis is an important step towards the new paradigm in regenerative and personalized medicine where the emphasis is on producing the future generation of LOC devices so-called “organ-on-chip” with the final goal of arriving at personalized “human-on-chip” platforms.